The Role of *CDKN1B*-p27kip1 Deregulation in the Pathogenesis of Pediatric T-cell Acute Lymphoblastic Leukemia

Sara Colomer-Lahiguera

DOCTORAL THESIS UPF / 2015

DEPARTMENT OF EXPERIMENTAL AND HEALTH SCIENCES

THESIS DIRECTORS

Dr. Sabine Strehl, Genetics of Leukemia group; CCRI, Children's Cancer Research Institute, St. Anna Kinderkrebsforschung, Vienna (Austria)

Dr. Jose Aramburu, Department of Expertimental and Health Sciences; Universitat Pompeu Fabra, Barcelona (Spain)

St Anna Kinderkrebsforschung
Children's Cancer Research Institute

To my five hundred million bells.

To my parents.

Acknowledgements

"I'm going to give you a present (…) When you look at the sky at night, because I'll be living on one of them, because I'll be laughing on one of them, to you it will sound as if all the stars are laughing… It will be as if, instead of stars, I'd given you lots of laughing bells."

Today I'm sitting in front of my laptop trying to write this "acknowledgements" section. Today I'm looking back at the past; this thesis represents many things.

At the personal level, it represents a milestone in my life and in my professional career. A career I started almost ten years ago, full of changes, cities, countries, languages, challenges, ups and downs… but that achieves today its academic "maturation".

I remember the day I entered a pediatric oncology unit for the first time. I immediately felt I became part of a unique and special family and I realized what I wanted to do. This thesis somehow symbolizes my continued motivation and commitment to the pediatric oncology field since that day.

My first and most heartfelt thanks go to all the children and their families I had the honor and the privilege to meet during my years working as a pediatric oncology nurse. You have been my gift. Words can't really explain… Thank you for teaching me everyday, for giving me the chance to share so many special moments with you. You have accompanied me each day; you are my real motivation.

I would like to thank Dr. Sabine Strehl, for giving me the chance to perform my PhD in her group. Thank you Sabine for your support during these four years, but most of all, thank you for trusting this pediatric nurse with aspirations and for this huge opportunity! Thanks Klaus, Dagmar and Amy for your help and scientific advice and of course for teaching me the Austrian way of life -unpronounceable dialect included- *wie nie!* (Cited from *Österreich* or *Heute*). Thanks Margit for your energy and all your

work with the FISH! And to my *alter ego* in the lab, Micky, “Ph.D.” stands for *Permanent head Damage* or *Proudly half Dead*, now we know.

Thanks to Dr. Jose Aramburu. I am so grateful you accepted being my co-director! Jose, not only have you been supervisor but also a life and personal coach! You always have comforting and cheering words. Thank you for your faith and support!

Special thanks to Iris, for the extraordinary years sharing interests, projects, goals and ideas. You changed my life and opened a completely new world to me. You taught me to be strong and to keep pushing for my dreams. I will be always grateful for your help and your support. This is also a bit yours.

I would also like to thank the many people I have been working with over the years. In particular Eugenia and Marisol, my two “nurse mentors”. Marisol, I will never forget my first days working at the pediatric transplantation unit and the firsts night shifts. I was so scared! I will be forever grateful for your patience teaching me and for your support. Eugenia…what can I say. You basically pushed me eight years ago and told me to think big and to do big things. I hope a PhD in Biomedicine and the European Pediatric Oncology Nurses group reaches at least the threshold! I am really happy to count on you for all the new projects.

To the man with the mustache who was working in 2002 at the Secretariat of the Nursing School in Valencia: I still remember your words: “*With your literary background you will never be able to access the Nursing degree*”. I did it. I even managed to do a PhD in Biomedical Sciences. It was just a matter of time, effort and motivation. But thanks for triggering my pigheadedness.

To my Viennese family… Eleni, Iro, Carmen, Iñaki, Jon, Paola, Karin… you have been my Mediterranean breeze. And without breathing one cannot survive. As simple but as vital as this.

Aizea, thanks for your patience and for your support day after day. You encouraged me along the way. You brought some light –not only the

flashes- and you brought a smile. It was a hard decision and it has been a hard time, but we got over it! We started from scratch and what we have now is all ours. We have to be proud!

This thesis is also the achievement of one of my goals. Mum, I remember sitting next to you during your evening lectures at the University. Those were the mid-80's, you psychologists were crazy at this time! I was 6, but I already got the small spark of this "way-of-life". This spark became bonfire with Prof. Lorenzo Ferrer Figueras and his life dedicated to the Academia and research. I could also feel your enthusiasm while discussing about projects, your commitment and your passion… The day had only 24 hours, too little for you. I grew up getting questions as answers and many resources as solution. To prepare an omelette for dinner was a nice exercise to develop algorithms and any existential doubt was the excuse to (re)read together Carl Sagan or Marvin Harris. Weekends were the time for arts&crafts and nature. Dad, you taught me the respect for life, the value of care, the empathy and the patience, to see deep and beyond. Thanks mum and dad for all this. Thank you for bringing me up in -supervised- freedom and teaching me the meaning and the value of taking each and every decision. If I would have to raise me up again, I wouldn't change anything.

"…And at night, I love listening to the stars.
It is like hearing five hundred million bells."

-Antoine de Saint-Exupéry-
The Little Prince

Agradecimientos

"Voy a hacerte un regalo (…) Cuando mires al cielo por la noche, como estaré viviendo en una de ellas, como estaré riendo en una de ellas, será para ti como si todas las estrellas estuvieran riendo… Será como si en lugar de estrellas, te regalase millones de cascabeles que ríen."

Hoy estoy sentada delante del portátil intentando escribir esta sección de "agradecimientos". Hoy miro al pasado. Esta tesis representa muchas cosas.

A nivel personal, significa un paso más en mi vida y en mi carrera profesional. Una carrera que empecé casi diez años atrás, llena de cambios, ciudades, países, idiomas, retos, altibajos… pero que alcanza hoy su "madurez" académica.

Recuerdo el día que entré por primera vez en una unidad de pediatría oncológica. De inmediato sentí que formaba parte de una familia única y especial, y me dí cuenta de que quería dedicar mi vida a esto. Esta tesis simboliza de algún modo, mi motivación y dedicación al campo de la pediatría oncológica desde aquel día.

Mi primer y más sentido agradecimiento es para todos los niños y familias que tuve el honor y el privilegio de conocer durante mis años trabajando como enfermera en oncología pediátrica. Vosotros habéis sido mi regalo. No se puede explicar con palabras… Gracias por enseñarme cada día, por darme la oportunidad de compartir tantos momentos especiales con vosotros. Me habéis acompañado cada día y sois mi verdadera motivación.

También quiero dar las gracias a la Dra. Sabine Strehl por darme la oportunidad de llevar a cabo mi investigación en su grupo. Gracias Sabine por tu apoyo durante estos cuatro años, pero sobre todo, por confiar en esta enfermera pediátrica con aspiraciones! Gracias Klaus, Dagmar y Amy por vuestra ayuda y consejo científico y por supuesto por enseñarme el modo de vida austriaco, dialectos impronunciables incluidos. Gracias Margit por tu energía y todo tu trabajo de FISH! Y a mi

alter ego en el laboratorio, Micky, "Ph.D." significa *Daño cerebral Permanente* u *Orgullosamente medio muerto*, ahora lo sabemos (lo siento, esto no tiene tanta gracia en castellano…).

Gracias al Dr. Jose Aramburu, estoy tan feliz de que aceptases ser mi co-director! No sólo has sido supervisor sino también asesor personal! Siempre tienes palabras de ánimo y reconfortantes. Gracias por tu fé y apoyo!

Un agradecimiento especial para Iris por los grandes años compartiendo intereses, proyectos, metas e ideas. Cambiaste mi vida por completo y abriste un nuevo mundo. Me enseñaste a ser fuerte y a luchar por los sueños. Siempre voy a estar agradecida por toda tu ayuda y apoyo. Esto es también un poco tuyo.

Quiero dar las gracias también a todas las personas con las que he trabajado durante estos años. En particular a Eugenia y Marisol, mis dos "mentoras" en enfermería. Marisol, nunca olvidaré mis primeros días en la unidad de trasplantes ni las primeras guardias de noche. Tenía tanto miedo! Gracias por tu paciencia al enseñarme y por tu apoyo. Eugenia… qué puedo decir. Básicamente me diste un empujón hace ocho años y me dijiste que pensase en grande y que hiciese grandes cosas. Espero que un doctorado en biomedicina y un grupo europeo de enfermería pediátrica oncológica cumpla los mínimos! Estoy muy contenta de poder seguir contando contigo para nuevos proyectos.

Al señor del bigote que trabajaba en 2002 en la Secretaría de la Escuela de Enfermería de Valencia, aún recuerdo tus palabras: "*Eres de letras, no vas a poder tener acceso a la Escuela de Enfermería*". Pues lo hice. Incluso accedí a un Doctorado en biomedicina. Era sólo cuestión de tiempo, esfuerzo y motivación. Pero gracias por despertar mi cabezonería.

A mi familia vienesa…Eleni, Iro, Carmen, Iñaki, Jon, Paola, Karin… Habéis sido mi "brisa" mediterránea. Y sin aire no se puede sobrevivir. Tan simple pero tan básico como eso.

Aizea, gracias por tu paciencia y tu apoyo día tras día. Me has dado ánimos a lo largo de todo este largo camino. Trajiste luz –y no me refiero sólo a los flashes- y trajiste la sonrisa. Fue una decisión complicada y han sido tiempos difíciles, pero los superamos! Empezamos con nada y lo que tenemos ahora es nuestro. Tenemos que estar orgullosas!

Esta tesis es el logro de una de mis metas. Mamá, recuerdo el sentarme a tu lado durante tus clases nocturnas en la Universidad. Era a mediados de los ochenta, y los psicólogos estabais locos por aquel entonces! Yo tenía seis años, pero ya pude sentir aquella chispita por de ese modo de vida. Chispita que se convirtió en fuego al conocer al Profesor Lorenzo Ferrer Figueras y su vida dedicada a la Universidad y a la investigación. También sentí vuestro entusiasmo mientras discutías proyectos, vuestra entrega, vuestra pasión… el día tenía 24 horas, muy pocas para ti. Crecí teniendo preguntas como respuesta y muchos recursos como solución. Preparar una tortilla para cenar era un magnífico ejercicio para desarrollar algoritmos y cualquier duda existencial era la excusa para (re)leer juntas Carl Sagan o Marvin Harris. Los fines de semana era el tiempo de manualidades y naturaleza. Papá, me has enseñado el respeto por la vida, el valor de cuidar, la empatía, la paciencia, el mirar y ver más allá. Gracias papá y mamá por todo eso. Gracias por educarme en libertad –controlada- y enseñarme el significado y valor de tomar decisiones. Si tuviera que volver atrás, no cambiaría absolutamente nada.

"…Y por las noches, me gusta escuchar las estrellas.
Es como escuchar quinientos millones de cascabeles."

-Antoine de Saint-Exupéry-
El Principito

Abstract

T-cell acute lymphoblastic leukemia (T-ALL) accounts for 10-15% of pediatric ALL. The oncogenic transformation of T-cell precursors is driven by a broad spectrum of genetic abnormalities. We have confirmed the high frequency of heterozygous loss of the haploinsufficient tumor suppressor *CDKN1B* in pediatric T-ALL samples as well as its reduced transcription also in patients without any evidence of *CDKN1B* deletions. Although we did not find a correlation between alterations in genes involved in *CDKN1B* regulation and frequently mutated in T-ALL and low *CDKN1B* transcript levels, we determined that *CDKN1B*-deleted patients have a significantly lower incidence of *CDKN2A/B* deletions and preferentially arise in immature/*MEF2C*-dysregulated T-ALL. We also show that *MEF2C* overexpression is not exclusively found in early immature T-ALL but is significantly associated with a poor response to glucocorticoid treatment. Furthermore, we investigated the effects of two small molecule inhibitors of SKP2 alone and in combinations with other therapeutic agents in T-ALL cell lines. Our results highlight the importance of defining the cell type-specific and genetic background-dependent biological effects of such compounds.

Resumen

La leucemia linfoblástica aguda de células T (LLA-T) representa el 10-15% de las leucemias pediátricas. La transformación oncogénica de precursores de células T es causada por un amplio espectro de complejas anomalías genéticas. En nuestro estudio hemos podido confirmar la alta frecuencia de la pérdida heterocigota del gen supresor de tumores *CDKN1B* en muestras de LLA-T pediátrica así como su reducida transcripción en pacientes que no mostraban evidencia de deleciones en *CDKN1B*. A pesar de no hallar una correlación entre alteraciones en genes involucrados en la regulación de *CDKN1B*, y frecuentemente mutados en LLA-T, y los bajos niveles de *CDKN1B*, determinamos que los pacientes que presentan deleción en *CDKN1B* tienen una menor incidencia de deleciones en *CDKN2A/B* y muestran una mayor preferencia por los subtipos inmaduros/*MEF2C*-desregulados de LLA-T. También demostramos que la sobrexpresión de *MEF2C* no se encuentra limitada exclusivamente al subtipo "precursor temprano T", pero sí está significativamente asociada con una pobre respuesta al tratamiento con glucocorticoides. Además, investigamos los efectos de dos moléculas inhibidoras de SKP2, solas o en combinación con otros agente terapéuticos, en líneas celulares de LLA-T. Nuestros resultados resaltan la importancia de definir el trasfondo genético y especificidad celular de los efectos biológicos producidos por dichos compuestos.

TABLE OF CONTENTS

RESULTS

INTRODUCTION

1. T-cell acute lymphoblastic leukemia

T-cell acute lymphoblastic leukemias (T-ALL) are highly aggressive hematological tumors resulting from the malignant transformation of T-cell progenitors and account for 10-15% of pediatric ALL cases. This disease typically presents with distinctive clinical features including very high numbers of lymphoblasts in the peripheral blood, involvement of the central nervous system, and with or without an anterior mediastinal mass (Gutierrez and Look, 2010). By treatment with intensive combination chemotherapy nowadays about 80% of T-ALL patients remain in long-term remission. However, 15-20% of the patients still relapse within the first two years following diagnosis and their prognosis remains dismal, emphasizing the need to gain a better understanding of the genetic alterations and molecular mechanisms responsible for disease development, progression, and therapy resistance (Pui and Evans, 2006).

1.1 Genetic alterations in T-ALL

In T-ALL, leukemic transformation is a multistep process throughout which numerous genetic lesions are acquired and cooperate in altering the mechanisms that control self-renewal, cell growth, proliferation, survival, and differentiation during thymocyte development (Graux et al., 2006; Van Vlierberghe and Ferrando, 2012). The oncogenic transformation of T-cell precursors is driven by specific genetic abnormalities, including chromosomal translocations, deletions, duplications, amplifications or mutations of genes, which are either exclusively or most frequently affected in T-ALL, or oncogenes and tumor suppressor genes whose genetic lesions are related to a broader spectrum of human cancers (Table 1).

In this context, constitutive activation of NOTCH1 signaling is the most prominent oncogenic pathway in T-cell transformation. In addition, several mutually exclusive chromosomal rearrangements resulting in the ectopic

expression of a number of transcription factors are considered as driving oncogenes, delineating distinct molecular T-ALL subtypes (reviewed in (Meijerink, 2010) and (Van Vlierberghe and Ferrando, 2012)).

Table 1. Recurrent molecular cytogenetic abnormalities in T-ALL

Subgroup	Rearrangement	Gene(s)	Frequency (%)
TAL/LMO	t(1;14)(p32;q11) t(1;7)(p32;q34) 1p32 deletion	TAL1	4-15
	t(7;9)(q34;q32)	TAL2	1–2
	t(11;14)(p15;q11) t(7;11)(q34;p15)	LMO1	1–2
	t(11;14)(p13;q11) t(7;11)(q34;p13) 11p13 deletion	LMO2	6-3
	t(7;12)(q34;p12)	LMO3	< 1
TLX1	t(10;14)(q24;q11) t(7;10)(q34;q24)	TLX1	5-10
TLX3	t(5;14)(q35;q32)[a]	TLX3	5-20
HOXA	inv(7)(p15q34) t(7;7)(p15;q34)	HOXA	3
	t(10;11)(p13;q14)	PICALM-MLLT10	5-10
	t(11;19)(q23;p13)[b]	MLL-ENL	2–5
	9q34 deletion	SET-NUP214	3
MYB	t(6;7)(q23;q34)	MYB	3
MYC	t(8;14)(q24;q11)	MYC	1
Proliferative	inv(14)(q13q32) t(7;14)(q34;q13)	NKX2-1	5
	t(14;20)(q11;p11)	NKX2-2	1
Immature	del(5)(q14)/	MEF2C	10
	t(5;14)(q34;q32)	BCL11B-NKX2-5	
	t(11;14)(p11.2;q32)	BCL11B-SPI.1	

a a number of alternative TLX3 translocations have been described
b ENL is the most common MLL translocation partner in T-ALL.

Modified from Van Vlierberghe, 2012.

Specific chromosomal translocations result in the aberrant expression of transcription factor oncogenes. Primarily, these chromosomal rearrangements place certain transcription factors under the control of

T-cell receptor (*TCR*) gene-specific enhancers, resulting in their ectopic expression. These alterations are frequently caused by erroneous V(D)J recombination events during T-cell development, thus linking the expression of particular oncogenes to the developmental arrest at a specific stage of normal thymocyte development. These oncogenic transcription factors include *TAL1* and *TAL2*, *LMO1* and *LMO2*, *TLX1*, *TLX3*, *NKX2,* and *HOXA* (Table 1; Fig. 1) (Graux et al., 2006; Van Vlierberghe and Ferrando, 2012). Furthermore, a number of different chromosomal rearrangements, which result in the expression of fusion genes, for example *SIL-TAL1, MLL*-fusions, *PICALM-MLLT10* (alias *CALM-AF10)*, and *NUP214-ABL1*, have been identified (Van Vlierberghe and Ferrando, 2012). These fusion genes encode potentially oncogenic chimeric proteins that alter proliferation, differentiation and survival of developing T-cells (Aifantis et al., 2008).

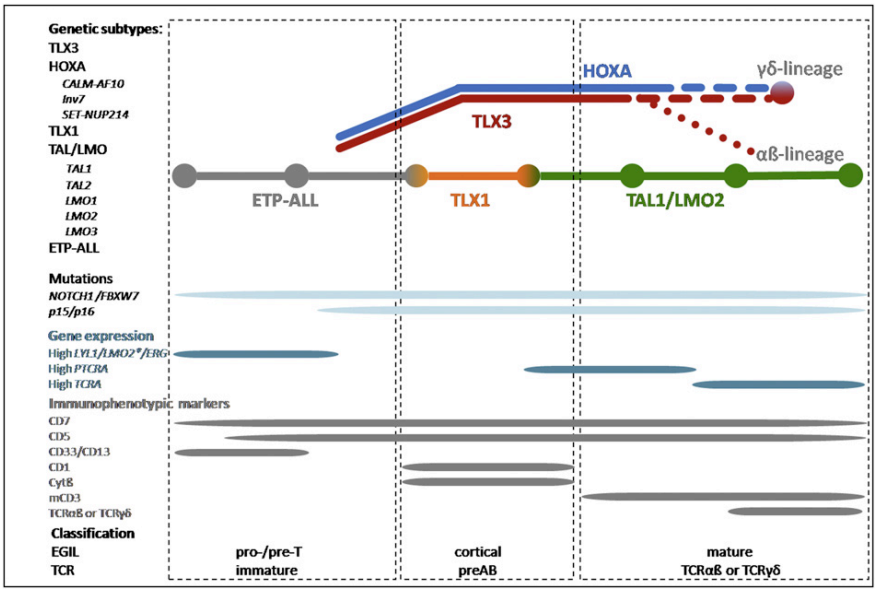

Figure 1. **T-ALL subtypes**. The HOXA, TLX3, TLX1, and TAL/LMO as well as the immature early T-cell phenotype (ETP) T-ALL subtypes are shown in relation to their arrest in a specific stage of T-cell development based on the European Group for the Immunological Characterization of Leukemias (EGIL) or TCR classification systems and the distribution of CDKN2A/B (p15/16) deletions and NOTCH1 pathway activating mutations (NOTCH1/FBXW7) is depicted. Modified from Meijerink, 2010.

Constitutive activation of NOTCH1 signaling by activating NOTCH1 and/or inactivating FBXW7 mutations, which provides stem cells or T-cell precursors with self-renewal capacity, is a hallmark of the disease (Tzoneva and Ferrando, 2012). Furthermore, cryptic deletions leading to the loss of the tumor suppressor gene, cyclin-dependent kinase inhibitor p16 (*CDKN2A*) are found in more than 70% of all T-ALL cases (De Keersmaecker et al., 2005; Graux et al., 2006; Van Vlierberghe and Ferrando, 2012). Therefore, NOTCH1 activation cooperates with an impairment of cell cycle control in T-cell transformation and constitutes the core of the oncogenic program in the pathogenesis of T-ALL (Van Vlierberghe and Ferrando, 2012).

NOTCH1 is a transmembrane receptor, which is activated upon ligand-induced progressive cleavage steps. The initial proteolytic cleavage of the NOTCH1 precursor protein yields an extracellular and a transmembrane (TM) subunit, which are held together by the heterodimerization (HD) domain and stabilized through three LIN-12/NOTCH1 repeats (LNRs). Ligand binding triggers a conformational change in the HD-LNR complex, exposing the S2 cleavage site in the extracellular domain to ADAM-like metalloproteases, which is a prerequisite for subsequent cleavage by the γ-secretase complex at the S3 site within the TM domain. This final step releases intracellular NOTCH1 (ICN1) from the membrane and allows its translocation to the nucleus, where it converts the CSL repressor into an activator to drive target gene expression (Aster et al., 2008).

In T-ALL, activating NOTCH1 mutations cluster in exons 26-27 and 34, encoding the HD and PEST domains, respectively (Weng et al., 2004). While PEST domain mutations result in a loss of the domain and increased ICN1 levels due to its impaired proteasomal degradation, HD mutations induce ligand-independent activation of NOTCH1. Most HD mutations, comprising single amino acid substitutions and small in-frame deletions and insertions (class 1 mutations), destabilize the HD-LNR interaction and reduce heterodimer stability. In rare cases, the insertion of extra amino acids between the distal part of the HD and the S2 cleavage

site (class 2 mutations) displace the S2 away from the protective effects of the LNR-HD complex and expose it to cleavage by ADAM-like metalloproteases (Malecki et al., 2006; Weng et al., 2004). In addition, a new class of NOTCH1 mutations in exon 28 encoding the extracellular juxtamembrane domain, termed juxtamembrane expansion mutations (JEMs), which distance the LNR-HD complex from the membrane and allow ligand-independent proteolytic processing of S2, has been identified (Sulis et al., 2008).

Furthermore, recurrent PI3K/AKT pathway aberrations have been found in about 15-20% of pediatric T-ALLs, among which *PTEN* mutations or deletions have been reported in 8-20% and 10% of the cases, respectively (Bandapalli et al., 2013; Gutierrez et al., 2009; Larson Gedman et al., 2009; Zuurbier et al., 2012). Interestingly, the lack of PTEN expression has been associated with a failure to block NOTCH1 signaling by γ-secretase inhibitors (Palomero et al., 2008), intertwining these two key signaling pathways in the development of treatment resistance in T-ALL.

Additionally, a number of recurrent genetic alterations, shared by all subgroups or associated with one or the other, which affect cellular processes such as cell cycle control, proliferation, differentiation, chromatin remodeling, and signal transduction pathways have been identified (Table 2) (Graux et al., 2006; Van Vlierberghe and Ferrando, 2012). For example, in contrast to *NOTCH1* mutations and *CDKN2A* deletions, which occur across all T-ALL subtypes, T-ALL with *TLX1* or *TLX3* rearrangements harbor specific cooperating mutations (Van Vlierberghe and Ferrando, 2012), including the *NUP214-ABL1* fusion (Graux et al., 2009) and mutations in *PTPN2* (Kleppe et al., 2010), *WT1* (Renneville et al., 2010; Tosello et al., 2009), and *PHF6* (Van Vlierberghe et al., 2010).

Table 2. Recurrent genetic abnormalities in T-cell acute lymphoblastic leukemia

	Genetic alteration	Gene(s)	Frequency (%)
Cell cycle defects	9p21 deletion/ hypermethylation	CDKN2A/2B	70
	t(7;12)(q34;p13) t(12;14)(p13;q11)	CCND2	<1
	12p deletion	CDKN1B	12
	13q14 deletion	RB1	4
NOTCH pathway	t(7;9)(q34;q34)	NOTCH1	<1
	activating mutation	NOTCH1	>60
	inactivating mutation	FBXW7	8–30
Signal transduction	10q23.3 deletion	PTEN	10
	inactivating mutation	PTEN	8-20
	activating mutation	AKT	2
		PI3K	7
	episomal 9q34 amplification	NUP214-ABL1	4
	t(9;14)(q34;q32)	EML1-ABL1	<1
	t(9;12)(q34;p13)	ETV6-ABL1	<1
	t(9;22)(q34;q11)	BCR-ABL1	<1
	t(9;12)(p24;p13)	ETV6-JAK2	<1
	activating mutation	FLT3	2-4
		N/K-RAS	4-10
		JAK1	4-18
		JAK3	5
		IL7R	10
	17q11.2 deletion/mutation	NF1	3
	18p11 deletion	PTPN2	6
Chromatin remodeling	inactivating mutation/deletion	EZH2	10-15
		SUZ12	10
		EED	10
		PHF6	20-40
Cell growth/tumor suppressors	inactivating mutation	ETV6	13
		WT1	13
		BCL11B	10
		RUNX1	10-20
	duplication	MYB	8-15
	t(8;14)(q24;q11)	MYC	1

Modified from Van Vlierberghe, 2012.

1.2 Gene expression signatures in T-ALL

During the last decade, gene expression profiling and whole genome sequencing provided a more comprehensive view of the pathways and genetic alterations involved in pathogenesis of T-ALL. Microarray-based expression studies significantly contributed to the identification and better understanding of the altered transcriptional programs in T-ALL and revealed at least four different well-defined T-ALL molecular subgroups with unique gene expression signatures reflecting distinct stages of thymocyte development (Ferrando et al., 2002; Soulier et al., 2005).

These expression signatures include the *TAL*/*LMO*, *TLX1*, *TLX3*, and *HOXA* clusters, and pointed to the existence of an additional immature T-ALL subgroup, first identified as “immature cluster” by Soulier *et al*. and further characterized a few years later by Homminga and colleagues (Homminga et al., 2011; Soulier et al., 2005). This cluster is enriched for cases with immunophenotypically immature blast cells expressing CD34 and frequently coexpressing myeloid markers (Zuurbier et al., 2014) and overlapped with the previously identified LYL1 subtype delineated by Ferrando *et al.* and the early T-cell precursor (ETP) subset described by Coustan-Smith *et al.* (Coustan-Smith et al., 2009; Ferrando et al., 2002). In addition, a new group, distinct from the established genetic subgroups and denoted as “proliferative cluster” due to its enrichment for genes associated with cell cycle and spindle assembly, was identified. Further analysis of the new immature and proliferative T-ALL subtypes revealed overexpression of *MEF2C* and *NKX2-1*, respectively, as driving oncogenes (Fig. 2) (Homminga et al., 2011).

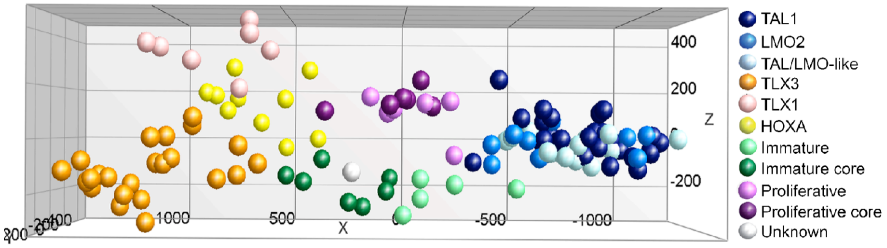

Figure 2. Principal component analysis of pediatric T-ALL patients based on the top 100 most significant differentially expressed probe-sets among the major T-ALL subtypes (Homminga et al., 2011).

MEF2C, a member of the MADS-box transcription factor family, is a key regulator of lymphoid development and is expressed in early stages (pre-DN1 (CD4/CD8 double-negative) and DN1) of normal thymocyte development and its expression decreases in DN2 cells. It has also been found highly expressed in *MLL*-rearranged myeloid leukemia and has been identified as a HOXA9 target gene in *MLL-AF9* transgenic mice (Krivtsov et al., 2006). In T-ALL, *MEF2C* is aberrantly expressed due to 5q14 deletions or upregulated via genetic rearrangements affecting *SPI1* encoding PU.1 or *NKX2-5* and *NCOA2,* and its ectopic expression seems to drive the arrest of developing T-lymphocytes at an immature stage (Homminga et al., 2011).

NKX2-1 belongs to the NK-like (NKL) homeobox family of transcription factors with highly cell type-specific important functions in cell fate and embryogenesis (Homminga et al., 2012). Although *NKX2-1* and *NKX2-2* are not expressed during normal T-cell development they are highly expressed in a subset of T-ALL and in about 30% of the cases their expression is driven by their juxtaposition to *TCR* promotor/enhancer elements (Homminga et al., 2011). These cases share similar expression signatures, characterized by a high expression of genes involved in proliferation, with T-ALL patients overexpressing *TLX1*, another member of the NKL homeobox family. Some of the latter cases also expressed *NKX2-1*, but albeit at lower levels compared with *NKX2-1*-rearranged

T-ALL. In the majority of these cases the lymphoblasts show an arrest at the early cortical stage of T-cell development (Homminga et al., 2011).

Both TLX1 and TLX3 belong to the homeobox family of transcription factors, which are essential for embryonic development, and their aberrant expression defines a large subgroup of T-ALL with a cortical thymic developmental arrest (Meijerink, 2010). Dadi *et al.* showed that this maturation arrest is due to binding of TLX1/TLX3 to ETS1, leading to repression of TCRA enhanceosome activity and blocked *TCR-Jα* rearrangement (Dadi et al., 2012). TLX1 and TLX3 expressing leukemias share a similar mechanism of leukemic transformation and similarities in their gene expression signatures. The oncogenic role of TLX1 in T-cell transformation has been well-established using TLX1 transgenic mouse models (De Keersmaecker et al., 2010) and, more recently, integrative genomic approaches unraveled the binding profile of TLX1 in human T-ALL, confirming that ETS1 and RUNX1 are critical co-factors in TLX1-driven transcriptional repression (Durinck et al., 2015).

The homeobox A (HOXA) gene cluster is one of the four major homeobox gene clusters involved in embryogenesis, stem cell renewal, cell fate and differentiation in hematopoiesis and thymocyte development. The T-ALL subtype characterized by a *HOXA* signature shows a differentiation arrest at the DN1 to DN2 stage, similar to *TLX1* expressing cases (Soulier et al., 2005). Aberrant expression of *HOXA* genes is not only triggered by the *TRB-HOXA* fusion but also MLL as well as the PICALM-MLLT10 and SET-NUP214 fusion proteins (Van Vlierberghe et al., 2008). Thus, T-ALLs with different molecular cytogenetic defects may share highly similar expression profiles.

Leukemic arrest at the late cortical stage of normal thymocyte development (DP, CD4/CD8 double-positive cells) is characterized by the expression of TAL1/LMO. LIM domain proteins (LMO) were first described in T-ALL cases harboring the t(11;14)(p15;q11) and t(11;14)(p13;q11) translocations involving the *LMO1* and *LMO2* genes, respectively (McGuire et al., 1989; Royer-Pokora et al., 1989). Although *LMO1* and

LMO2 activating rearrangements or deletions occur only in a minor proportion of cases, up to 45% of T-ALL display aberrant *LMO2* expression, suggesting that other mechanisms lead to its upregulation (Van Vlierberghe and Ferrando, 2012). TAL1 is a member of the basic helix-loop-helix (bHLH) family of transcription factors implicated in hematopoiesis and involved in chromosomal translocations in 5-15% of T-ALL cases (Meijerink, 2010). However, a substantial proportion of T-ALLs overexpress *TAL1* but lack a rearrangement of the *TAL1* locus. Intriguingly, a recent study revealed that mutations of the *TAL1* enhancer create a super-enhancer upstream of the *TAL1* oncogene activating its expression (Mansour et al., 2014). Since *TAL1* and *LMO2* may be overexpressed in the same samples, according to Ferrando *et al*. these two genes defines a unique T ALL subtype (Ferrando et al., 2002).

1.3. Prognostic relevance of genetic alterations in T-ALL

Unlike B-cell precursor ALL, which can be divided into meaningful genetically distinct prognostic subgroups (Hunger and Mullighan, 2015; Inaba et al., 2013), such entities are not readily apparent in T-ALL, and the predictive value of specific genetic lesions or combinations thereof is still controversially discussed. For example, the prognostic impact of *TLX3* rearrangements appears to be dependent on the treatment protocol and may be codependent on associated genetic lesions such as *NUP214-ABL1* (Attarbaschi et al., 2010).

Several studies have addressed the impact of *NOTCH1* and *FBXW7* mutations, however their prognostic value remains as well unclear. While in some studies these mutations had a poor or no impact on overall survival (Clappier et al., 2010; Zhu et al., 2006; Zuurbier et al., 2010), others found a positive correlation with long-term outcome (Breit et al., 2006; Fogelstrand et al., 2014; Gao et al., 2014; Mansur et al., 2012). Moreover, in the context of the ALL-BFM 2000 study it has been shown that *PTEN* mutations are generally associated with therapy resistance and

a poor prognosis. However, patients with a combination of *PTEN* inactivation and NOTCH1 pathway activating mutations showed a higher treatment sensitivity and a more favorable outcome than those with *PTEN* mutations alone (Bandapalli et al., 2013). The latter observation is contradicted by recent data from the MRC UKALL2003 trial, in which, though, *PTEN* mutations did as well not change the favorable outcome of patients with *NOTCH1/FBXW7* mutations, the presence of *PTEN* mutations alone had also no impact on therapy response or long-term survival (Jenkinson et al., 2015).

Along this line, different studies have reported either a favorable (Cave et al., 2004) or unfavorable outcome (Mansur et al., 2009) trend for *SIL-TAL1* positive patients and a recent study showed basically no difference in the overall survival for *SIL-TAL* positive and negative patients (D'Angio et al., 2015). Furthermore, it has been suggested that T-ALL patients with *TAL1* gene rearrangements in general tend to have a more favorable outcome (Kikuchi et al., 1993; van Grotel et al., 2006). In contrast, in a stratified analysis of pediatric T-ALL patients *LMO2* rearrangements predicted a poor outcome, at least with borderline significance (Van Vlierberghe et al., 2006), which however, contradicted a previous study (Ferrando and Look, 2003).

Additionally, it has been shown that the early immature/ETP subtype of T-ALL determined by immunophenotyping or gene expression profiling (Coustan-Smith et al., 2009; Inukai et al., 2012; Ma et al., 2012; Neumann et al., 2012) as well as patients with an absence of biallelic *TCRG* deletions have a very poor prognosis (Gutierrez et al., 2010). This observation was recently contradicted by a study of Zuurbier and co-workers, in which they found that in their cohort of immature/ETP-ALL patients treated on the COALL-97 protocol the outcome and sensitivity towards conventional chemotherapy was not inferior compared to other T-ALL patients (Zuurbier et al., 2014).

Hence, due to the heterogeneity of the disease in terms of genetic alterations, therapy response and outcome, further molecular genetic

insights into the pathobiology of T-ALL are required to determine the prognostic significance of single genetic lesions or combinations thereof. In addition, the delineation of novel molecular targets for therapeutic intervention is crucial for the improvement of T-ALL treatment and outcome.

1.4 Treatment strategies in ALL

Despite the fact that due to therapy intensification the prognosis of ALL patients has dramatically improved reaching over 80% of 5 year event free survival rates, patients with T-ALL experience a higher frequency of treatment failure and early relapse with a very poor outcome (Pui and Evans, 2006; Roti and Stegmaier, 2014).

Due to the heterogeneity of the disease, tailored treatment decisions are mainly based on the phenotype, genotype and risk determined for each patient. The classification into the categories low/standard, intermediate/medium risk and high-risk patients is based on several factors, including early response to therapy, genetic characteristics of the leukemic cells and clinical and pharmacogenetic features of the host. In ALL, initial response to therapy is an independent prognostic factor for long-term survival. Generally, therapy response is assessed by the peripheral blast cell count after a 7-day pre-phase treatment with glucocorticoids or by the evaluation of the minimal residual disease (MRD) load at different time-points post-induction therapy by the polymerase chain reaction (PCR)-based detection of leukemic clone-specific immunoglobulin and T-cell receptor gene rearrangements or by flow cytometry. In contemporary ALL-BFM clinical trails low or no PCR-based MRD load at day 33 (end of induction phase) and at week 12 (just before consolidation treatment) serves to stratify patients into the low/standard risk group, while patients with high MRD levels at week 12 are treated in the high-risk arm (Conter et al., 2010; Flohr et al., 2008).

The specific treatment approaches differ between the various pediatric study groups but consistently emphasize remission-induction therapy

followed by intensification (or consolidation) therapy and continuation treatment to eliminate residual leukemia (Inaba et al., 2013). The goal of remission-induction therapy is to eradicate more than 99% of the initial burden of leukemia cells and to restore normal hematopoiesis. This treatment phase almost always includes the administration of a glucocorticoid (GC) – prednisone (PDN) or prednisolone or dexamethasone (DEX) – vincristine (VCR), and asparaginase (ASP) with or without anthracycline in standard-risk cases. Patients with intermediate or high-risk disease receive four or more drugs. Therapy directed at the central nervous system or extended triple intrathecal therapy, starts early in the clinical course and, depending on the patients' risk of relapse, will determine the schedule and the intensity of systemic treatment. Intensification (consolidation) therapy is given after remission-induction treatment and aims to eradicate residual leukemic cells. High-dose methotrexate (MTX) with mercaptopurine is often given, as are frequent pulses of VCR and GC, uninterrupted ASP for 20–30 weeks, and reinduction therapy with drugs similar to those used during remission-induction therapy. Continuation therapy typically lasts 2 years or longer and comprises mainly daily mercaptopurine and weekly MTX with or without pulses of VCR and DEX.

Glucocorticoids (GCs) are small lipophilic compounds derived from the natural cortisol hormone. Synthetic GCs such DEX or PDN are used as immunosuppressive and anti-leukemic drugs and, because of their capacity to induce cell cycle arrest and apoptosis in lymphoid progenitor cells, play a fundamental role in the treatment of all lymphoid malignancies. However, GC resistance is strongly associated with treatment failure, relapse and a poor prognosis (Inaba and Pui, 2010). The BFM group classifies good-prednisone responders (GPR) and poor-prednisone responders (PPR) and in the ALL-BFM-90 trial showed that 10% of all patients were PPR with 34% of them having a 6-year event free survival (EFS) compared to 82% for those with a GPR (Reiter et al., 1994; Schrappe et al., 2000). Even for patients with cytogenetic or clinical features generally associated with a favorable outcome but presenting a

PPR, the outcome was poor, turning prednisone response into a powerful tool to assess early therapy response and also in the current ALL-BFM 2009 clinical trail poor responders are allocated to the high-risk treatment arm.

1.5 Innovative approaches to target T-ALL

Most of the drugs used in contemporary treatment protocols were developed before 1970; however, their dosages, schedules and combinations have been optimized. Nowadays, two of the priorities and challenges are to reduce the toxicity of the current chemotherapy regimens, which results in an increased morbidity and mortality of the patients, without increasing relapse rates, and to develop new selective drugs and/or drug combinations effective against relapsed T-ALL, which is generally associated with acquired chemotherapy resistance. These objectives require a better understanding of the molecular pathways underlying the pathogenesis of this disease as well as a comprehensive approach for assessing the specific pharmacogenetics of the host, which can critically influence the treatment efficacy and toxicity (Pui and Evans, 2006).

Recent genome-wide studies, including gene expression analysis and whole genome sequencing, have identified and characterized several key pathways, for example, the NOTCH1, BRD4/MYC, CDK4/6 or the PI3K pathway, involved in the pathogenesis of T-ALL, and have uncovered a number of potential therapeutic targets (reviewed in (Roti and Stegmaier, 2014)).

Since constitutive activation of NOTCH1 signaling is one of the most important oncogenic pathways in T-cell transformation (Malecki et al., 2006; Weng et al., 2004), NOTCH1 is considered as a promising target for drug development. NOTCH1 is activated upon ligand-induced progressive cleavage steps and the final release of intracellular NOTCH1 (ICN1) and its subsequent translocation to the nucleus, where it evokes its functions in transcriptional regulation, relies on the γ-secretase complex activity

(reviewed in (Tzoneva and Ferrando, 2012)). Modulation of NOTCH signaling has reached clinical trials and currently there are two main types of approaches, namely, inhibition of γ-secretase activity and the use of antibodies against the NOTCH receptors or their ligands. γ-secretase inhibitors (GSI) were originally identified as inhibitors of amyloid β in Alzheimer disease and have already been tested in preclinical and clinical studies (reviewed in (Roti and Stegmaier, 2014)).

However, in T-ALL, in a phase I clinical trial treatment with a GSI showed limited antitumor activity and its continuous administration was associated with severe gastro-intestinal toxicity (Clinical Trial Identifier: NCT00100152) (Deangelo et al., 2006). More recently, it has been shown that GSI restores GC sensitivity in T-ALL cell lines and primary leukemic blasts and that GC protects mice from GSI-induced gut toxicity (De Keersmaecker et al., 2008; Real et al., 2009), providing a rationale to incorporate a combination of GC and GSI in future clinical trials. An alternative approach to target NOTCH is based on the development of specific antibodies targeting components of the NOTCH receptors or their ligands; e.g. monoclonal antibodies against the NOTCH1-DLL4 interaction, decoy ligands, decoy receptor molecules or selective antibodies against the negative regulatory region of NOTCH1. The effectiveness of this kind of inhibitors has also been tested and they lead to a growth inhibition of T-ALL cell lines *in vitro* and in xenograft models (reviewed in (Roti and Stegmaier, 2014)). The discovery of aberrant NOTCH signaling in an increasing number of diseases and the better understanding of the NOTCH pathway will foster the development of more specific compounds and the initiation of early phase clinical trials (reviewed in (Andersson and Lendahl, 2014)).

NOTCH1 is also known to down-regulate the tumor suppressor *PTEN* (mediated by MYC and HES1), which in turn inhibits AKT. The PI3K/AKT pathway drives multiple cellular processes including cell growth, proliferation and survival. Notably, GSI-resistant T-ALL cell lines showed mutational loss of PTEN, which is also observed in about 15% of T-ALL

patients (Palomero et al., 2008). Therefore, inhibitors of the PI3K/AKT pathway (e.g. Pan-PI3K, mTOR, dual TORC1/TORC2 inhibitors), which are already in development, may be first-rate candidates for future therapeutic approaches.

Furthermore, also *MYC* is a direct target of NOTCH1 and its expression activates the mTOR pathway in a subset of T-ALL (Chan et al., 2007; Palomero et al., 2006b). *In vitro* data and a mouse model of T-ALL have shown synergistic effects when applying GSI and Rapamycin, an mTOR inhibitor (Chan et al., 2007; Cullion et al., 2009). The relevance of using drug combinations is supported by another independent study, in which Shepherd *et al.* showed that inhibition of the PI3K/mTOR pathway alone led to an upregulation of the NOTCH1-MYC pathway, whereas simultaneously targeting both pathways enhanced cell cycle arrest and cell death (Shepherd et al., 2013).

Remarkably, in a T-ALL mouse model Dail and colleagues demonstrated that targeting PI3K signaling alone resulted in the development of drug resistance (Dail et al., 2014). In the refractory T-ALLs the NOTCH1 pathway was downregulated, indicating a loss of NOTCH1 addiction, and these leukemias exhibited a cross-resistance to γ-secretase inhibitors. These findings raise the question whether combinatorial drug regimens, at least under certain circumstances, might undermine the efficacy of some inhibitors by facilitating selection of drug resistant clones (Dail et al., 2014).

NOTCH1 also positively regulates the NF-kB pathway (Vilimas et al., 2007) and in T-ALL cell lines inhibition of NF-kB with Bortezomib results in apoptotic cell death and its combination with GSI has synergistic effects (Koyama et al., 2014).

In addition, the application of BET bromodomain inhibitors has recently emerged as potential therapeutic option in leukemia. For example, JQ1 binds selectively to the acetyl lysine recognition pockets of BET bromodomain proteins, such BRD4, and displaces them from chromatin leading to the repression of BRD4 transcriptional targets, like *MYC* or

MYCN. Treatment with JQ1 showed a dose-dependent decrease in cell growth accompanied by a reduction of MYC protein levels and induced cell cycle arrest and apoptosis in T-ALL cell lines and primary cells, including treatment-refractory pediatric T-ALL (Knoechel et al., 2014; Roderick et al., 2014). These data indicate that also bromodomain inhibitors, several of which have been shown to be effective in other diseases and are already in clinical trials, may also be useful for the treatment of T-ALL (Roti and Stegmaier, 2014).

Moreover, it has been shown that overexpression of cyclin D is a common feature of T-ALL and that NOTCH1 signaling is also involved in its regulation. D-type cyclins associate and activate the cyclin-dependent kinases CDK4 and CDK6, thus contributing to cell cycle progression and leukemogenesis (Joshi et al., 2008; Li et al., 2008). CDK4/CDK6 inhibitors prevent retinoblastoma (RB) protein phosphorylation in early G1 phase, thereby preventing CDK-mediated G1-S transition and cell cycle entry. Therefore, also the inhibition of D-type cyclin-CDK complexes may reduce tumor burden, and indeed, in animal models of T-ALL targeting cyclin D-CDK4/6 with small molecules inhibits cell cycle entry and disease progression (Aleem and Arceci, 2015; Sawai et al., 2012).

2. Cell cycle regulation

The collective results derived from a multitude of studies in various eukaryotes have demonstrated that progression through the cell cycle is a highly conserved and tightly controlled biological process, which is regulated by cyclins and their associated cyclin-dependent kinases (CDKs). Cell cycle progression is driven by changes in the substrate specificity and subcellular localization of the CDKs, which are modulated by the cyclins, CDK-activating and CDK-inhibiting kinases, and the cyclin-dependent kinase inhibitors (CDKIs). Regulation of the cell cycle is critical for normal development and the complexity of its regulation is also reflected in the plethora of different alterations leading to aberrant cell proliferation and tumorigenesis.

2.1 Cyclin-dependent kinase activation

The balance between CDK activation and inactivation determines whether cells proceed through G1 into S phase and from G2 to mitosis (M phase), via regulatory mechanisms that are conserved in more complex eukaryotes. In mammalian cells at least four different CDKs (CDK1, CDK2, CDK4, and CDK6) and four cyclin families (cyclin D1, D2, D3; cyclin E1, E2; cyclin A1, A2; cyclin B1, B2, B3) are known to be involved in cell cycle regulation (Fig. 3). CDKs are serine/threonine kinases present in constant excess throughout the normal cell cycle and their regulation is primarily post-translational (reviewed in (Malumbres, 2014)). CDK activation requires an association with a cyclin regulatory subunit and phosphorylation (Fig. 3B). The oscillation in their activity depends on corresponding oscillations of their regulatory subunits: the cyclins. The different cyclin types are expressed and degraded at different stages of the cell cycle (Fig. 3A), resulting in the formation of a series of cyclin-CDK complexes, each of them promoting the activation of the next in the sequence, thus ensuring that the cell cycle progresses in an ordered fashion (reviewed in (Hochegger et al., 2008)).

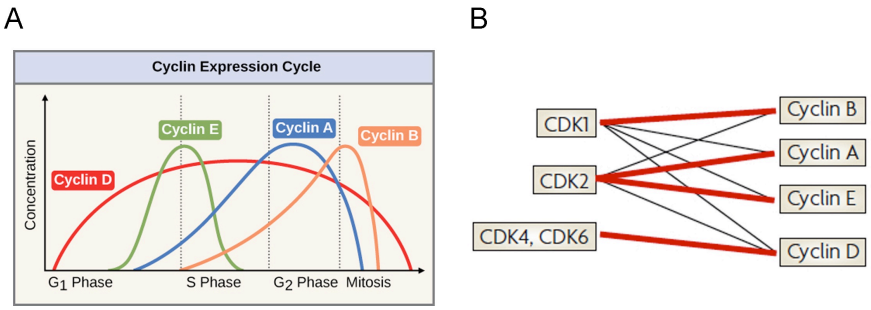

Figure 3. Cell cycle regulation by cyclins and CDKs. (A) D-type cyclins regulate events in early G1, cyclin E triggers S phase entry, cyclin A regulates the completion of S phase, and cyclin B is responsible for mitosis. (B) CDK1 and CDK2 show promiscuity in their choice of cyclin partners and can bind to cyclins A, B, D, and E, whereas CDK4 and CDK6 only partner D-type cyclins. Thick lines represent the preferred pairing for each kinase. Modified from Hochegger, 2008.

Upon mitogenic signals, these cyclin-CDK complexes are required to promote cell cycle entrance and progression from quiescence to G1 phase and the transition from G1 to S phase. During G1, the phase in which cells prepare to initiate DNA synthesis, D-type cyclins preferentially bind and activate CDK4 and CDK6. Activation of these complexes leads to phosphorylation and partial inactivation of the pocket proteins – RB (retinoblastoma) and the RB-like proteins RBL1 (p107) and RBL2 (p130) – allowing for the expression of E-type cyclins, which bind and activate CDK2 (Malumbres, 2014). The cyclin E-CDK2 complexes further hyperphosphorylate these pocket proteins, leading to their complete inactivation. Finally, A-type cyclins activate CDK2 at the late stages of DNA replication (G2 phase) to drive the transition from S to M phase, followed by the activation of CDK1, at the end of interphase to facilitate the initiation of mitosis. A-type cyclins are then degraded, supporting the formation of the cyclin B-CDK1 complexes responsible for driving cells through mitosis (reviewed in (Hochegger et al., 2008)).

The basic concept of this model that each phase of the cell cycle is driven by specific CDKs has been assessed by genetic studies, in which the knockout of CDK loci in the mouse germline showed that embryos develop normally until mid gestation in the absence of all interphase CDKs (CDK2, CDK4, and CDK6). In contrast, loss of each of these CDKs

alone results in developmental defects in highly specialized cell types. For example, CDK4 is essential for the proliferation of pancreatic β-cells, loss of CDK6 causes minor defects in cells of the erythroid lineage, and while mice without CDK2 do not display any detectable defects in mitotic cells it is essential for meiotic division of both male and female germ cells. Only the elimination of the mitotic kinase CDK1 causes cell cycle arrest, preventing embryos from developing beyond the two-cell stage (reviewed in (Malumbres and Barbacid, 2009)).

2.2 Cyclin-dependent kinase inhibition

Apart from the fluctuation in the expression of their regulatory subunits, i.e. the cyclins, the CDKs remain constant throughout the cell cycle and their activities are regulated by specific inhibitors, the CDKIs (Fig. 4). These proteins counteract the activity of the CDK complexes by directly blocking their activation or by barring their access to their substrates or ATP. Based on their structures and functional properties, CDKIs are divided into two families, named because of their ability to inhibit the activities of the different CDKs: the INK4 (inhibitors of CDK4) and the CIP/KIP family (reviewed in (Malumbres, 2014)).

The INK4 family comprises p16 (INK4a, encoded by *CDKN2A*), p15 (INK4b, *CDKN2B*), p18 (INK4c, *CDKN2C*), and p19 (INK4d, *CDKN2D*) and specifically binds to and inhibits the catalytic subunits of CDK4 and CDK6. These proteins are characterized by the possession of a common structural ankyrin-like repeat domain and crystallography and site-directed mutagenesis studies suggested that the third ankyrin repeat is crucial for the interaction of the INK4 proteins with CDK4 and CDK6 (Pavletich, 1999).

The other family is the so-called CIP/KIP family, comprising p21Cip1 (encoded by *CDKN1A*), p27kip1 (*CDKN1B*), and p57Kip2 (*CDKN1C*) (Harper et al., 1993; Lee et al., 1995; Polyak et al., 1994). These proteins, which interact with a broader range of substrates, such as cyclins E-, A-, and B-dependent kinases, control more features of the cell cycle (Sherr

and Roberts, 1999). The CIP/KIP family members share a conserved N-terminal domain, which mediates their binding to cyclins and CDKs, but diverge in the remainder of their sequence, indicating that each of these proteins has distinct regulatory functions. In this regard, p57Kip2 plays an important role in the regulation of the cell cycle during embryonic development and has a tissue-restricted expression pattern during embryogenesis and in the adult (Pateras et al., 2009). In contrast, p21Cip1 and p27kip1 are ubiquitously expressed. While p21Cip1 is an important transcriptional target of TP53 and can induce cell cycle arrest in G1 or G2 upon DNA damage, p27kip1 expression is generally higher during quiescence and in mitogen-starved cells and is rapidly degraded as cells enter the cell cycle (Besson et al., 2006).

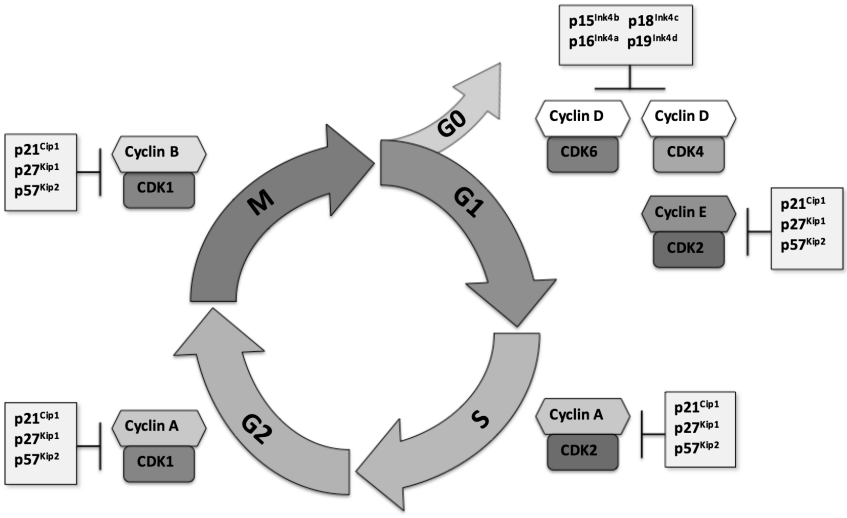

Figure 4. Cell cycle regulation. Cell cycle is tightly controlled by cyclin-dependent kinases (CDKs), which are regulated by the cyclins through phosphorylation and by the CDK inhibitors. Taken from Slingerland and Pagano, 2000.

3. *CDKN1B*-p27kip1

As outlined in the previous chapter „Cell cycle regulation“, p27kip1 is a member of the CIP/KIP family of CDK inhibitors and plays an important role in coordinating cell cycle control. This protein was first described as an inhibitor of cyclin-CDK complexes in cells arrested upon TGFB1 induction, contact inhibition or lovastatin treatment (Toyoshima and Hunter, 1994) and its encoding gene, *CDKN1B* located on chromosome 12p13, was cloned in 1994 (Polyak et al., 1994). Two years later, the crystal structure of the p27kip1-cyclin A-CDK2 complex was resolved, delineating the p27kip1 regions responsible for its binding to cyclin A and to CDK2 (Russo et al., 1996). These studies also revealed the high amino acid homology between members of the CIP/KIP family – a 60-amino-acid segment, 44% identical to p21Cip1 and 47% to p57Kip2 – responsible for the recognition of and its inhibitory effect on the CDKs, and the separated binding sites for the cyclin and CDK subunits (Fig. 5).

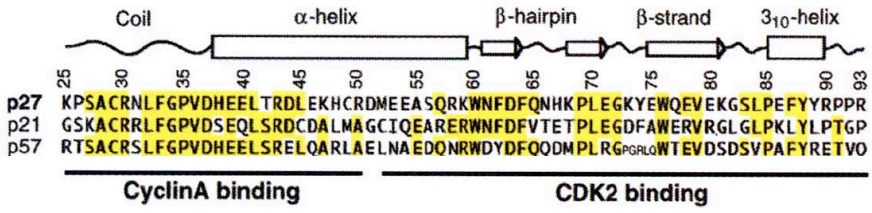

Figure 5. Conserved domains of the CIP/KIP family. Sequence of p27kip1 inhibitory domain showing its secondary structure elements and the homology with the corresponding domains of the p21Cip1 and p57Kip2 CIP/KIP family members. Residues identical in two or more family members are highlighted in yellow. Adapted from Russo, 1996.

3.1. Functions of p27kip1

The CIP/KIP proteins play a central role in cell cycle regulation; however, they appear to have more functions than just cell cycle regulatory ones. Several studies suggest that not only p21Cip1 and p57kip2 but also p27kip1 is involved in the regulation of other cellular processes, including transcription, apoptosis, and migration, which may be oncogenic under certain circumstances (reviewed in (Starostina and Kipreos, 2012)).

3.1.1 Role of p27kip1 in cell cycle regulation

The cell cycle may be controlled by two major routes: either by mitogenic signals promoting proliferation or by antimitogenic signals leading to cell cycle exit and p27kip1 serves as mediator of these extracellular mitotic and antimitotic signals (Fig. 6). p27kip1 is expressed at high levels during quiescence but is downregulated upon mitogenic stimulation, facilitating the progression through G1 and entering of the S phase.

Nuclear p27kip1 was first described to inhibit the kinase activity of cyclin E-CDK2 complexes in response to TGFB1 signaling (Polyak et al., 1994). However, upon mitogenic signals, which activate D-type cyclins, p27kip1 is phosphorylated by cyclin E-CDK2 and targeted by the nuclear export protein CRM1 (Connor et al., 2003). In the cytoplasm, p27kip1 promotes the assembly, stabilization and nuclear import of cyclin D-CDK4/6 complexes (Larrea et al., 2008). Once in the nucleus, these cyclin D-CDK complexes allow hyperphosphorylation of the phospho-protein RB, causing its inactivation, thereby releasing the transcription factor E2F and allowing the transcription of genes required for S phase induction (Sherr and Roberts, 1999). Collectively, p27kip1 links proliferative and antiproliferative signals (Fig. 6), and its shuttling between cyclin E-CDK2 and cyclin D-CDK4/6 complexes facilitates to establish the balance between proliferation (when associated with CDK4) and cell cycle arrest (when associated with CDK2) (reviewed in (Borriello et al., 2011)).

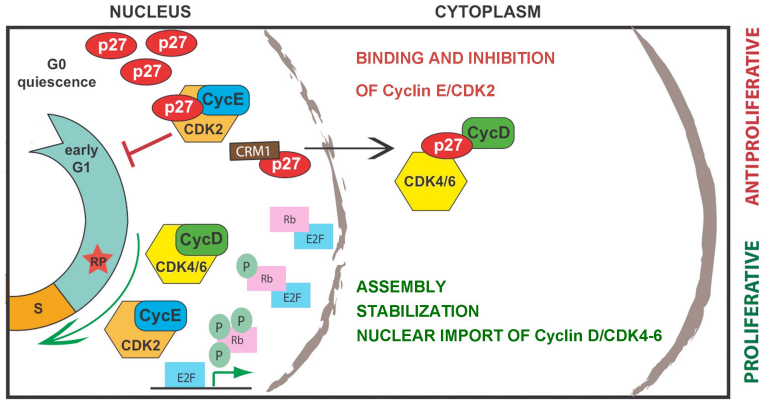

Figure 6. Cell cycle regulatory functions of p27kip1.

3.1.2 Transcriptional regulatory functions of p27kip1

One of the first evidences suggesting a function of p27kip1 beyond cell cycle control was its implication in the regulation of the human telomerase reverse transcriptase (h*TERT*) gene. Overexpression of p27kip1 in human malignant glioma cells suppressed telomerase activity by interfering with the binding of the positive regulators MYC and SP1 to the h*TERT* core promoter, thereby hindering (h*TERT* transcriptional activation (Kanzawa et al., 2003).

More recently, Pippa and colleagues demonstrated that p27kip1 can behave as transcriptional regulator by its association with the p130/E2F4 repressor complexes, silencing genes involved in important cellular functions, such as processing and splicing of RNA, mitochondrial organization and respiration, translation and cell cycle (Pippa et al., 2012). When p27kip1 is located on the promoters of specific genes it plays a key role in controlling the timing of gene transcription in G1 by recruiting and regulating specific cyclin D-CDK complexes required for the phosphorylation of p130 in mid G1 and subsequent progression through the cell cycle (Orlando et al., 2015).

In addition, in a breast cancer cell line model, Jeon and colleagues demonstrated once more the negative transcriptional regulatory function of p27kip1. In this case p27kip1 modulates the association of estrogen receptor α (ERα) with cyclin D1 and BRCA1 by driving cyclin D1 from the ERα transcriptional machinery and recruiting BRCA1, which results in a block of ERα transcription (Jeon et al., 2012).

3.1.3 p27kip1 in survival and apoptosis

The role of p27kip1 in survival and apoptosis remains controversially discussed and appears to be highly dependent on the experimental model system. While some studies reported a proapoptotic effect of p27kip1, others showed how the induction of p27kip1 could prevent apoptosis (Besson et al., 2008).

Based on the hypothesis that the ability of the CDKIs to prevent apoptosis may occur via their negative regulation of the CDKs, it has been suggested that overexpression of the CIP/KIP family in endothelial and breast cancer cell lines results in a caspase-mediated cleavage of p21Cip1 and p27kip1, thereby up-regulating CDK2 activity and enhancing the apoptotic program (Levkau et al., 1998). Along the same line, overexpression of p27kip1 decreased CDK2 and cyclin B-CDK1 activity, induced cell cycle arrest and promoted apoptosis in different cancer cell lines (Jaruga-Killeen and Rayford, 2005; Katayose et al., 1997). Accordingly, Naruse and colleagues showed in lung cancer cell lines that cells required phosphorylated RB in addition to p27kip1 in order to undergo apoptosis, but that cells arrested in G1 phase were protected from apoptosis (Naruse et al., 2000). However, due to the use of adenoviral vectors and cancer cell lines in which cell cycle regulation may already be aberrant and may differ notably from normal cells, the relevance of these studies for physiological conditions remains uncertain.

On the other hand, it has been shown that the CIP/KIP proteins p21Cip1 and p57Kip2 may block apoptosis in a CDK-independent mode by preventing stress-induced apoptosis mediated by the JNK and p38 MAP kinase signaling pathways (Asada et al., 1999; Huang et al., 2003). Liang *et al.* showed that under stress conditions (growth factor withdrawal), activation of the LKB1-AMPK pathway results in p27kip1 stabilization by its phosphorylation on T198 allowing cells to survive the metabolic stress through autophagy and that p27kip1 knockdown in these cells results in apoptosis (Liang et al., 2007). These findings picture a role of p27kip1 in apoptosis prevention, which may contribute to tumor cell survival under growth factor deprivation, disrupted energy metabolism or during stress due to chemotherapeutic agents. This observation together with the fact that accumulation of p27kip1 in certain cancer types may support resistance to apoptosis induced by cytotoxic drugs or irradiation needs to be taken into consideration before designing any cancer therapy, which interferes with the functions of the CIP/KIP family (Ishii et al., 2004).

3.1.4 p27kip1 and cell motility

The CIP/KIP family members p21cip1, p27kip1, and p57kip2 are mainly localized in the nucleus but all of them may also be found in the cytoplasm, where they display functions independent of their cell cycle regulatory roles.

In this regard, CIP/KIP proteins can regulate cell motility through interaction with the RHOA-ROCK-LIMK pathway, thereby altering the actin cytoskeletal dynamics and regulating cell migration (Besson et al., 2004). Particularly p27kip1, when localized in the cytoplasm, can enhance cell migration by modulating RHOA activity through its C-terminal domain, a region called “scatter domain”, which is necessary for the interaction with Rac-GTPase (Besson et al., 2004). RHOA-p27kip1 binding is facilitated by p27kip1 phosphorylation at T198, which is driven by p90 ribosomal S6 kinase (RSK1) activity, and its cytoplasmic relocation, ultimately results in an inhibition of the RHOA-ROCK pathway and a loss of actomyosin stability (Larrea et al., 2009).

However, in contrast to these findings, several studies reported an opposite effect, showing that p27kip1 can act as an inhibitor of cell migration in different tissues, including muscle cells, endothelial cells, neurons and oral carcinoma cells (reviewed in (Borriello et al., 2011)). Also in fibrosarcoma cells and normal mouse fibroblasts cultured in 3D matrices, p27kip1 has been shown to interact and impair the function of stathmin, a microtubule-associated protein, leading to the accumulation of stabilized microtubules, thus regulating cell morphology and motility. In the absence of p27kip1 a decrease in microtubule stability seems to be responsible for the increased motility and invasive potential of the tumor cells (Baldassarre et al., 2005). Along this line, it has been demonstrated that p27kip1 can regulate lipid raft trafficking and Rho GTPase activity via its interaction with stathmin and that this molecular pathway is probably involved in the control of cell morphology and motility in 3D environments (Belletti et al., 2010).

3.2 Regulation of p27kip1

Due to its highly relevant functions, *CDKN1B*-p27kip1 is itself tightly regulated at the transcriptional, translational and post-translational level. The p27kip1 protein is mainly regulated by proteasomal degradation but its nuclear functions may also be inactivated by nuclear exclusion, i.e. cytoplasmic localization, and/or by phosphorylation at specific sites. Moreover, some transcription factors bind to the *CDKN1B* promoter region and regulate its expression on the transcriptional level. Together, the abundance and activity of p27kip1 is regulated at the level of *CDKN1B* transcription and mRNA translation rates as well as protein stability and degradation and is further modulated by its subcellular localization (Roy and Banerjee, 2015; Servant et al., 2000).

3.2.1 Transcriptional regulation of *CDKN1B*

While cell cycle-dependent changes in p27kip1 are mainly post-translationally regulated, several transcription factors also act on the *CDKN1B* promoter (Chu et al., 2008). In 1999, Kamiyama and Inoue characterized the 5´-flanking regulatory region of the human *CDKN1B* promoter and described two regions containing CCAAT and GGGCGG boxes, which are essential for the promoter activity driven by the transcription factors SP1 and NF-Y (Inoue et al., 1999; Kamiyama et al., 1999).

CDKN1B is also a direct target of the transcription factor E2F1**,** a critical regulator of cell cycle (Wang et al., 2005). Remarkably, the decrease in p27kip1 levels in early- to mid-G1 phase allows free cyclin E-CDK2 complexes to hyperphosphorylate RB, which in turn releases the E2F1 transcription factor, suggesting the existence of a negative feedback mechanism (Wang et al., 2005).

Furthermore, Medema *et al.* and Dijkers *et al.* were the first to show that the effect of AKT signaling on the Forkhead transcription factors (FOXOs: FOXO1, FOXO3, FOXO4, and FOXO6) inversely correlated with *CDKN1B*

expression, providing evidence that FOXOs can directly regulate *CDKN1B* promoter activity resulting in increased p27kip1 protein levels (Dijkers et al., 2000; Medema et al., 2000). In the absence of AKT signaling, all FOXO members are located in the nucleus in an active form. AKT activation results in their phosphorylation, leading to their release from DNA and relocalization into the cytoplasm, thus blocking their transcriptional activity and suppressing the expression of cell cycle and apoptosis related genes (reviewed in (Dansen and Burgering, 2008)). As an additional player in *CDKN1B* transcriptional regulation by FOXOs, SKP2 indirectly controls *CDKN1B* expression by promoting the degradation of FOXO1 (Huang et al., 2005).

Although MYC mainly acts at the post-translational level, it can also transcriptionally repress *CDKN1B* by binding to the promoter region of the gene (Yang et al., 2001). In this context, it has been shown that MYC and FOXO3 compete for the occupation of the *CDKN1B* promoter and that the PI3K signaling pathway coordinately and inversely controls both an activator (FOXO3), presumably mediated by AKT, and a repressor (MYC) of *CDKN1B* transcription (Chandramohan et al., 2004).

Also HES1, which is known to play a crucial role in the control of differentiation and proliferation of neuronal, endocrine, and T-lymphocyte progenitors, has been suggested to promote progenitor proliferation through transcriptional repression of *CDKN1B* (Murata et al., 2005). Interestingly, MYC and HES1, both transcriptional repressors of *CDKN1B*, are directly controlled by NOTCH1, which is constitutively activated in more than 60% of T-ALL (Jarriault et al., 1998; Palomero et al., 2006b). Moreover, both HES1 and MYC bind to regulatory sequences in the *PTEN* proximal promoter, with HES1 acting as a strong transcriptional repressor and MYC as a weaker transcriptional activator, so that the overall output downstream of NOTCH1 activation is a controlled downregulation of *PTEN* transcripts resulting in an indirect regulation of *CDKN1B* transcription via activation of the PI3K-AKT signaling pathway (Palomero et al., 2007).

Also the TLX1 homeobox transcription factor is involved in the transcriptional regulation of *CDKN1B*. Expression analysis of *TLX1* positive primary leukemia samples and ectopic expression in the T-ALL cell line Jurkat determined that TLX1 regulated genes are mainly involved in the G1/S transcriptional networks, amongst them *E2F* and *MYC* and genes modulated by AKT signaling. Also *CDKN1B* expression was reduced in *TLX1* overexpressing leukemia and downregulated following introduction of TLX1 (Riz and Hawley, 2005). Interestingly, in a recent paper the genome-wide binding profile of TLX1 in human T-ALL was analyzed and identified binding peaks in the vicinity of genes that define T-cell lineage identity and tumor suppressors, including *CDKN1B* (Durinck et al., 2015).

3.2.2 Post-transcriptional regulation of *CDKN1B*

p27kip1 levels are elevated in quiescent cells but decrease drastically following mitogen stimulation and entry into G1 (Besson et al., 2006; Sherr and Roberts, 1999) and this oscillation in protein levels is at least in part controlled at the translational level. The accumulation of p27kip1 in non-proliferating cells is due to an increase in the amount of *CDKN1B* mRNA in the polyribosomes and enhanced translation rates. The regulation of translation rates occurs via specific elements in the 5'-untranslated region (UTR) of *CDKN1B,* which interact with RNA-binding and RNA-processing proteins in a cell cycle phase-specific manner (Hengst and Reed, 1996; Kullmann et al., 2002; Millard et al., 2000).

Alternatively, the post-transcriptional regulation of p27kip1 protein abundance may be caused by microRNAs (miRNAs). These small non-coding RNAs associate with the 3'-UTRs of protein coding genes and control protein synthesis via translational repression or mRNA decoy, depending on the complementarities between the miRNAs and their targets. Specifically, miR-221 and miR-222, two polycistronic miRNAs sharing the same seed sequence, have been shown to control p27Kip1 translation but not mRNA stability (le Sage et al., 2007). Upregulation of

these miRNAs has been found in several human cancers and their downregulation increased p27kip1 levels and inhibited tumor proliferation (le Sage et al., 2007; Medina et al., 2008). Also in T-ALL and T-cell lymphoma miRNA-221 is upregulated, suggesting that it contributes to the regulation of p27kip also in T-cell malignancies (Gimenes-Teixeira et al., 2013; Mussolin et al., 2014).

3.2.3 Post-translational modifications and subcellular localization of p27kip1

Although *CDKN1B*-p27kip is in part regulated at the transcriptional and translational level, protein activity is mainly regulated at the post-translational level via p27kip1 phosphorylation and redistribution between the nucleus and the cytoplasm. The p27kip1 protein possesses multiple tyrosine, serine or threonine residues whose phosphorylation regulates its activity (Table 3).

Table 3. List of postranslationally phosphorylated p27kip1 residues and their functions

Residue modified	Modified by	Localization	Effects of modification
Y74	SRC kinase	Nucleus	Inhibits p27kip1 mediated CDK2 inhibition, promotes proteolysis of p27
Y88	ABL kinase, SRC kinase	Nucleus	Converts p27kip1 into a non-inhibitor of cyclin-CDK complex, required for efficient phosphorylation on T187 by CDK2
Y89	ABL kinase	Nucleus	Converts p27kip1 into a non-inhibitor of cyclin-CDK complex
T198	AKT	Cytoplasm	Sequesters p27kip1 in the cytoplasm by binding to 14-3-3
T157	AKT	Cytoplasm	pT157 within the NLS domain of p27kip1 prevents its nuclear import
S10	DYRK1B, KIS, AKT, ERK	Cytoplasm	Increases stability, induces nuclear export, thus reducing the threshold of cyclin-CDK2 activation
T187	Cyclin E-CDK2	Nucleus	Docking site for CSK1 and SKP2 followed by ubiquitination mediated degradation

Modified from Roy, 2015.

In quiescent cells, p27kip1 is mainly located in the nucleus exerting its antiproliferative role by binding to and inhibiting the Cyclin E-CDK2 complex. During early G1, phosphorylation at tyrosines 74 (Y74) and 88/89 (Y88/Y89), mediated by ABL and SRC kinases, impairs the ability of p27kip1 to inhibit the activity of CDK, thus contributing to cyclin E-CDK2 activation, which is then followed by threonine 187 (T187) phosphorylation and proteolysis through the SCF-SKP2 complex (Fig. 7). Phosphorylation at serine 10 (S10) allows CRM1-dependent cytoplasmic export and KPC-mediated proteolysis. Once in the cytoplasm, PI3K-AKT activation promotes p27kip1 phosphorylation at threonines 157 (T157) and 198 (T198), sequestering p27kip1 in the cytoplasm and allowing the assembly of cyclin D-CDK-p27kip1 complexes. T198 phosphorylation also promotes p27kip1 binding to RHOA, disrupting RHOA-ROCK activation and inhibiting the activity of the GTPase RHOA, required for focal adhesion, and thereby promoting cell migration (reviewed in (Chu et al., 2008) and (Roy and Banerjee, 2015)).

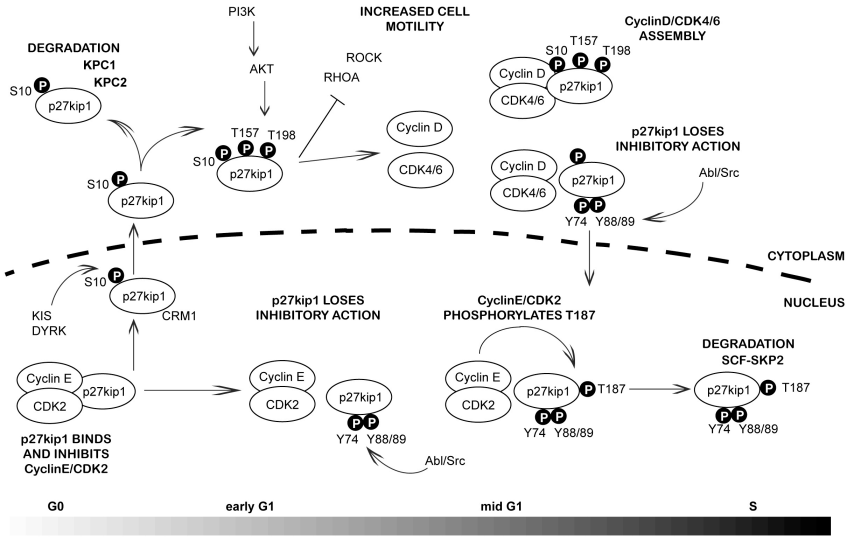

Figure 7. **Model of signaling pathways that regulate p27kip1.**
Modified from Chu, 2008.

3.2.4 Protein degradation by the proteasome pathway

As soon as cells exit cellular quiescence and progress into G1, p27kip1 protein levels decline dramatically, which is mainly controlled through its proteasomal pathway-mediated degradation (Fig. 7). The best characterized protein targeting p27kip1 for degradation is the S-phase kinase-associated protein 2 (SKP2), an F-box protein of the SKP1-CUL1-F-box-protein (SCF) complex (Pagano et al., 1995). SKP2 knockout mice show an accumulation of p27kip1, slow growth and have smaller organs compared to control littermates, suggesting that loss of SKP2 leads to changes in cell proliferation. They also present prominent cellular phenotypes with nuclear enlargement accompanied by polyploidy and centrosome overduplication. Loss of p27kip1 rescues the defects observed in SKP2 mutant mice, clearly indicating that p27kip1 is the principal target of SKP2 (Nakayama et al., 2000).

In this context, SKP2 binds to T187-phosphorylated p27kip1, which is phosphorylated by cyclin E-CDK2, and mediates its degradation in the nucleus during S phase. Subsequent studies showed that the efficient interaction between the SKP2 ubiquitin ligase complex and its substrate p27kip1 requires the participation of an additional protein, CKS1, which facilitates the recognition of the phosphorylated site (reviewed in (Chu et al., 2008) and (Roy and Banerjee, 2015)).

Notably, several genes and their encoded proteins, which are deregulated in cancer in general and also in T-cell leukemia play a role in the p27kip1 degradation pathway. For example, PTEN modulates p27kip1 abundance by reducing the expression of *SKP2* (Mamillapalli et al., 2001), and consequently, the mutational inactivation of PTEN leads to an augmented p27kip1 degradation. In addition, MYC not only represses the *CDKN1B* promoter, but also directly induces *SKP2* expression at the mRNA level by binding to *SKP2* regulatory elements (Bretones et al., 2011). Furthermore, MYC can also indirectly regulate p27kip1 levels by inducing other genes, for example, *CUL1* and *CKS1B*, encoding proteins which are involved in p27kip1 proteolysis (Keller et al., 2007; O'Hagan et al., 2000). Importantly,

activation of NOTCH1 signaling induces both *MYC* and *SKP2* expression, emphasizing its role as a crucial player in p27kip1 regulation (Dohda et al., 2007; Sarmento et al., 2005).

A second ubiquitin-proteasome pathway responsible for p27kip1 degradation in the cytoplasm mediated by the KIP1 ubiquitination-promoting complex (KPC) has been described (Kamura et al., 2004). KPC is composed of KPC1, a ring finger protein, and KPC2, which contains ubiquitin-like and ubiquitin-associated domains. Certain discrepancies between the spatial and temporal expression patterns of p27kip1 and SKP2 suggested the existence of another p27kip1 degradation pathway. While p27kip1 has its peak during G0, SKP2 is not expressed until late G1-S phase. Moreover, p27kip1 is exported to the cytoplasm at early G1 and is sensitive to proteasome inhibitors in SKP2 knockout cells, suggesting a SKP2-independent proteasome-dependent mechanism (Hara et al., 2001; Nakayama et al., 2004). This KPC-mediated degradation requires the nuclear export of p27kip1 by CRM1 in G1 phase (Starostina and Kipreos, 2012).

4. Involvement of p27kip1 and SKP2 in cancerogenesis

The first *Cdkn1b* knockout mice were generated in 1996 by Fero and colleagues (Fero et al., 1996). The p27kip1-deficient animals showed an apparently normal prenatal development but an overall increase in cell proliferation resulting in an increase in body size and multiorgan hyperplasia, conferring an important antiproliferative role to p27kip1 (Fero et al., 1996). In addition, the animals showed a disorganization of sensory epithelia in the retina and inner ear and displayed female sterility due to defective ovarian and uterine functions (Fero et al., 1996). Notably, not only p27kip1 null mice but also heterozygous ones showed an increased predisposition to tumorigenesis in multiple organs when exposed to carcinogens and irradiation, indicating that p27kip1 is a haploinsufficient tumor suppressor (Fero et al., 1998; Lee and Kim, 2009; Nakayama et al., 1996).

Decreased *CDKN1B* and/or p27kip1 expression levels have been observed in many types of cancer and it is generally accepted that p27kip1 is implicated in the development and progression of human malignancies and that it has tumor suppressor functions (Chu et al., 2008; Slingerland and Pagano, 2000).

4.1 Solid tumors

As mentioned above, decreased *CDKN1B* and/or p27kip1 levels have been observed in several malignancies and appear to be a poor prognostic factor (Chu et al., 2008; Slingerland and Pagano, 2000; Wander et al., 2011). In primary tumors and cancer cell lines both *CDKN1B* alleles are rarely inactivated, supporting the notion that *CDKN1B*-p27kip1 is not a tumor suppressor in the classical sense but rather functions in a haploinsuffcient state (Chu et al., 2008).

Recent data also suggests a role of p27kip1 as oncoprotein, implying a function for p27kip1 beyond the regulation of cyclin-CDK complexes,

which may enhance tumorigenesis. Increasing evidence indicates that the cytoplasmic sequestration of p27kip1 may be critical for its oncogenic function (Besson et al., 2007; Vervoorts and Luscher, 2008). The current model suggests that p27kip1 suppresses tumorigenesis when located in the nucleus by inhibiting the active cyclin-CDK complexes but exerts other functions in the cytoplasm that are potentially oncogenic (Chu et al., 2008). Several studies investigating the subcellular localization of p27kip1 in tumors suggest that – while the loss of nuclear p27kip1 is commonly observed – its localization in the cytoplasm correlates with high tumor grade and a poor prognosis (Chu et al., 2008; Lee and Kim, 2009). The potential oncogenic function of p27kip1 is supported by mouse models, in which its cytoplasmic mislocalization promoted metastasis formation (Denicourt et al., 2007).

Since ubiquitin-mediated degradation of p27kip1 is mainly controlled by SKP2, the overexpression of the latter observed in several types of cancer most likely represents the major cause of p27kip1 protein downregulation (Frescas and Pagano, 2008). SKP2 knockout mice are smaller than wild-type ones and show organ hypoplasia, phenotypes, which are rescued in SKP2-p27kip1 double knockout mice (Cardozo and Pagano, 2004). Moreover, also SKP2 levels may represent a prognostic marker in patients suffering from various human cancers. In line with this notion, patients with breast cancer, gastric cancer or melanoma expressing higher levels of SKP2 have a poorer prognosis, suggesting a potential usefulness of SKP2 as a predictive biomarker (reviewed in (Wang et al., 2014)).

Importantly, because of its relevant role in tumorigenesis, SKP2 has emerged as a promising target for novel therapeutic approaches and small molecule inhibitors are currently developed (Chan et al., 2013; Wu et al., 2012).

4.2 T-cell malignancies

There is increasing evidence that haploinsufficiency of *CDKN1B*-p27kip1 may also play a role in the pathogenesis of T-cell malignancies. In this regard, in about 50% of T-cell prolymphocytic leukemia (T-PLL) heterozygous deletions of *CDKN1B* have been found and the absence of biallelic mutations in virtually all tumors emphasizes its haploinsufficiency mechanism in tumorigenesis. Notably, a significant number of T-PLL cases displayed decreased levels of *CDKN1B* transcripts without any evidence for heterozygous deletions or mutations (Hetet et al., 2000; Le Toriellec et al., 2008).

In pediatric T-ALL genome-wide studies of copy number alterations have revealed that heterozygous *CDKN1B* deletions are one of the most frequent numerical aberrations occurring in about 12% of the cases (Mullighan et al., 2007; Remke et al., 2009). In addition, like in T-PLL, also in T-ALL decreased *CDKN1B* expression is frequently observed in *CDKN1B* wild-type cases, strongly suggesting that other mechanisms contribute to its downregulation. Analysis of the *CDKN1B* promoter in primary T-ALL samples did not show involvement of hypermethylation in the downregulation of the gene (Kraszewska et al., 2012).

Furthermore, it has been shown that NOTCH1 signaling in T-ALL controls the expression levels of *SKP2* and its target protein p27kip1, leading to a more rapid cell cycle progression. Pharmacologically blocking NOTCH1 signaling decreases SKP2 and increases p27Kip1 expression (Dohda et al., 2007). Interestingly, in T-lymphoma cells treatment with GCs reduces both the protein and mRNA levels of SKP2 and increases p27kip1 expression, identifying both as key players in GC-induced growth suppression (Kullmann et al., 2013).

5. Regulatory network of *CDKN1B*-p27kip1 in T-ALL

Based on published data we have generated a regulatory network how specific genetic alterations frequently found in T-ALL may contribute to the suppression of *CDKN1B*-p27kip1 (Fig. 8).

Constitutive activation of NOTCH1 signaling – either by NOTCH1 activating and/or FBXW7 inactivating mutations – is recurrently found in T-ALL (Park et al., 2009; Weng et al., 2004). Activation of this signaling pathway may result in the downregulation of *CDKN1B*-p27kip1 via two different routes: NOTCH1 up-regulates both *MYC* (Palomero et al., 2006b; Weng et al., 2006) and *HES1* (Jarriault et al., 1998) and in turn both proteins suppress *CDKN1B* transcription (Murata et al., 2005; Yang et al., 2001). Loss of FBXW7 function prevents targeting NOTCH1 and MYC for proteasome-mediated degradation, thus, stabilizing these proteins (Thompson et al., 2007). Furthermore, both NOTCH1 and MYC transcriptionally up-regulate *SKP2* (Dohda et al., 2007; Sarmento et al., 2005), leading to an enhanced ubiquitin-dependent proteasome-mediated degradation of p27kip1 by the SCF-SKP2 complex (Bretones et al., 2011).

An additional important player in the regulatory network of *CDKN1B*-p27kip1 is the main negative regulator of AKT signaling, PTEN (Carracedo and Pandolfi, 2008). In T-ALL, PTEN function is not only lost by mutational inactivation, which occurs in 10-15% of the cases, but may also be impaired by NOTCH1-mediated upregulation of HES1 and MYC, which directly bind to the *PTEN* promoter, inhibiting its transcription (Palomero et al., 2007). Thus, MYC – as direct target of NOTCH1 – reinforces the downregulation of *CDKN1B*-p27kip1 by directly repressing both the *PTEN* and *CDKN1B* promoter activity. However, PTEN only indirectly regulates *CDKN1B* via the FOXO transcription factors, which are key mediators of tumor suppression downstream of PTEN (Dansen and Burgering, 2008). More specifically, inactivation of PTEN activates AKT signaling, which leads to the phosphorylation of FOXO members, their

nuclear exclusion, and therefore, their inactivation and cell cycle re-entry (Burgering and Kops, 2002).

On the one hand, inactivation of FOXOs prevents the transcriptional induction of *CDKN1B* (Dijkers et al., 2000; Medema et al., 2000), and, on the other hand, it has been proposed that FOXOs also function as negative regulators of SKP2 (Paik et al., 2007; Wu et al., 2013). Conversely, induction of SKP2 expression promotes the ubiquitin-dependent degradation of FOXOs, suggesting the presence of a feedback loop between inactivation of FOXOs and enhanced SKP2 function (Dehan and Pagano, 2005; Huang et al., 2005).

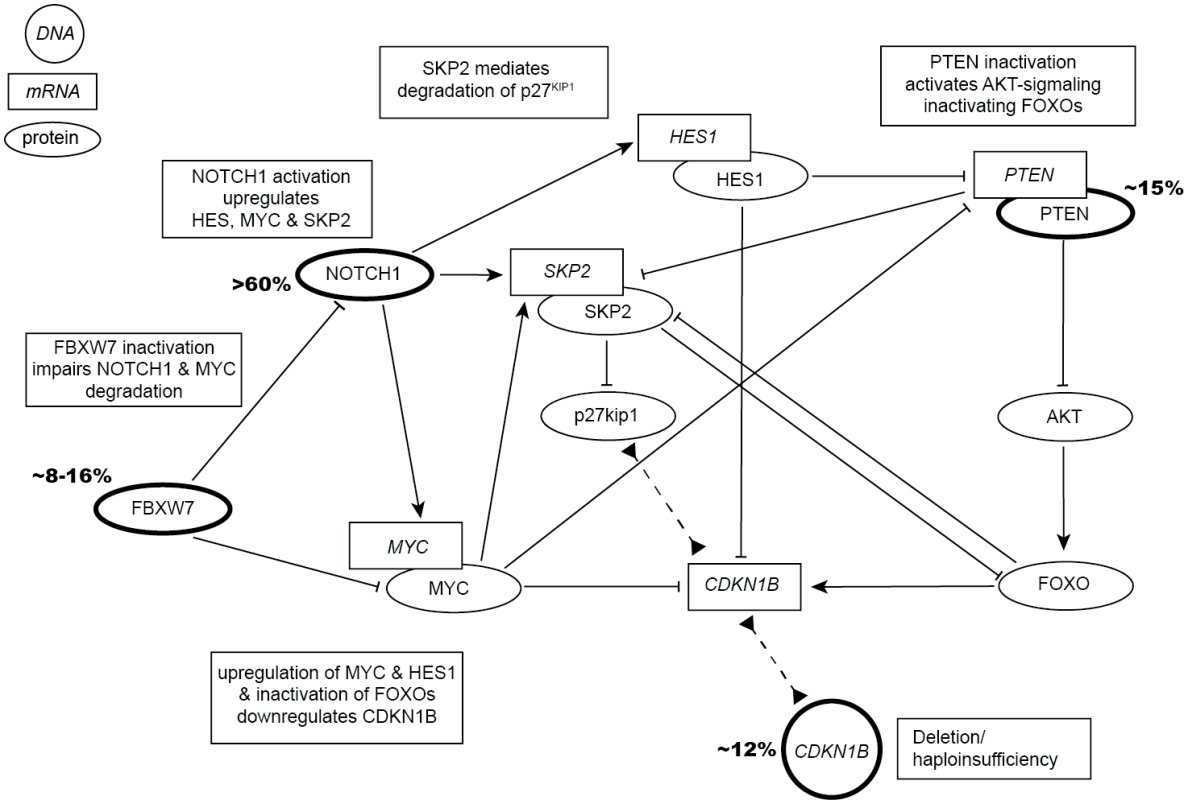

Figure 8. *CDKN1B*-p27kip1 regulatory network. The major players involved in *CDKN1B*-p27kip1 regulation and frequently mutated in T-ALL are depicted. Percentages indicate the mutation frequencies in T-ALL.

RATIONALE AND OBJECTIVES

Downregulation of the haploinsufficient tumor suppressor CDK inhibitor p27kip1, encoded by *CDKN1B*, has been found in several human cancer types and correlates with a poor prognosis. In T-ALL, *CDKN1B* is affected by heterozygous deletions in about 12% of the cases. Intriguingly, also cases carrying two copies of the gene showed low *CDKN1B* transcript levels, indicating that other mechanisms are involved in its regulation.

Based on the *CDKN1B*-p27kip1 regulatory network described above, we hypothesized that genetic alterations of *NOTCH1*, *FBXW7* or *PTEN*, frequently present in T-ALL, may independently or in conjunction be related to the transcriptional repression of *CDKN1B* and/or the regulation of p27kip1 protein levels.

The purpose of this thesis was to elucidate the role of heterozygous *CDKN1B* deletions or reduced *CDKN1B*-p27kip1 levels in T-ALL by conducting a comprehensive analysis of the selected genes involved in its regulation in T-ALL cell lines and primary leukemia samples and to determine whether interfering with p27kip1 protein degradation may open a new avenue for therapeutic intervention.

The main objectives were:

- To elucidate whether *CDKN1B* deletions occur mutually exclusive from or in combination with other specific genetic alterations associated with T-ALL
- To determine whether deletion of *CDKN1B* results in lower transcript levels compared to wild-type T-ALL
- To determine if *NOTCH1*, *FBXW7*, or *PTEN* mutations correlate with a reduction of *CDKN1B* transcript levels
- To assess whether in T-ALL cell lines *CDKN1B* transcription correlates with p27kip1 protein levels and whether its subcellular distribution is affected
- To elucidate whether *CDKN1B* deletions may define a T-ALL subtype with specific biological features

- To assess the impact of novel small molecule inhibitors of SKP2 in T-ALL
- To determine whether inhibition of SKP2 in combination with other treatments might be a feasible therapeutic approach

RESULTS

RESULTS I

Correlation of *CDKN1B* expression with the mutation status of genes implicated in its regulation in T-ALL

In T-cell malignancies, 50% of T-PLL (Hetet et al., 2000; Le Toriellec et al., 2008) and 12% of pediatric T-ALL (Remke et al., 2009) carry heterozygous deletions of *CDKN1B* and a decreased expression was also observed in several wild-type cases, suggesting that *CDKN1B* transcription is regulated by other mechanisms. Since several genes, amongst them *NOTCH1*, *FBXW7*, and *PTEN*, encoding proteins directly or indirectly involved in *CDKN1B*-p27kip1 regulation are frequently affected by genetic alterations in T-ALL, we analyzed whether *CDKN1B* expression correlates with specific mutation patterns.

I.1. Characterization of T-ALL cell lines

Mutation screening and *CDKN1B*-p27kip1 expression in T-ALL cell lines

To study the regulation of *CDKN1B*-p27kip1, we analyzed a panel of T-ALL cell lines, which not only permitted to assess transcript but also protein levels. First, we confirmed the authenticity of the cell lines by fluorescence in situ hybridization (FISH) and molecular analysis for known genetic markers, including *TLX3* and *TCR* rearrangements (data not shown) as well as characteristic mutations in the genes of interest (*NOTCH1*, *FBXW7*, and *PTEN*) by direct sequencing of PCR amplification products. Except for TALL-1, which was wild-type for all three genes, all other cell lines showed at least one mutation (Table 4). Further analysis by Western blotting confirmed the impact of these alterations on the presence or absence of the respective proteins (Fig. 10A).

Table 4. Summary of mutations in T-ALL cell lines

	NOTCH1 HD/TM	NOTCH1 PEST	FBXW7	PTEN
DND-41	MUT	MUT	WT	WT
MOLT-4	MUT	MUT	WT	MUT
RPMI-8402	MUT	WT	MUT	MUT
Jurkat	MUT	WT	MUT	MUT
CCRF-CEM	MUT	WT	MUT	DEL
MOLT-16	WT	WT	WT	MUT
Loucy	WT	WT	WT	DEL
HSB-2	WT	WT	MUT	WT
TALL-1	WT	WT	WT	WT

HD, heterodimerization domain; TM, transmembrane domain; WT, wild-type; MUT, mutated; DEL, deleted.

Next, we determined the *CDKN1B* transcript levels by RT-qPCR. The T-ALL cell lines showed variable and some very low *CDKN1B* mRNA expression levels, which correlated only to some extent with the respective protein levels (Fig. 9A). For example, RPMI-8402 expressing the highest level of *CDKN1B* showed rather low amounts of p27kip1 protein, supporting the well-documented post-transcriptional regulation of p27kip1 (Slingerland and Pagano, 2000; Vervoorts and Luscher, 2008).

Notably, in the cell line Loucy, neither *CDKN1B* mRNA expression nor any p27kip1 protein was detectable. In order to investigate whether the lack of transcripts and protein in Loucy is due to a homozygous deletion, we designed a series of *CDKN1B*-specific primer pairs covering different regions of the gene and performed standard PCRs using genomic DNA (Fig. 9B). The presence of specific PCR amplification products of the predicted sizes demonstrated that in this cell line no homozygous deletion of the gene was responsible for the lack of *CDKN1B* expression (Fig. 9B), indicating that the transcriptional regulation occurs via other mechanisms.

However, no correlation between *CDKN1B* expression levels and the genetic lesions in *NOTCH1*, *FBXW7*, and/or *PTEN* was observed (Table 4, Fig. 9A).

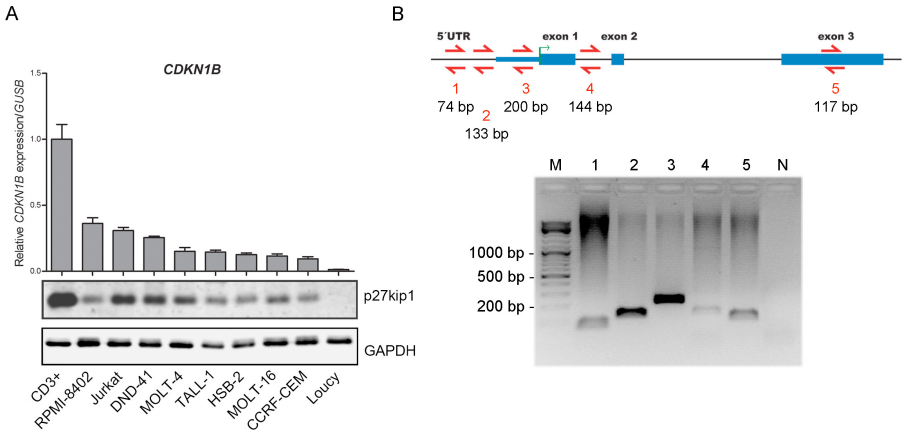

Figure 9. *CDKN1B*-p27kip1 expression in T-ALL cell lines. (A) *CDKN1B* transcript levels were assessed by RT-qPCR and normalized to the reference gene *GUSB* and to a pool of CD3+ T-cells isolated from peripheral blood of three healthy donors. Western blot analysis of p27kip1. GAPDH was used as loading control. (B) Standard genomic PCR of Loucy. Schematic representation showing the localization of the *CDKN1B* primers used. The presence of amplification products of the expected sizes excluded the presence of a homozygous deletion. M, DNA marker; lanes 1-5, genomic PCR with different primer pairs; N, non-template control.

NOTCH1-HES1/MYC/SKP2 in the regulation of *CDKN1B*-p27kip1 in T-ALL cell lines

Based on regulatory network we have generated, the NOTCH1 signaling pathway is one of the major axis in the transcriptional and post-translational regulation of *CDKN1B*-p27kip1. To verify the relationship between NOTCH1 activation and the induction of *MYC*, *HES1*, and *SKP2* previously described (Dohda et al., 2007; Jarriault et al., 1998; Larson Gedman et al., 2009; Palomero et al., 2006b; Sarmento et al., 2005; Weng et al., 2006), the T-ALL cell lines were subjected to mRNA and protein expression analysis (Fig. 10).

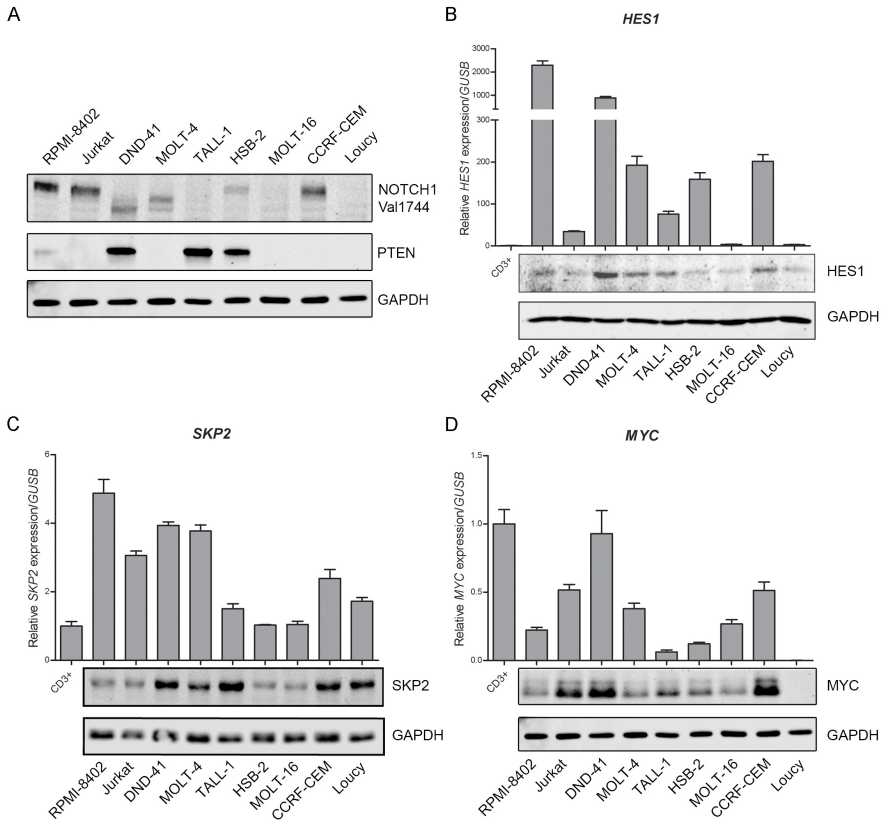

Figure 10. Analysis of T-ALL cell lines with regard to the correlation between NOTCH1 signaling and *HES1*, *MYC*, and *SKP2*. (A-D) Western blots of T-ALL cell lines. Whole protein lysates from the different T-ALL cell lines were probed with the indicated antibodies. GAPDH was used as a loading control. (A) Cleaved NOTCH1 was detected in all cell lines, except for TALL-1, MOLT-16, and Loucy, which harbor neither a mutation in NOTCH1 nor FBXW7. Only the cell lines DND-41, TALL-1, and HSB-2 express wild-type PTEN protein. (B-D) RT-qPCR was used to assess the transcript levels of the genes of interest and normalized to *GUSB* reference gene and to a pool of CD3+ T-cells from three healthy individuals. (A-D) NOTCH1 activation (A) was generally associated with HES1 (B), SKP2 (C), and MYC (D) expression but not with *CDKN1B*-p27kip1 levels. *Note*: The cell lines are ordered according to their *CDKN1B* transcript levels: from left to right – highest to lowest mRNA expression.

The presence of cleaved active intracellular NOTCH1 in the cell lines RPMI-8402, Jurkat, DND-41, MOLT-4, and CCRF-CEM was consistent with the mutations found in the most frequently mutated NOTCH1 domains (Table 4, Fig. 10A). Also in the cell line HSB-2, which carries a FBXW7 inactivating mutation, leading to an impairment of intracellular NOTCH1 degradation, cleaved NOTCH1 was detectable (Table 4,

Fig. 10A). PTEN protein was only present in the three wild-type cell lines DND-41, HSB-2, and TALL-1 (Table 4, Fig. 10A). We detected also a weak signal in RPMI-8402, which contains both a truncating and a missense mutation in the *PTEN* gene, however, it has been previously described that this cell line expresses only non-functional PTEN protein (Palomero et al., 2007; Shepherd et al., 2013).

NOTCH1 activation was generally associated with the induction of *HES1*, *SKP2*, and *MYC* transcript levels (Fig. 10). Of note, although the cell line TALL-1 harbors neither a NOTCH1 nor a FBXW7 mutation it nevertheless expresses *HES1*, indicating that NOTCH1 activation is caused by a different mechanism, which is supported by the sensitivity of the cells to γ-secretase inhibitors (De Keersmaecker et al., 2008; Shepherd et al., 2013; Tammam et al., 2009). In most of the cases, *HES1*, *MYC*, and *SKP2* transcript levels correlated with the respective protein levels (Fig. 10), indicating that mRNA expression may, at least to a certain extent, be used as surrogate for protein levels.

Remarkably, although in several types of tumors p27kip1 protein expression inversely correlated with SKP2 and HES1 expression (Miyamoto et al., 2010; Murata et al., 2005; Rosner et al., 2009; Sarmento et al., 2005), in the T-ALL cell lines this association was not readily apparent, suggesting that p27kip1 levels might not always be as tightly linked to SKP2 or HES1 expression.

p27kip1 subcellular localization in T-ALL cell lines

Cytoplasmic mislocalization of p27kip1 has been reported in many types of cancer and is often associated with a poor outcome (reviewed in (Chu et al., 2008; Lee and Kim, 2009)). p27kip1 shuttles between the nuclear and cytoplasmic compartments, however, its aberrant cytoplasmic retention impedes its cell cycle inhibitory function and has been described to have oncogenic consequences (Besson et al., 2004; Serres et al., 2011).

One known factor responsible for the cytoplasmic sequestration is the direct phosphorylation of p27kip1 by AKT (Fujita et al., 2003; Liang et al., 2002; Viglietto et al., 2002a).

Therefore, we investigate the subcellular distribution of p27kip1 in our panel of T-ALL cell lines and we asked whether its localization correlated with loss of PTEN, the main negative regulator of AKT signaling, which has been found mutated or deleted in about 15% of T-ALL cases (Bandapalli et al., 2013; Zuurbier et al., 2012).

Western blotting of fractionated proteins showed both cytoplasmic and nuclear localization of p27kip1 in all cell lines (Fig. 11A). Therefore, we did not observe a virtually complete nuclear exclusion of p27kip1 as seen in other tumor subsets (reviewed in (Chu et al., 2008)) However, the PTEN wild-type T-ALL cell lines DND-41, TALL-1, and HSB-2 (Table 4, Fig. 10A) showed an accumulation of cytoplasmic p27kip1 as compared to the PTEN-inactivated ones (except for CCRF-CEM), corroborating its AKT-mediated functional inactivation and cytoplasmic relocalization (Fig. 11A).

AKT signaling also results in phosphorylation, nuclear exclusion and inactivation of FOXOs (Brunet et al., 1999; Burgering and Kops, 2002). As FOXOs have been described to regulate *CDKN1B* transcription (Dijkers et al., 2000; Medema et al., 2000; Paik et al., 2007), we analyzed by Western blotting whether the PTEN status of the cell lines correlated with the subcellular localization of FOXO3 and *CDKN1B* expression (Fig. 11B). In the majority of the cell lines FOXO3 showed a mainly cytoplasmic localization, but in the PTEN wild-type cell lines DND-41 and TALL-1, FOXO3 was found in the nucleus, confirming its regulation by PTEN (Fig. 11B). In HSB-2 this correlation was not that obvious and the reasons for that remain to be determined. Notably, in our panel of T-ALL cell lines also the subcellular distribution of FOXO3 did not correlated with *CDKN1B* transcript levels.

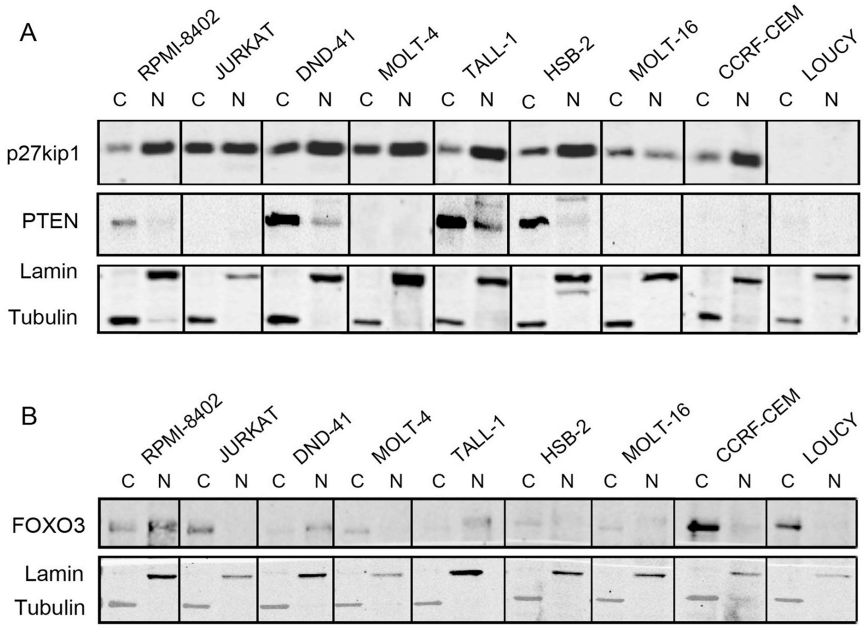

Figure 11. Subcellular distribution of proteins in T-ALL cell lines. (A) Localization of p27kip1 and PTEN. PTEN wild-type cell lines show an accumulation of protein in the cytoplasmic fraction compared to PTEN-inactivated ones (except for CCRF-CEM). (B) Subcellular distribution of FOXO3 in cytoplasmic and nuclear protein fractions. Lamin and tubulin served as loading controls for the cytoplasmic and nuclear protein fractions, respectively. *Note*: The cell lines are ordered according to their *CDKN1B* transcript levels: from left to right – highest to lowest mRNA expression. C, cytoplasmic; N, nuclear.

I.2. Characterization of pediatric *CDKN1B*-deleted T-ALL

Based on the data available from a previous BAC tiling path array comparative genomic hybridization (aCGH) study of 102 samples of pediatric T-ALL (Pisecker M, Ullmann R, Strehl S, *unpublished*) twelve cases carrying heterozygous deletions of *CDKN1B* were identified. The size of the deletions was highly variable, ranging from 1.2-27.8 Mb, but the minimal region of deletion always included *CDKN1B* (Table 5), indicating that indeed, this haploinsufficient tumor suppressor represents a key gene targeted by these deletions. Two further cases were detected by routine cytogenetics showing deletions at 12p13, encompassing the *CDKN1B* locus.

Table 5. *CDKN1B*-deleted pediatric T-ALL cases detected by aCGH

Sample	Start *	End *	Size in Mb	No. of genes	Selected genes
90-0130	10844955	13749846	2,905	>50	CDKN1B
92-1410	3945234	23344563	19,399	>100	CDKN1B
96-0885	16595	27822752	27,806	>100	CDKN1B
98-2805	16595	27805680	27,789	>100	CDKN1B
99-2697	9793879	13152331	3,359	>50	CDKN1B
99-3248	16595	26700467	26,684	>50	CDKN1B
01-1426	11945983	13152331	1,206	19	BCL2L14, LRP6, MANSC1, LOH12CR2, LOH12CR1, DUSP16, CREBL2, GPR19, CDKN1B, APOLD1, DDX47, RPL13AP20, GPRC5A, GPRC5D, HEBP1, LOC100506314, HTR7P1, KIAA1467, GSG1
02-3018	8623654	13749846	5,126	>100	CDKN1B
02-3977	11528797	21412933	9,884	>50	CDKN1B
04-3370	16595	24439697	24,423	>100	CDKN1B
04-3511	16595	20226572	20,210	>100	CDKN1B
05-5035	16595	27395869	27,379	>100	CDKN1B

***** The genome coordinates correspond to the NCBI Build 36.1, hg18 assembly.

The presence of the *CDKN1B* deletions was verified by quantitative genomic PCR in fourteen cases of which sufficient material was available and we detected heterozygous deletions in thirteen of the cases and in case 02-3018 even a homozygous one (Fig. 12).

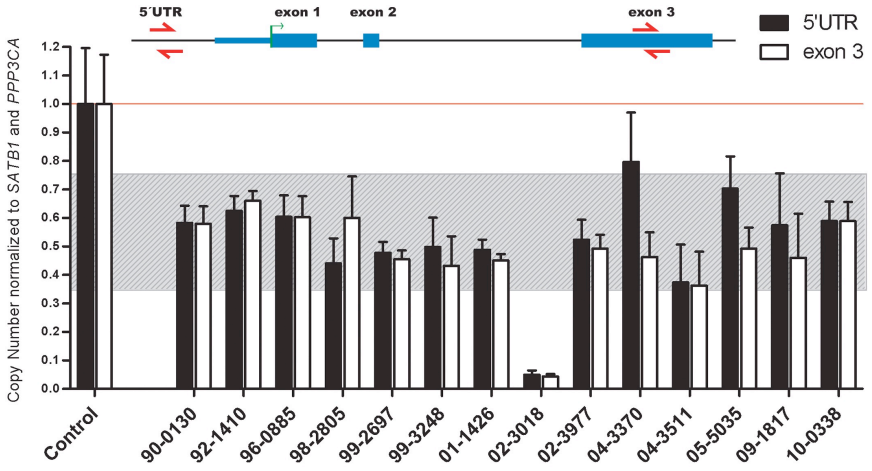

Figure 12. Detection of *CDKN1B* deletions. Quantitative genomic PCR for copy number alterations using primers located in the 5' UTR and exon 3 of *CDKN1B* and normalized to the reference genes *SATB1* and *PPP3CA*. A value of 1 indicates two copies; values between 0.75-0.35 indicate a heterozygous, and ≤0.35 a homozygous deletion. Red arrows, localization of primer pairs.

To determine whether *CDKN1B*-deleted T-ALLs show any specific genetic or biological characteristics they were analyzed in more detail. First, employing RT-qPCR we assessed the *CDKN1B* expression levels in the *CDKN1B*-deleted cases and compared them to the levels in a pool of normal CD3+ T-cells isolated from peripheral blood of three healthy individuals. In several of the cases *CDKN1B* showed lower transcript levels than expected in case of heterozygous deletions (Fig. 13B), corroborating our hypothesis that *CDKN1B* expression is repressed by other mechanisms.

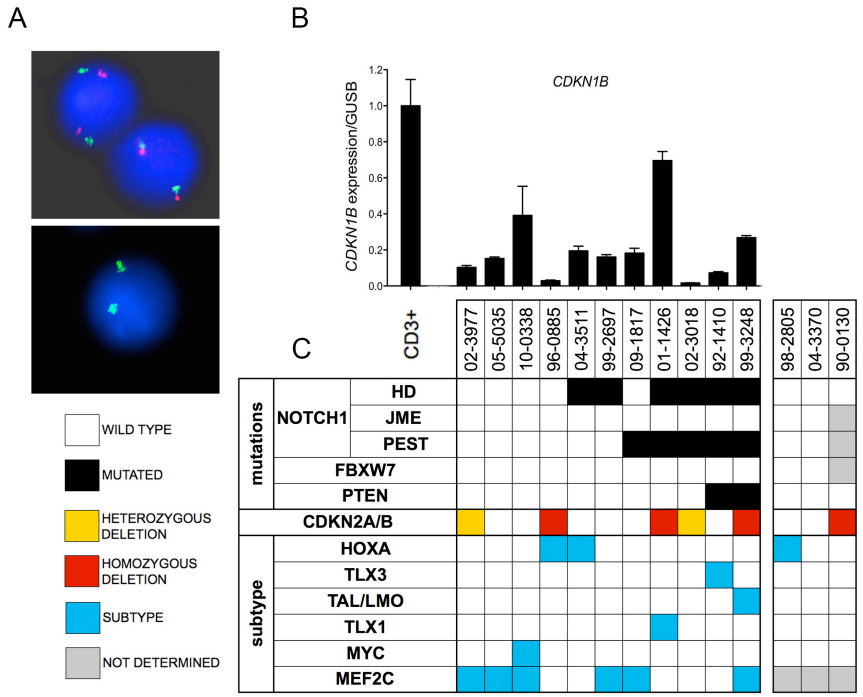

Figure 13. Characterization of 14 *CDKN1B*-deleted T-ALL patients. (A) FISH analysis with *CDKN2A/B* (red signals) and chromosome 9 centromere-specific probes (green signals) showing a sample with normal *CDKN2A/B* status (upper image) and one with a homozygous deletion (lower image). (FISH images were provided by M. König). (B) *CDKN1B* transcript levels were normalized to the *GUSB* reference gene and pooled CD3+ T-cells from three healthy individuals. (C) Summary of genetic alterations in *CDKN1B*-deleted cases and assignment to the major T-ALL subtypes. HD, heterodimerization domain; JME, juxtamembrane expansion. *Note*: The cases are clustered based on the mutation status of the genes implicated in *CDKN1B* transcriptional regulation – NOTCH1, FBXW7, and PTEN.

To determine whether alterations of *NOTCH1, FBXW7*, and *PTEN,* potentially directly or indirectly implicated in *CDKN1B* regulation, are associated with *CDKN1B* expression levels, we conducted a mutation screening of these genes (Fig. 13C, Table 6). However, in line with the observations in the T-ALL cell lines, also in the primary leukemia samples, neither a correlation between mutation patterns and *CDKN1B* expression levels nor a specific association of any mutation with *CDKN1B* deletions was found. In fact, the frequencies of mutations in the investigated genes were highly similar to those in unselected T-ALL cohorts (Table 6).

In addition, the major T-ALL subtypes including the *TAL*/*LMO*, *TLX1*, *TLX3*, and *HOXA* clusters as well as the immature subgroup, characterized by expression of *MEF2C* and the proliferative cluster in about 30% of the cases associated with T-cell receptor rearrangements (*TRAD* and *TRB*), were identified by FISH and/or RT-qPCR.

These analyses revealed that one case each was positive for *TLX1*, *TLX3*, *TRAD-MYC, KMT2A-MLLT4* (alias *MLL-AF6*), *PICALM-MLLT10* (*alias CALM-AF10*), and *TRB-HOXA*; and one case harbored a cryptic *LMO2*-activating deletion detected by aCGH. Therefore, 21% (3/14) of the *CDKN1B*-deleted cases belong to the *HOXA* cluster and only 7% (1/14) to the *TLX3* subtype, which usually account for 10% and 20-25% of all T-ALL cases, respectively (Van Vlierberghe and Ferrando, 2012; Van Vlierberghe et al., 2008). 54% (6/11) of the *CDKN1B*-deleted patients showed an increased *MEF2C* expression and were, thus, assigned to the immature T-ALL subtype (Fig. 5C), which generally accounts for roughly 10% of the cases (Homminga et al., 2011). (For the detailed description and analysis of these cases see section Results II "*MEF2C* dysregulation in *CDKN1B*-deleted T-ALL"). None of the cases showed a *TRAD* or *TRB* translocation indicative of the T-cell receptor to *NKX2-1* or *NKX2-2* rearrangements and of belonging to the proliferative cluster. However, since this cluster is usually defined by gene expression profiling (Homminga et al., 2011), we cannot rule out that one or the other of the cases belongs to this T-ALL subtype.

In terms of other copy number alterations, which were determined by aCGH and/or FISH analyses (Fig. 13A-C), the incidence of *CDKN2A/B* deletions in *CDKN1B*-deleted cases was lower as compared to *CDKN1B* wild-type cases (43% (6/14) vs 79% (71/90); 2-tailed Fisher's exact test, p=0.067). Although not statistically significant, these data support the notion that deletion of *CDKN1B* may represent another mechanism to impair cell cycle regulation, which is one of the core oncogenic pathways in T-ALL (Van Vlierberghe and Ferrando, 2012).

Table 6. Frequencies of genetic alterations in *CDKN1B*-deleted compared to unselected T-ALL cohorts

Genetic alterations	*CDKN1B*-deleted patients	*CDKN1B* wild-type patients	Unselected T-ALL cohorts*
Mutations			
NOTCH1	(7/13) 54%	(19/28) 68%	>60%
HD	(2/13) 15%	(11/28) 39%	20%
PEST	(1/13) 8%	(0/28) -	5%
PEST+HD	(4/13) 31%	(5/28) 18%	20%
JME	(0/13) -	(3/28) 10%	3%
FBXW7	(0/13) -	(5/28) 18%	8-30%
PTEN	(2/14) 14%	(2/28) 7%	10%
Copy number alterations			
CDKN2A/B deletion	(6/14) 43%	(21/28) 75%	>70%
Molecular subtype			
TAL/LMO	(1/14) 7%	(5/28) 18%	20-35%
TLX3	(1/14) 7%	(8/28) 29%	20-25%
TLX1	(1/14) 7%	(2/28) 7%	5-10%
HOXA	(3/14) 21%	(1/28) 4%	5-10%
MEF2C	(6/11) 54%	(4/28) 14%	10%

* these data have been retrieved from the literature (Graux et al., 2006; Homminga et al., 2011; Van Vlierberghe and Ferrando, 2012). HD, heterodimerization domain; JME, juxtamembrane expansion.

In summary, we show that *CDKN1B* deletions frequently arise in the *HOXA*/immature T-ALL subtype and that such cases have a lower incidence of *CDKN2A/B* deletions. Furthermore, *CDKN1B*-deleted cases may express lower levels of gene transcripts than expected in case of heterozygous *CDKN1B* deletions. However, low *CDKN1B* transcript levels were neither associated with mutations in *NOTCH1* and/or *FBXW7* nor *PTEN*.

I.3. *CDKN1B* expression in unselected T-ALL cases

To verify the previously finding that also *CDKN1B* wild-type cases may express low *CDKN1B* levels (Remke et al., 2009) we assessed the *CDKN1B* transcript levels in 28 *CDKN1B* non-deleted pediatric T-ALL cases. The selection of these patients was solely based on material availability and RNA quality and only samples with a RNA Integrity Number (RIN) value ≥5 were analyzed. Quantitative analysis of *CDKN1B* expression confirmed that indeed also *CDKN1B* non-deleted cases display heterogeneous and frequently very low *CDKN1B* transcript levels (Fig. 14A).

Also these samples were analyzed for mutations in *NOTCH1*, *FBXW7*, and *PTEN*, however, like in the *CDKN1B*-deleted cases, also in the *CDKN1B* wild-type samples no correlation with mutations in these genes and *CDKN1B* transcript levels was observed (Fig. 14B). The genetic characteristics of these cases showed the mutation patterns and major subtype frequencies usually observed in unselected cohorts of T-ALL (Table 6). For example, 68% (19/28), 18% (5/28), and 7% (2/28) of the cases were found to carry mutations in the *NOTCH1*, *FBXW7,* and *PTEN*, respectively. Furthermore, 29% (8/28) cases showed a *TLX3* rearrangement and 7% (2/28) a rearranged *TLX1*, but only 4% (1/28) belonged to the *HOXA* subtype. In one case (09-3756) we detected a *TRAD* rearrangement possibly with *NKX2-2*, which was subsequently confirmed by RT-PCR (Fig. 14C).

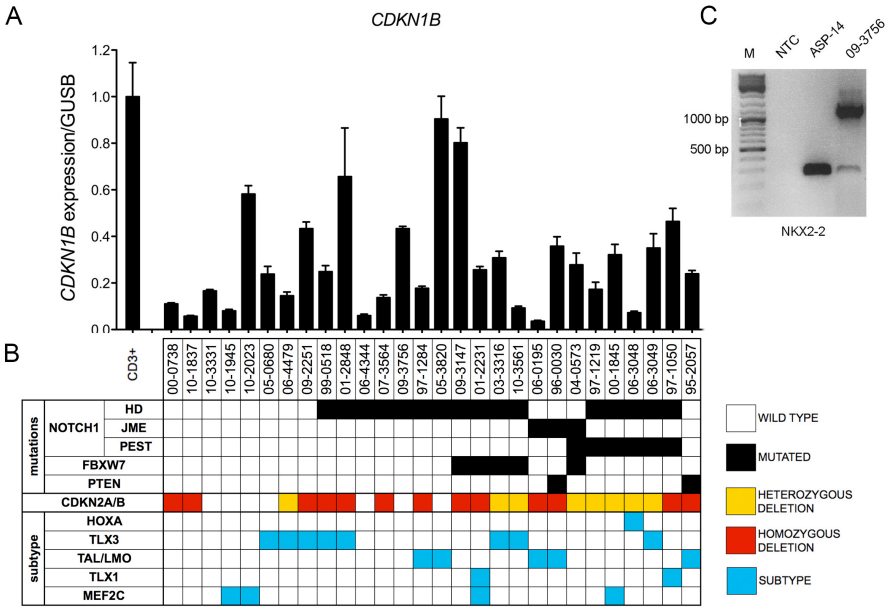

Figure 14. Characterization of *CDKN1B* wild-type T-ALL patients. (A) RT-qPCR for *CDKN1B* expression levels normalized to the *GUSB* reference gene and pooled CD3+ T-cells from three healthy donors showed variable and in some cases very low *CDKN1B* expression. (B) Mutations in *NOTCH1*, *FBXW7*, *PTEN*, and *CDKN2A/B* status and the specific T-ALL subtypes are depicted. *Note*: The cases are clustered based on the mutation status of the genes implicated in *CDKN1B* transcriptional regulation – NOTCH1, FBXW7, and PTEN. (C) RT-PCR confirming *NKX2-2* expression in case 09-3756 (lower band, 267 bp *NKX2-2* RT-PCR product; upper band, 1192 bp amplification product of genomic DNA contamination). HD, heterodimerization domain; JME, juxtamembrane expansion; ASP-14, sarcoma cell line used as positive control; NTC, non-template control; M, DNA marker.

Intrigued by these rather unexpected findings that contradict the concept that activation of NOTCH1 signaling via upregulation of *HES1* represses *CDKN1B* transcription (Murata et al., 2005), we further analyzed the *CDKN1B*-deleted and non-deleted primary T-ALL samples for the expression of *HES1*.

We generally observed a positive correlation between elevated *HES1* levels and NOTCH1/FBXW7 mutations. However, *HES1* expression did not correlate with that of *CDKN1B*, neither in the *CDKN1B*-deleted nor in the wild-type cases (Fig. 15). Of note, in some cases *HES1* expression did not correlate with NOTCH1 and/or FBXW7 alterations, supporting the notion that distinct mutations in different domains as well as specific

mutation patterns have a different relative strength on NOTCH1 signaling, and consequently on *HES1* expression levels, and that other triggers may as well activate the NOTCH1 signaling pathway (Larson Gedman et al., 2009).

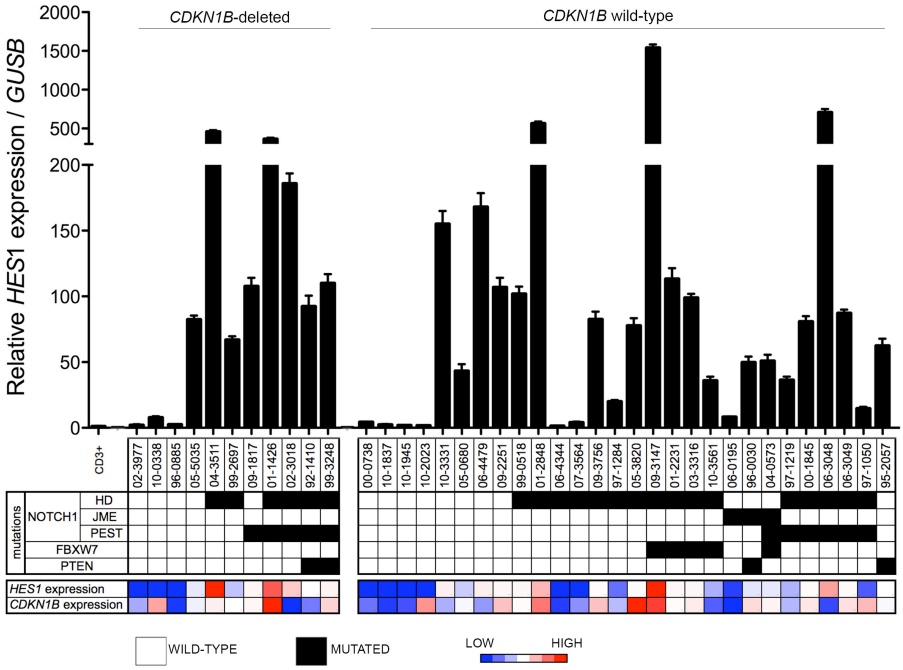

Figure 15. *HES1* expression in the T-ALL samples. Correlation with NOTCH1 signaling pathway mutations (NOTCH1, FBXW7) and *CDKN1B* expression. *HES1* expression levels normalized to the *GUSB* reference gene and pooled CD3+ T-cells from three healthy individuals generally correlated with the mutation status, but in most of the cases did not inversely correlate with *CDKN1B* expression levels. *Note*: The cases are clustered based on the mutation status of the genes implicated in *CDKN1B* transcriptional regulation – NOTCH1, FBXW7, and PTEN.

I.4. Complexity of Juxtamembrane NOTCH1 mutations

Interestingly, screening of NOTCH1 in the 39 T-ALL patients, revealed the presence of a rare type of mutations in three of them, located in the vicinity of exon 28 encoding the extracellular juxtamembrane domain, termed juxtamembrane expansion mutations (JEMs) (Sulis et al., 2008).

Generally, the mutation hotspots within NOTCH1 are the heterodimerization domain (HD), the PEST, and the juxtamembrane (JM) domains. Most HD mutations, comprising single amino acid substitutions and small in-frame deletions and insertions (class 1 mutations), destabilize the LNR-HD (LIN-12/NOTCH1 repeats) interaction and reduce heterodimer stability. In rare cases, insertions of extra amino acids between the distal part of the HD (HD-C) and the S2 cleavage site (class 2 mutations) displace the S2 away from the protective effects of the LNR-HD complex and expose it to cleavage by ADAM-type metalloproteases (Malecki et al., 2006; Weng et al., 2004). Generally, both HD-C class 2 and JME mutations are generated by relatively long insertions resulting from, at least partial, internal tandem duplications (ITDs). However, in case of class 2 HD-C NOTCH1 mutations, aberrant S2 cleavage is induced by the insertion of extra amino acids immediately proximal to the S2 cleavage site, which is displaced closer to the membrane and out of reach of the protective effects of the LNR-HD complex (Tzoneva and Ferrando, 2012). In contrast, JME insertions are located distal to the S2 cleavage site and displace the LNR-HD complex and the S2 site away from the membrane without altering the primary structure of any of these elements (Gordon et al., 2009; Malecki et al., 2006; Sulis et al., 2008).

In three T-ALL cases (3/39; 7.7%) we detected insertions in exon 28, which were analyzed in detail by sequence analysis of the cloned PCR products (Fig. 16A) and resulted in in-frame insertions of 7 (06-0195), 13 (96-0030) or 14 (04-0573) amino acids in the extracellular juxtamembrane region (Fig. 17). Of note, in cases 96-0030 and 06-0195 the mutations led to amino acid substitutions at the insertion sites but only the actual

number of amino acids expanding the protein were counted (Fig. 17). Remarkably, in case 04-0573 the ITD of 14 amino acids created a potential second S3 γ-secretase cleavage site. Furthermore, while in two of the cases (96-0030 and 04-0573) the inserted amino acids included an ITD, in the third case (06-0195) they were completely unrelated to NOTCH1 sequences (Fig. 17). Additionally, in the latter case a heterozygous point mutation leading to an F1736L amino acid change was detected (Fig. 16A, Fig. 17).

To obtain a more comprehensive picture of the amino acid compositions of JME mutations, we examined all cases with such mutations previously reported (Asnafi et al., 2009; Fogelstrand et al., 2014; Sulis et al., 2008; Zhu et al., 2006) and deposited in the COSMIC database (http://cancer.sanger.ac.uk/cosmic). Our analysis revealed an additional patient (case 29) showing a *de novo* insertion rather than an ITD (Fig. 17). Consequently, these two cases (06-0195 and 29) lacked the common tetrapeptide QLHF motif present in the JME mutants previously identified (Sulis et al., 2008), and case 4018 displayed only a tripeptide LHF sequence (Fig. 17), supporting the notion that NOTCH1 activation by JME mutants is not dependent on this motif (Sulis et al., 2008).

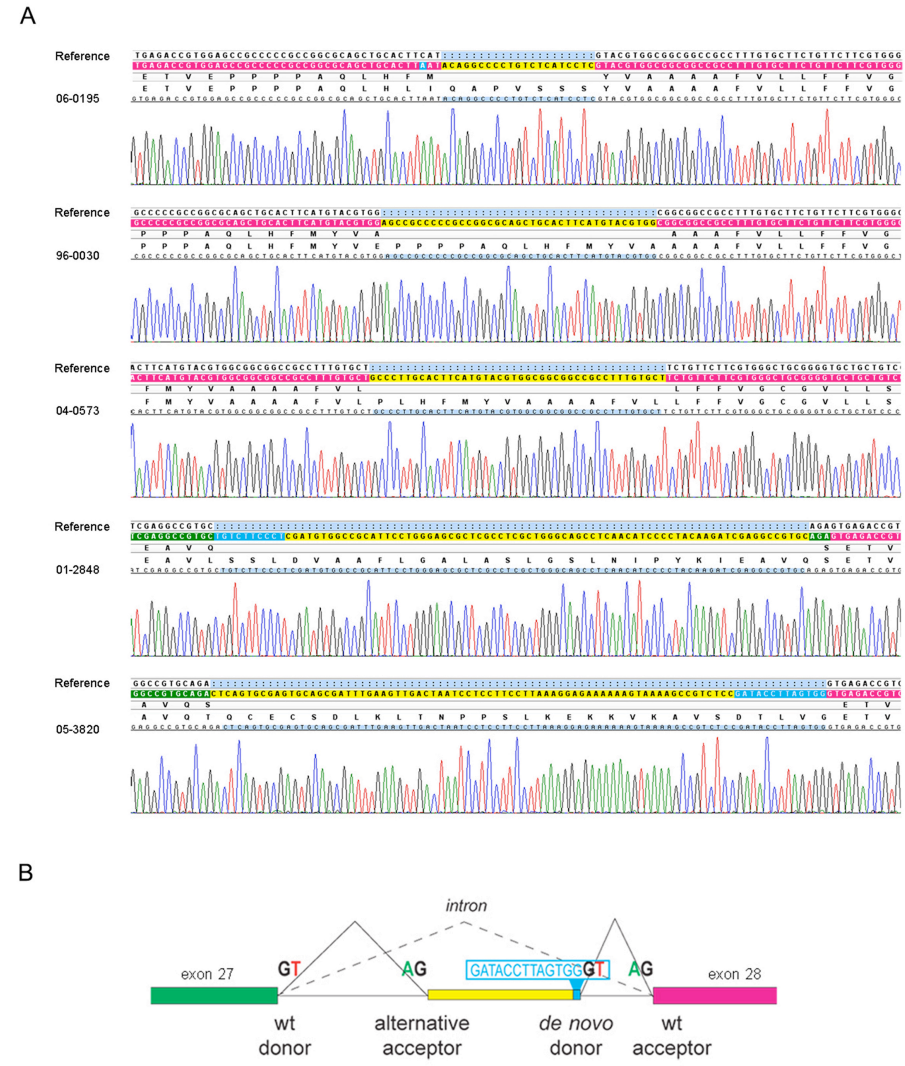

Figure 16. Analysis of NOTCH1 juxtamembrane insertion mutations. (A) Sequence analysis of cloned RT-PCR products showing the duplications and *de novo* insertions marked in yellow and blue, respectively. (B) Schematic representation (not drawn to scale) of the partial intron retention (yellow bar) and the *de novo* insertion (blue sequence) in case 05-3820 creating a new splice donor site and resulting in alternative acceptor splice site usage. wt, wild-type.

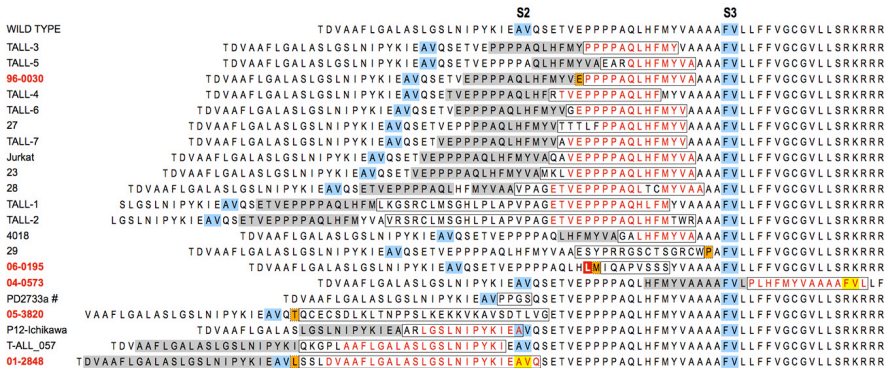

Figure 17. Prediction of the amino acid changes of NOTCH1 juxtamembrane expansion mutations detected in T-ALL cell lines and primary leukemia samples retrieved from the COSMIC database and the cases described herein (marked in bold/red) arranged based on the S3 cleavage site. S2, ADAM-type metalloproteases cleavage site; S3, γ-secretase cleavage site; boxed amino acids, insertions; red, tandem duplicated amino acids (ITDs); gray, duplicated amino acids; light blue, S2 and S3 cleavage sites; yellow, potential *de novo* cleavage sites; orange, amino acid substitutions; red square, missense mutation. #*Of note*: Due to differences in the description of the mutation in case PD733a in the original publication and the COSMIC database, we have reanalyzed the sequence and these data are shown.

In addition, we detected two cases (2/39; 5.4%) with rare juxtamembrane insertion mutations (Fig. 16A) in the NOTCH1 HD-C domain adjacent to the S2 cleavage site. Similarly to the mutations described above, also these resulted in amino acid substitutions at the insertion sites and also in these cases just the actual numbers of introduced amino acids were considered as expansion. In case 01-2848 the mutation was a 28 amino acids long, almost perfect ITD creating a potential second S2 site and in 05-3820 an insertion of 29 entirely NOTCH1-unrelated amino acids (Fig. 17). Sequence analysis of the cloned RT-PCR product of the latter case uncovered a partial retention of intron 27 followed by a small *de novo* insertion (Fig. 16A). Genomic PCR using primers located in the mutation flanking sequences followed by direct sequencing of the PCR product confirmed the insertion in intron 27. Notably, *in silico* splice site prediction revealed the presence of an alternative acceptor splice site in intron 27 and the generation of a new donor splice site by the insertion, suggesting that aberrant alternative splicing is involved in the generation of the mutated NOTCH1 protein (Fig. 16B).

Although insertion mutations in this region have already been described (Breit et al., 2006; Maser et al., 2007; Weng et al., 2004), it is interesting to note that – except for one case (PD2733a) with a short 4 amino acids long insertion distal to the S2 site – all mutations retrieved from the COSMIC database were located at the N-terminal rather than the C-terminal side of the S2 cleavage site (Fig. 17). While insertions at the S2 C-terminal side may well displace the NOTCH1 negative regulatory region and leave the S2 site unprotected, it is tempting to assume that those on its C-terminal side are more similar to JME mutations. However, in case 05-3820 the ITD of the region containing the S2 cleavage site might also displaces at least one of the sites away from the protective effects of the LNR-HD complex. Remarkably, in case 01-2848 harboring the HD-C insertion mutation, creating a second S2 cleavage site, *HES1* expression was extremely elevated (Fig. 15), indicating that the presence of two such sites may enhance the accessibility to ADAM-like metalloproteases.

Taken together, insertion expansion mutations in the NOTCH1 juxtamembrane region may be generated by complex mechanisms including tandem duplications, *de novo* insertions and partial intronic retention events in combination with alternative splicing.

RESULTS II

MEF2C dysregulation in CDKN1B-deleted T-ALL

Recently, Homminga and colleagues characterized the so-called "immature" T-ALL subtype, which overlapped with the immature cluster previously identified by Soulier *et al.* (Soulier et al., 2005), the LYL subgroup defined by Ferrando *et al*. (Ferrando et al., 2002), and the early T-cell precursor phenotype T-ALL (ETP-ALL) described by Coustan-Smith *et al*. (Coustan-Smith et al., 2009), suggesting that all these subgroups might constitute a single disease entity characterized by *MEF2C* overexpression (Homminga et al., 2011).

As shown in Results I "Characterization of pediatric *CDKN1B*-deleted T-ALL", several of the *CDKN1B*-deleted cases did not fall into any of the *TAL*/*LMO*, *TLX1*, *TLX3*, and *HOXA* clusters and therefore, to further classify these cases we determined whether they belong to the subtype characterized by *MEF2C* expression.

II.1. *MEF2C* expression in pediatric T-ALL samples

In order to compare *CDKN1B*-deleted and wild-type patients both groups were subjected to quantitative gene expression for *MEF2C*. The expression values were normalized to that of the cell line Loucy, known to have an ETP-like phenotype and to express *MEF2C* due to a del(5)(q14q35) (Homminga et al., 2011; Nagel et al., 2008; Van Vlierberghe et al., 2011). As additional controls we included the cell lines RPMI-8402, CCRF-CEM, and MOLT-16 previously described to express *MEF2C* as well as the *MEF2C* negative cell lines HSB-2, TALL-1, and DND-41 (Nagel et al., 2008). RPMI-8402 also carries a 5q14 deletion and CCRF-CEM harbors a t(5;14)(q35.2;q32.2) rearrangement, resulting in the ectopic expression of *NKX2-5* by its juxtaposition to the *BCL11B*

enhancer, and consequently leading to the induction of *MEF2C* by NKX2-5 (Homminga et al., 2011; Nagel et al., 2003; Nagel et al., 2008; Nagel et al., 2007; Przybylski et al., 2006).

Intriguingly, 45% (5/11) of the *CDKN1B*-deleted patients showed high levels of *MEF2C* expression, and one case (10-0338), harboring a *TRA-MYC* translocation also displayed at least a moderate increase of *MEF2C*, which was comparable to that in the T-ALL cell line MOLT-16 positive for the same genetic alteration (Fig. 10, Table 4). Notably, MEF2C is able to synergize with MYC in driving cellular transformation (Homminga et al., 2011). In contrast, only 14% (4/28) *CDKN1B* wild-type cases displayed elevated *MEF2C* levels (Fig. 18). Hence, including the *TRA-MYC*-positive case, *CDKN1B*-deleted patients showed a statistically significant higher frequency of *MEF2C* dysregulation as compared to the wild-type cases (6/11 vs 4/28; p=0.017; 2-tailed Fisher's exact test).

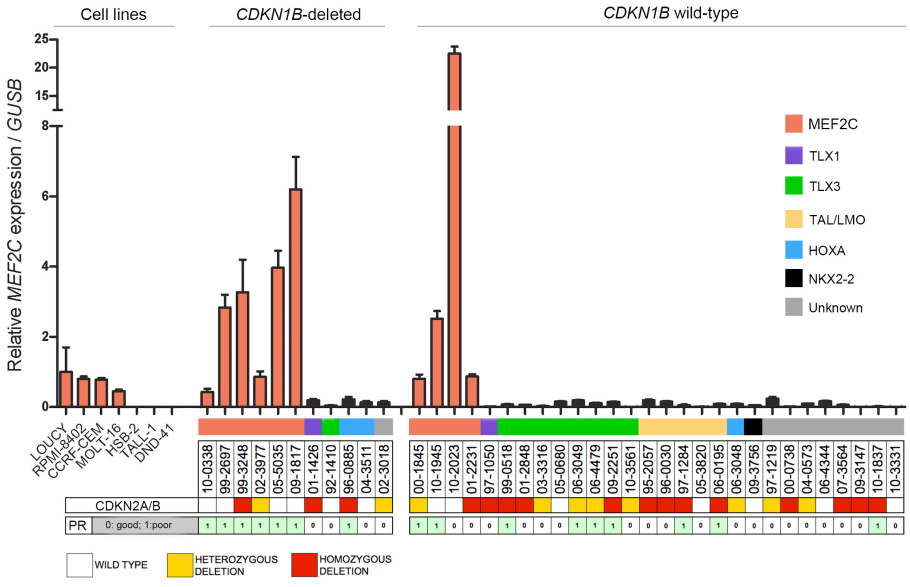

Figure 18. *MEF2C* expression in T-ALL patients and T-ALL cell lines. *MEF2C* expression levels normalized to the *GUSB* reference gene and to the cell line Loucy known to express *MEF2C* due to a del(5)(q14q35). Patients are clustered according to the main T-ALL subtypes. PR, prednisone response.

Since a variety of distinct genetic alterations, in particular *BCL11B*-mediated activation of *NKX2-5*, converge on the activation of *MEF2C* (Homminga et al., 2011; Nagel et al., 2008), we analyzed the *MEF2C* expressing cases with unknown primary subtype-defining alterations by FISH for rearrangements of the *BCL11B* locus. However, only two patients showed an altered FISH signal pattern indicating a *BCL11B* driven upregulation of *NKX2-5.*

Amongst the *CDKN1B*-deleted cases, 02-3977 showed a split signal for the *BCL11B* probes and RT-PCR for *NKX2-5* expression detected an upregulation of the gene, indicating the presence of a *BCL11B-NKX2-5* rearrangement (Fig. 19, Table 7). Moreover, in one of the cases (09-1817), for which no aCGH data were available, cytogenetics showed a der(5) chromosome, possibly indicating upregulation of *MEF2C* by the previously described *MEF2C*-activating 5q14 deletion (Homminga et al., 2011; Nagel et al., 2008). However, a more detailed analysis will be required to determine whether this mechanism of *MEF2C* upregulation indeed applies to this case.

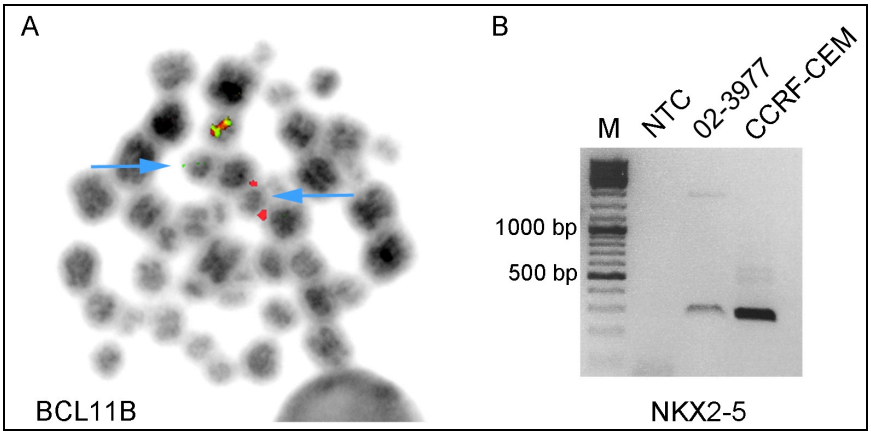

Figure 19. *BCL11B-NKX2-5* rearrangement identified by FISH and RT-PCR. (A) Metaphase FISH for case 02-3977 showing a split signal using *BCL11B* locus-specific probes (blue arrows) (picture provided by M. König). (B) RT-PCR confirming the presence of *NKX2-5* expression. CCRF-CEM carrying a t(5;14)(q35.2;q11.2) was used as positive control. NTC, non-template control; M, DNA marker.

Of the four *CDKN1B* wild-type patients, case 10-2023 displaying a *MEF2C* dysregulation, but with unknown T-ALL subtype, showed a gain of the *BCL11B* locus-specific probe, which contains the enhancer generally driving ectopic expression of the translocation partner (Nagel et al., 2007). Metaphase FISH analysis indicated a *BCL11B* rearrangement with a novel partner gene located at 6q27 (data not shown). These data confirm that a broad spectrum of different genetic alterations, several of which remain to be determined, result in the induction of *MEF2C* expression (Homminga et al., 2011; Nagel et al., 2008).

The distribution of characteristic T-ALL genetic lesions (*NOTCH1*, *FBXW7* or *PTEN*) did not differ between the patients expressing *MEF2C* and the non-expressing cases (Table 7). However, *CDKN2A/B* deletions were found in a lower proportion of the *CDKN1B*-deleted patients as compared to the wild-type cases (40% (4/10) *vs* 75% (22/29), p=0,056; 2-tailed Fisher's exact test), suggesting that in these cases impaired cell cycle regulation may be rather related to p27kip1 haploinsufficiency than to the loss of p16 function.

Table 7. Genetic characteristics of *CDKN1B*-deleted and *MEF2C*-dysregulated cases

Case	Karyotype	Rearrangement	MEF2C	CDKN1B	CDKN2A	NOTCH1	FBXW7	PTEN
90-0130	47,XX,+8[8]/46,XX[12]	unknown	ND	+/-	-/-	WT	ND	WT
92-1410	46XY,del(12)(p11),M7[20]	TRB-TLX3	-	+/-	+/+	MUT	WT	MUT
96-0885	46,XY[7]	PICALM-MLLT10	-	+/-	-/-	WT	WT	WT
98-2805	46,XX,del(11)(q22),add(12)(p13)[15] 46,XX,del(6)(q23),del(11)(q22),add(12)(p13)[4] 46;XX[11]	KMT2A-MLLT4	ND	+/-	+/+	WT	WT	WT
99-2697	48,XY,+Y,del(5)(q13q33),+10,inv(17)(p13q22?)[20]	unknown	+	+/-	+/+	MUT	WT	WT
99-3248	45,XY,t(12;18)(p13;q11?)[8]	LMO2 (activating deletion)	++	+/-	-/-	MUT	WT	MUT
01-1426	46,XY,del(9)(p21)[14]/46,XY,inv(2)(p25q34?),del(9)(p21)[5]/ 46,XY[2]	N-TLX1	-	+/-	-/-	MUT	WT	WT
02-3018	46XX,del(1)(p21p32),del(9)(p11)[14]/46,XX[6]	unknown	-	-/-	+/-	MUT	WT	WT
02-3977	45,XY,-7,add(9)(p24?),-12,+mar[3]/46,XY[3]	BCL11B-NKX2-5	+	+/-	+/-	WT	WT	WT
04-3370	46,XY,add(5)(q35),add(12)(p13),add(16)(p13)[6]/46,XY[2]	unknown	ND	+/-	+/+	WT	WT	WT
04-3511	46,XY,del(12?)(p13?)[3]/46,XY[2]	TRB-HOXA	-	+/-	+/+	MUT	WT	WT
05-5035	46,XX,+del(1)(p22)[7],del(2)(q27)[6],der(2)t(2;12)(q37;q11), -5,add(7)(p22),del(7)(p15)[4],-12,add(19)(p13),+1- 2mar[cp8]/46,XX[22]	unknown	++	+/-	+/+	WT	WT	WT
09-1817	47,XY,der(5),del(9)(q1?3q2?2),del(12)(p11~22),+13[5]/47,X Y,der(5),del(12)(p11~ 22),+13[3]/46,XY[12]	unknown	++	+/-	+/+	MUT	WT	WT
10-0338	46,XY[12]	TRAD-MYC	+	+/-	+/+	WT	WT	WT

Table 7. Genetic characteristics of *CDKN1B*-deleted and *MEF2C*-dysregulated cases (continued)

Case	Karyotype	Rearrangement	MEF2C	CDKN1B	CDKN2A	NOTCH1	FBXW7	PTEN
00-1845	46,X,del(Y)(q11),der(9)[10]	unknown	+	+/+	+/-	MUT	WT	WT
01-2231	46,XX[20]	TRAD-TLX1	+	+/+	-/-	MUT	MUT	WT
10-1945	46,XY[12]/47,XY,+11[1]	unknown	++	+/+	+/+	WT	WT	WT
10-2023	46,XY[8]	BCL11B-N	+++	+/+	+/+	WT	WT	WT

CDKN1B and *CDKN2A* deletions: +/+ wild-type, +/- heterozygous, -/- homozygous deletion; *MEF2C* expression: - negative, + moderate, ++, high, +++ very high; ND, not determined; WT, wild-type; MUT, mutated.

II.2. Immunophenotypic characteristics of *CDKN1B*-deleted and *MEF2C*-expressing T-ALL

Given that *MEF2C* upregulation is highly associated with an immature expression signature, which closely resembles that of ETP-ALL (Coustan-Smith et al., 2009; Ferrando et al., 2002; Soulier et al., 2005), we aimed to determine whether *CDKN1B* deletions and/or *MEF2C* dysregulation are associated with particular immunophenotypic characteristics (Table 5). Since the defining immunophenotypic criteria for ETP-ALL are still controversially discussed, we applied two different cell surface marker expression patters to determine whether any of these cases might fulfill ETP-ALL criteria (Coustan-Smith et al., 2009; Zuurbier et al., 2014).

However, only three of the *MEF2C* expressing cases, of which a complete immunophenotype was available (09-1817, 10-1945, and 10-2023) showed the originally defined ETP phenotype: absence of CD1a and CD8 (<5% positive lymphoblasts, absent or weak expression of CD5 (in ≤75% of total cells or ≥10-fold lower than in normal T-cells), and expression of one or more of the myeloid/stem cell antigens CD117, CD34, HLA-DR, CD13, CD33, CD11b, or CD65 on ≥25% of total cells (Coustan-Smith et al., 2009). In contrast, for example, case 99-3248 expressed CD1a and 01-2231 was positive for both CD1a and CD8, thus not fulfilling these ETP criteria.

Also the ETP phenotype CD1a-, CD4-/CD8-, CD34/CD33/CD13+ proposed by Zuurbier *et al*. (Zuurbier et al., 2014), which is thought to better reflect the ETP-ALL underlying gene expression signature than the *bone fide* ETP immunophenotype suggested by others (Coustan-Smith et al., 2009), did only apply to the minority of the cases (Table 5). However, for several of the primary leukemia samples only historic flow cytometry data were available and therefore, various markers nowadays used for assessing ETP-ALL were not available. Most importantly, CD5 expression was in former days mostly just judged as positive or negative without referring to its quantitative expression in relation to normal T-cells.

Therefore, in some of the cases the immunophenotype might not be completely accurate.

Nevertheless, virtually all of the *MEF2C* expressing cases expressed one or the other myeloid- or B-lineage-specific marker such as CD13, CD65s, or CD79A, suggesting a certain lineage plasticity of leukemic blasts (Table 5).

Together, these data indicate that *MEF2C* dysregulation, though associated with the currently defined ETP-like phenotype, is not restricted to this subtype of T-ALL. This notion is also supported by the gene expression data available from the Pediatric Cancer Genome Project, which shows that *MEF2C* expression does not exclusively occur in ETP-ALL (http://explore.pediatriccancergenomeproject.org/).

[1] **Legend to Table 8**. Numbers represent percentage of positive blast cells. According to EGIL criteria >20% and >10% of blast cells positive for surface and cytoplasmic markers, respectively, is considered as positivity of the leukemic blast cell population. Negative CD markers are marked in grey, borderline 15-25% positivity for surface markers and 8-10% for cytoplasmic markers in yellow, and positive ones in orange, white fields indicate not determined. In case 09-1817 the percentage of CD33+ cells was not available; My, myeloid; B, B-cell; nd, not determined; na, not available.

Table 8. Immunophenotypic characteristics of *CDKN1B*-deleted and *MEF2C*-dysregulated pediatric T-ALL cases [1]

	LabID	EGIL	MEF2C	ETP-like	cyCD3	sCD3	CD7	CD2	CD5	CD1a	CD4	CD8	Tα/β	Tγ/δ	CD34	CD117	TdT	HLA-DR	CD79A	CD10	CD5/10	CD13	CD33	CD65s
CDKN1B deleted	92-1410	T-II	-	no	97	10	90		30	0	10	3			4		40	0		0		0	0	0
	02-3018	T-III	-	no	90	2	92	9	92	73	93	0			11		61	46	1		22	0		
	04-3511	T-III	-	no	97	37	92	1	39	48	45	14			0	3	80	1			18			
	01-1426	T-III	-	no	93	2	97	97		90	90	79	1	3	2		89	3	2	43				
	96-0885	T-IV/My+	-	no	96	85	90		90	10	0	35	1	77	0		75	0		30		0	0	35
	10-0338	T-IV	+/-	no	78	72	97	88	67	3	3	1	4	70	8	4	1	15	9	2	0	0		
	02-3977	T-II/My+/B+	+	no	90	4	95	4	69	0	2	2	3	1	0		10	3	34	3	3	92		
	99-2697	T-II/My+	+	no	97	0	99	14	84	0	0	0	0	0	98		54	7		0		0	9	23
	99-3248	T-III/My+	++	no	95	3	97	98	96	92	26	73			0	1	71	2		0		0	0	31
	05-5035	T-II/My+	++	no	92	8	96	95	93	3	5	3	8	1	67	0	38	19	2	11	7	58		
	09-1817	T-II/My+	++	**yes**	67	7	99	97	10	17	7	0	7	1	83	0	68	24	7	0	0	17	na	
	98-2805	T-IV	nd	no	84	89	96	97		5	10	1	0	81	84		32	5	3				3	
	04-3370	T-IV	nd	no	85	91		15	91	24	1	90	4	94	22	2	40	15			6			
	90-0130	T-II	nd	no	80		90			10	80	80					0	0		0		0	0	0
CDKN1B wt	00-1845	T-II/B+	+	no	98	0	99	99	98	0	6	37			0		74	2	80	91	91	1	1	1
	01-2231	T-III	+	no	84	9	87	91		70	68	4	8	1	1		69	11	7	16		4	2	
	10-1945	T-II	++	**yes**	21	0	95	81	2	1	1	1	2	0	54	88	0	98	0	1	1	21		
	10-2023	T-II	+++	**yes**	57	3	95	99	0	0	2	1	1	0	3	0	83	65	1	0	0	22		

II.3. *MEF2C* expression predicts poor response to glucocorticoid therapy

Interestingly, samples of patients with a poor response to glucocorticoids, which constitute essential components of pediatric ALL therapy, expressed significantly higher *MEF2C* levels (Table 8, Fig. 20), corroborating the finding that *in vitro* *MEF2C*-dysregulated ETP-ALL is more resistant to prednisolone treatment (Zuurbier et al., 2014) and the resistance to treatment observed in patients with ETP-ALL (Coustan-Smith et al., 2009).

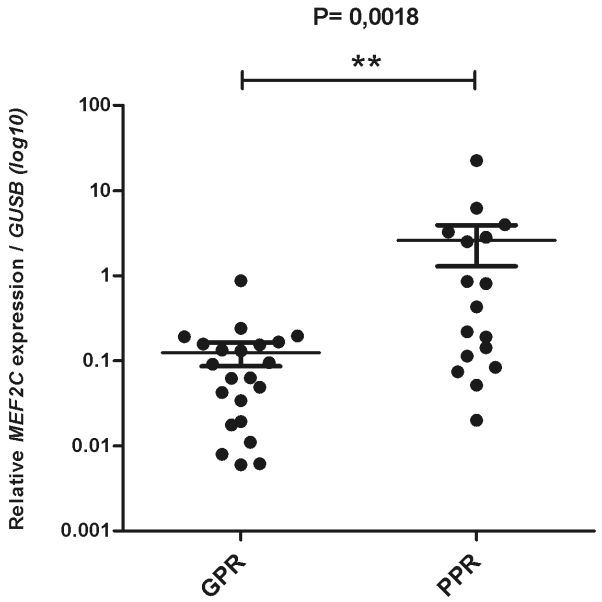

Figure 20. Prednisone response in correlation with *MEF2C* expression. Patients with poor prednisone response had a significant lyhigher expression of *MEF2C* (p=0,0018). Bars indicate median and standard deviation. Mann-Whitney test. GPR, good prednisone response; PPR, poor prednisone response.

RESULTS III

The role of SKP2 inhibitors in T-ALL

Proteolysis of p27kip1 is a critical event, which allows cells to transit from quiescence to a proliferative state, and is primarily regulated via ubiquitination by the S phase kinase-associated protein 2 (SKP2) and degradation via the ubiquitin-proteasome pathway (Nakayama and Nakayama, 2006). An inverse correlation between SKP2 and p27kip1 expression has been reported in several types of tumors and overexpression of SKP2 appears to be associated with a rather poor prognosis, suggesting that SKP2 inhibitors may hold promise for therapeutic intervention (reviewed in (Hershko, 2008)).

Therefore, efforts have been directed towards therapeutically targeting the ubiquitin-proteasome system in order to reduce protein degradation and consequently, small molecule inhibitors of SKP2 have been recently developed. For example, a compound termed C1 has been described to specifically target the interface between SKP2 and CKS1, an accessory protein responsible for the recognition of T187-phosphorylated p27kip1 (Fig. 21) (Wu et al., 2012). A second compound, C25, interacts with SKP2 and prevents its binding to SKP1, thus inhibiting SKP2-SCF E3 ligase activity (Chan et al., 2013) (Fig. 21).

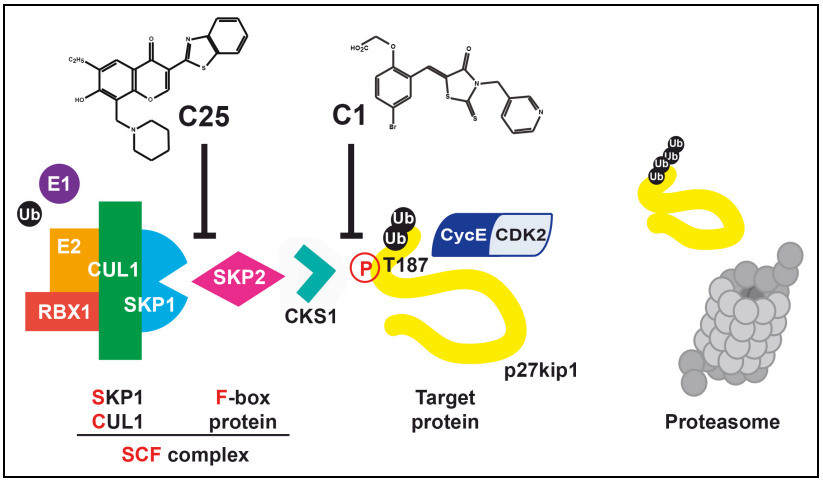

Figure 21. Small molecule inhibitors of SKP2 and their mechanisms of action. The SCF complex consists of four components, comprising S-phase kinase-associated protein-1 (SKP1), cullin-1 (CUL1), ring-box protein-1 (RBX1), and a variable F-box protein, which determines the specificity of the SCF ligase. Incorporation of SKP2 into the SCF complex triggers the ubiquitination of several targets, including p27kip1. Following phosphorylation at T187 by the cyclin E-CDK2 complex, the SCF-SKP2 complex recruits p27kip1 into the nucleus with the help of the accessory protein CKS1, which facilitates the binding between SKP2 and p27kip1. Polyubiquitinated p27kip1 is then degraded through the 26S proteasome. Compound C25 prevents the SKP1-SKP2 association and the SCF-SKP2 complex formation. Compound C1 interacts with SKP2 and hinders its fit into the molecular surface pocket at the SKP2-CKS1 interface and blocks p27kip1 ubiquitination.

III.1. Effects of small molecule inhibitors of SKP2 in T-ALL

As NOTCH1 is mutated in more than 60% of T-ALL and has been shown to induce transcription of *SKP2*, thereby promoting p27kip1 degradation and allowing cell cycle progression and proliferation (Dohda et al., 2007; Sarmento et al., 2005), we investigated the impact of the two small molecule inhibitors C1 and C25 of SKP2 in T-ALL. For this purpose, we selected four T-ALL cell lines (Jurkat, DND-41, TALL-1, and Loucy) with different mutational backgrounds (Fig. 22A) as a model system to determine the effects of these two compounds on the regulation of p27kip1 and used proliferation, apoptosis and cell cycle analysis as read-outs.

As already shown in RESULTS I “Characterization of T-ALL cell lines” and previously described by others (Dohda et al., 2007; Rodriguez-Rodriguez et al., 2014), SKP2 is up regulated in T-ALL cell lines compared to normal CD3+ T-cells. SKP2 transcript levels generally correlated well with the amount of protein, but only partially with the activation of NOTCH1 signaling, because TALL-1 and Loucy are both wild-type for NOTCH1 but nevertheless express relatively high levels of *SKP2* (Fig. 22B, C).

A

	NOTCH1	FBXW7	PTEN
Jurkat	Mut	Mut	Mut
DND-41	Mut	wt	wt
TALL-1	wt	wt	wt
Loucy	wt	wt	Del

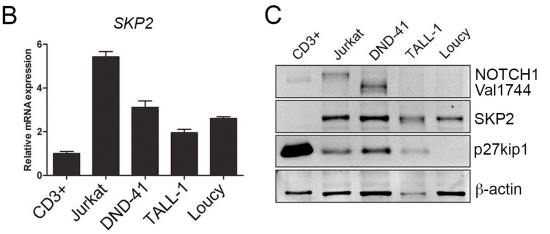

Figure 22. Gene and protein expression levels in T-ALL cell lines. (A) Table showing the mutational background of the selected T-ALL cell lines. Mut, mutated; Del, deleted; wt, wild-type. (B) Expression of *SKP2* was assessed by RT-qPCR and normalized to the reference gene *GUSB* and pooled CD3+ T-cells from healthy donors. (C) Western blots of total protein extracts showing active intracellular NOTCH1 in the cells carrying *NOTCH1* and/or *FBXW7* mutations. In all T-ALL cell lines rather high levels of SKP2 and low expression of p27kip1 were observed compared to normal CD3+ T-cells. Actin was used as loading control.

To ascertain that in T-ALL cell lines p27kip1 is degraded through the ubiquitin-proteasome system and that the protein levels can be upregulated by targeting this pathway, we treated the cells with the 26S proteasome inhibitor MG-132 and analyzed the protein levels by Western blotting (Fig. 23). We observed an induction of p27kip1 protein in the cell lines Jurkat, DND-41, and TALL-1, indicating that blocking the proteasome pathway indeed impedes the degradation of p27kip1 and promotes its accumulation. However, in Loucy we did not detect any trace of p27kip1 protein, suggesting that in this cell line its inactivation may be a pretranslational event. Whether in Loucy *CDKN1B* methylation, although not reported for T-ALLs (Kraszewska et al., 2012), the expression of certain non-coding RNAs or any other mechanisms play a role in *CDKN1B*-p27kip1 suppression remains to be determined.

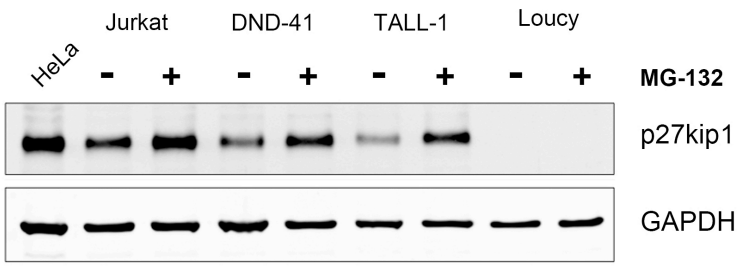

Figure 23. p27kip1 expression in T-ALL cell lines treated with proteasome inhibitor MG-132. Total protein extracts of the cells treated with 20 μM of the inhibitor for 5 hours were subjected to immunoblotting. HeLa was used positive and GAPDH as loading control.

Having shown that in T-ALL cell lines p27kip1 is degraded via the proteasome pathway, in a first step to study the effects of the SKP2 inhibitors C1 and C25 we determined the most appropriate concentrations for the treatment of the selected cell lines. C1 has so far been used in melanoma and breast cancer cell lines at concentrations between 5-10 μM for 16 hours (Wu et al., 2012), and for C25 concentrations of 10 μM and 20 μM were employed for the treatment of prostate adenocarcinoma cell lines (Chan et al., 2013).

Therefore, we first administered both compounds at concentrations of 10 μM for 16 hours; however, no effects were detectable (data not shown). Consequently, we extended the incubation times to 24, 48, and 72 hours and increased the concentration of C25 to 20 μM. Using these conditions, cell viability analysis by trypan blue (TB) exclusion staining, showed different sensitivities of the cell lines towards the two compounds (Fig. 24). While 20 μM C25 elicited some effect on cell growth in TALL-1, only minor effects in Loucy and DND-41, but none in Jurkat, all cell lines treated with C1 at a concentration of 10 μM showed a remarkable reduction in proliferation in a time-dependent manner and rapid cell death with an almost complete loss of viable cells after 3 days of treatment (Fig. 24).

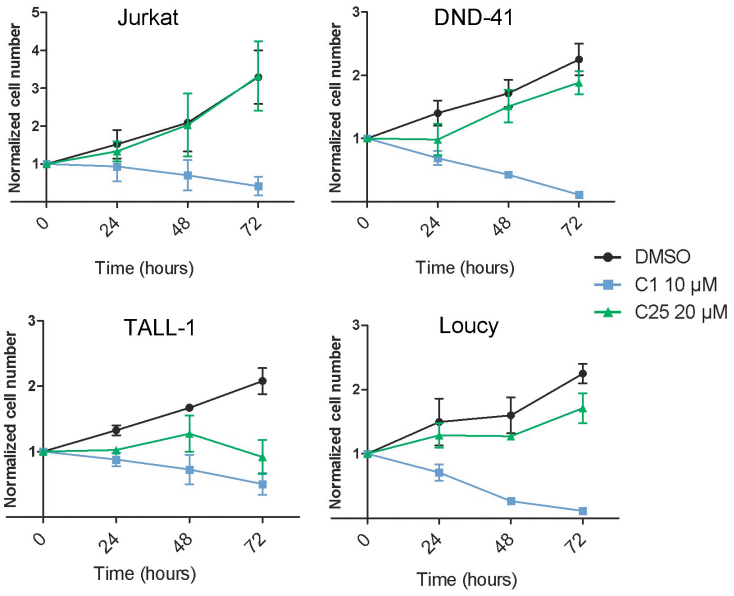

Figure 24. Growth curves upon treatment with C1 (10 µM) and C25 (20 µM). Proliferation was assessed after 24, 48, and 72 hours of drug treatment using TB exclusion staining. Means and standard deviations of two independent experiments are shown.

Western blot analysis for p27kip1 expression at least to some extent confirmed the differences regarding the sensitivity of the cell lines but the effects on p27kip1 were only minor (data not shown). In general, C25 resulted in a slight increase of p27kip1 protein levels after 24 and 48 hours. However, for C1 treated cells semi-quantification of the protein levels demonstrated basically no changes in the amount of p27kip1. In line with the results applying the proteasome inhibitor MG-132 (Fig. 23), neither of the compounds was able to induce p27kip1 in Loucy.

Based on these preliminary data we further optimized the concentrations of the compounds in that we determined the minimal concentrations required for an approximately 50% growth inhibition and a response in cell cycle without exceeding a maximum concentration of 1% DMSO (data not shown). Regarding compound C1, Jurkat was less sensitive to the drug and therefore, was treated with higher concentrations (4 µM and 8 µM) than DND-41, TALL-1, and Loucy (2,5 µM and 4 µM). Since we basically

did not observe any effects for compound C25, we decided to apply it at the maximal concentration of 20 µM used in another study (Chan et al., 2013).

III.2. Effects of C1 and C25 in T-ALL cell lines

Once the proper concentrations and time points for treatment and analysis were determined, we tested the effects of the compounds on proliferation, cell cycle and apoptosis. By counting viable cells, we observed that applying C1 resulted in a decrease of cell proliferation in a dose- and time-dependent manner in all cell lines as compared to untreated control cells (Fig. 25). In contrast, when using C25 only the cell line TALL-1 showed a slight reduction in cell growth (Fig. 25).

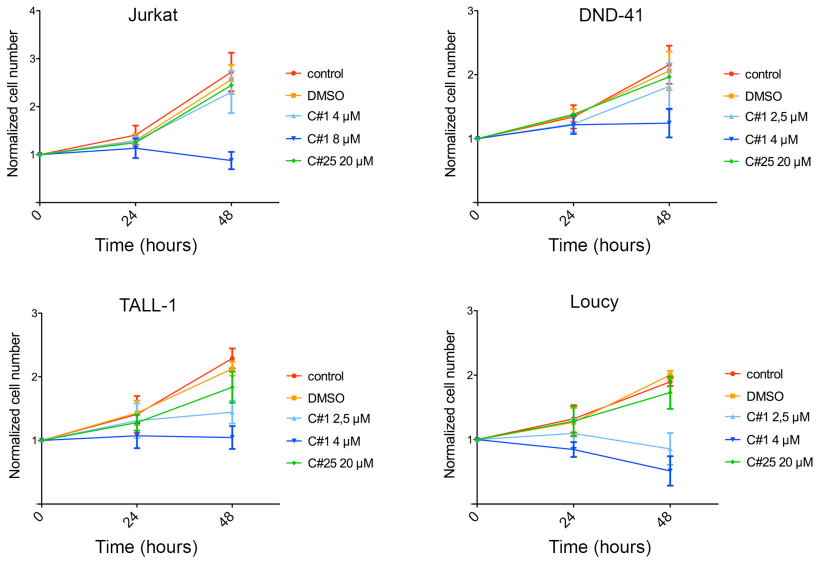

Figure 25: Effects of C1 and C25 on proliferation in T-ALL cell lines. Growth curves were generated based on cell viability determined by TB exclusion staining. Means and standard deviations of three independent experiments are shown.

To further investigate whether the lower rate of cell proliferation upon C1 treatment was related to apoptosis and cell death, we performed Annexin V/propidium iodide (Annexin V/PI) double staining followed by

flow cytometry analysis (Fig. 26A, B). This assay revealed that indeed the application of C1 induced apoptosis in the cell lines Jurkat and Loucy in a dose- and time-dependent manner, which was corroborated by the detection of cleaved PARP by Western blotting (Fig. 26C), but the effects were less pronounced in the cell lines DND-41 and TALL-1 (Fig. 26).

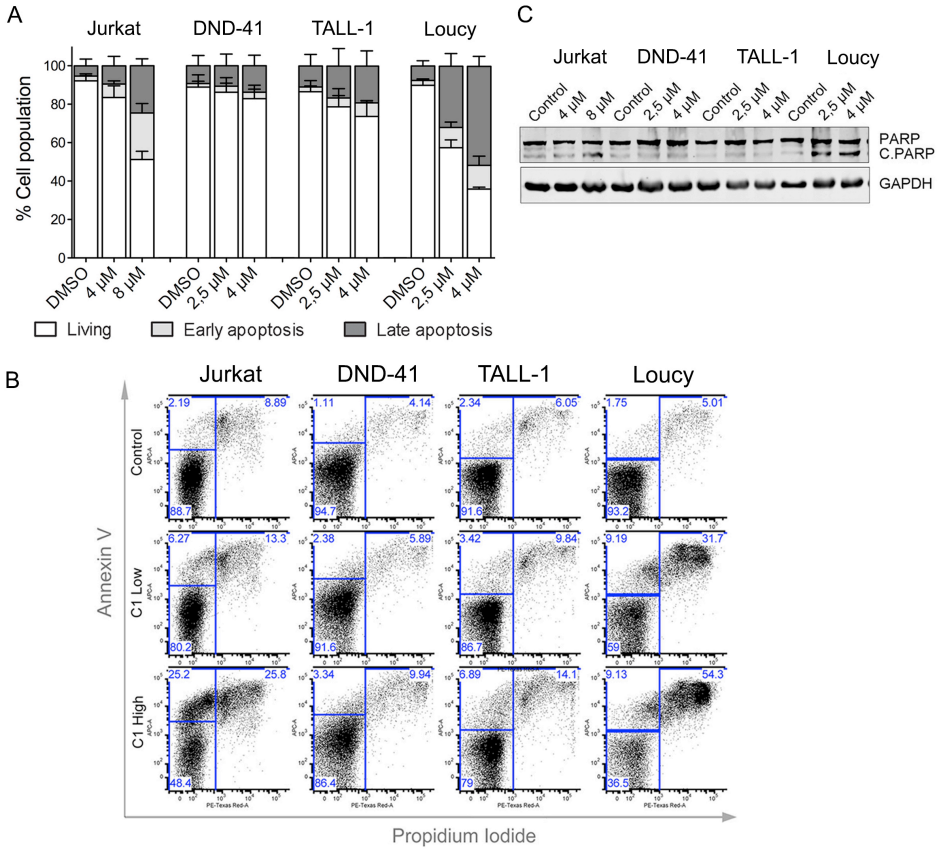

Figure 26. Effects of different concentrations of C1 on apoptosis after 48 hours of treatment. (A) The T-ALL cell lines showed different sensitivities against treatment with C1, e.g. Loucy displayed a higher sensitivity as compared to Jurkat. Means and standard deviations of three independent experiments are shown. (B) Representative FACS plots of Annexin V/PI staining. Left lower gate, living cells; left upper gate early and right gate late apoptotic cells. (C) Detection of cleaved PARP (C.PARP) by Western blotting confirmed the results observed by flow cytometry. GAPDH was used as loading control.

In contrast and consistent with the cell proliferation results shown in Fig. 25, compound C25 caused no significant changes with regard to apoptosis and cell death in any of the cell lines (Fig. 27).

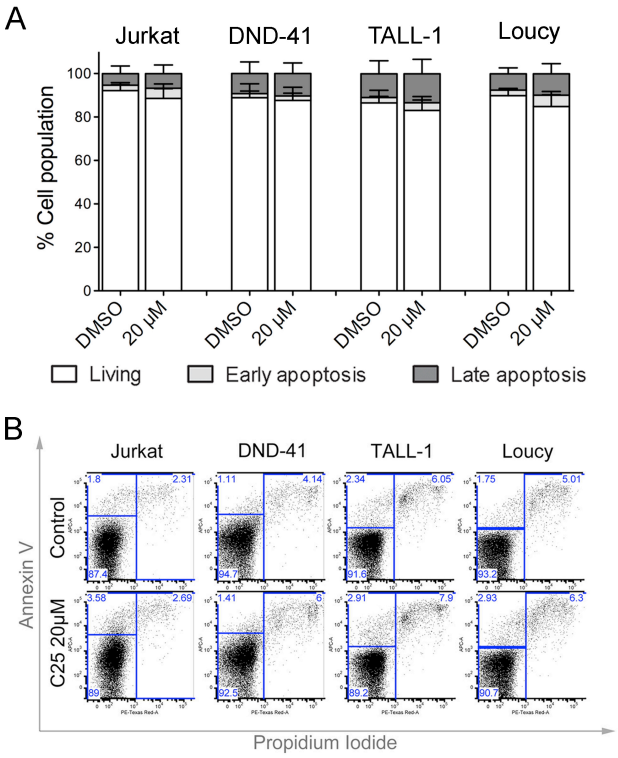

Figure 27. Effect of C25 on apoptosis after 48 hours of treatment. (A) Double staining with Annexin V/PI did not show any induction of apoptosis upon C25 treatment. Means and standard deviations of three independent experiments are shown. (B) Representative FACS plots of Annexin V/PI staining. Left lower gate, living cells; left upper gate early and right gate late apoptotic cells.

To further analyze the effects of the compounds we conducted cell cycle analysis using propidium iodide (PI) staining. Treatment with C1 resulted in a significant increase of cells in G2/M phase and a decrease in G1, except for in DND-41, which displayed only the G2/M arrest, in a dose-dependent manner (Fig. 28A). In Jurkat and TALL-1 the accumulation of cells in G2/M was accompanied by a reduction of p27kip1 protein levels, at the higher concentrations of the compound, and in TALL-1 with a minor decrease in SKP2 expression (Fig. 28B). SKP2 expression was markedly

affected only in Loucy cells, which displayed a significant drop in SKP2 protein levels with increasing concentrations of the compound.

Although p27kip1 typically inhibits the G1/S transition, it has also been reported that p27kip1 may have a function in controlling the G2/M transition, mainly by regulating the activity of CDK1 (Pagano, 2004). In line with our data, also Wu *et al*. observed that treatment of the cell line MCF-7 with compound C1 resulted in a G2 arrest (Wu et al., 2012).

However, our data also suggest that the G2 cell cycle arrest may, at least in some T ALL cell lines, occur independent of p27kip1. This notion is strongly supported by the fact that – quite unexpectedly – also the cell line Loucy, which lacks p27kip1 expression, showed a decrease in cell proliferation, increased cell death and achieved a G2 arrest (Fig. 26, Fig. 28).

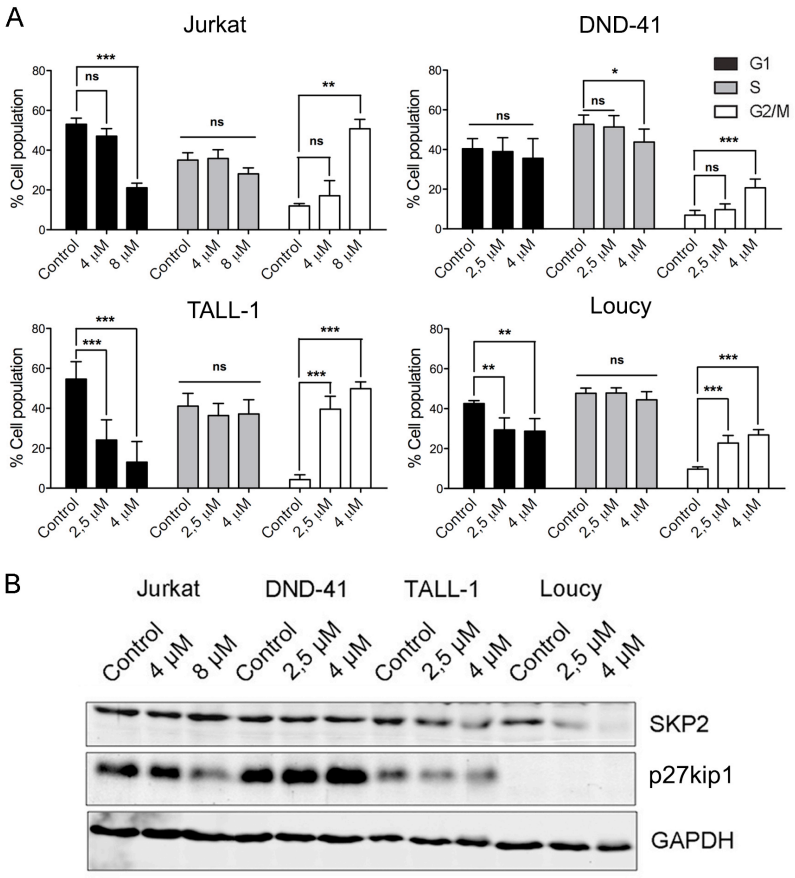

Figure 28. Effects of C1 on cell cycle and protein expression after 48 hours of treatment. (A) In all T-ALL cell lines C1 induced a significant accumulation of cells arrested in G2/M in a dose-dependent manner. Means and standard deviations of three independent experiments are shown. Significance levels were detremined by one-way repeated measures ANOVA; Dunnett's post hoc test; *p<0.05, **p<0.01, ***p<0.001. (B) Representative Western blots showing a moderate reduction of p27kip1 protein levels in Jurkat and TALL-1, and a decrease of SKP2 levels in TALL-1 and in particular in Loucy.

Concerning the effects of compound C25, in the T-ALL cell lines they were completely different from those previously reported in the prostate cancer cell line PC-3 (Chan et al., 2013). While in prostate cancer cells C25 caused a G2/M arrest, in two of the T-ALL cell lines, namely, DND-41 and TALL-1, it induced a significant accumulation of the cells in G1, but had no influence on Jurkat and Loucy (Fig. 29A). The G1 arrest was accompanied by an increase of p27kip1 protein, in particular in TALL-1

(Fig. 29B). Also in Jurkat cells, although the G1 arrest was insignificant, a slight increase of p27kip1 was observed (Fig. 29B).

In agreement with the results obtained by Chan *et al.* (Chan et al., 2013), administration of C25 downregulated SKP2 protein expression and stabilized p27kip1, at least in TALL-1 and to a lesser extent also in DND-41 (Fig. 29B). Of note, Loucy showed a decrease in SKP2 levels but – as always – no induction of p27kip1 expression (Fig. 29B).

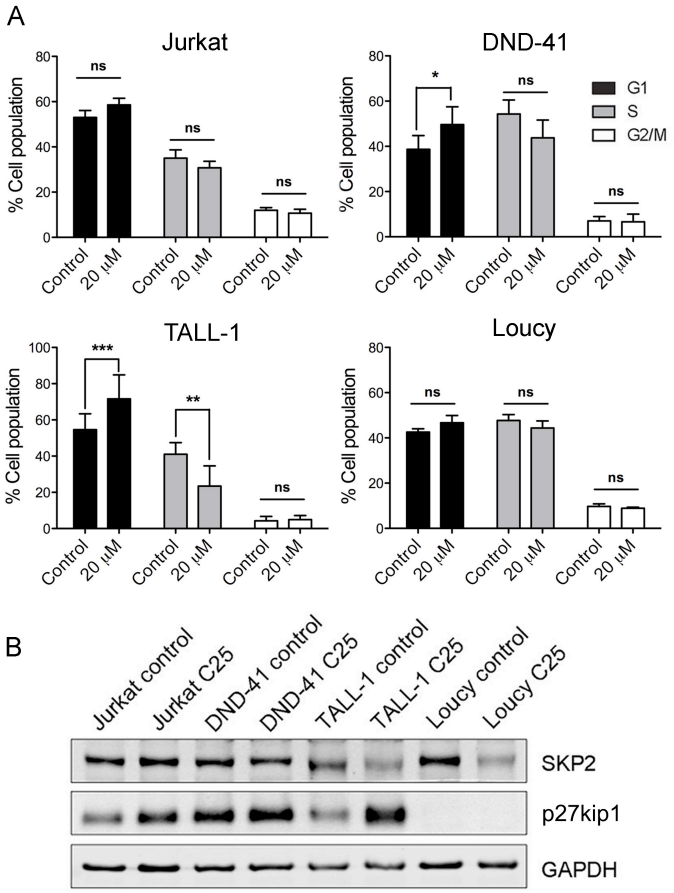

Figure 29. Effects of C25 on cell cycle and protein expression after 48 hours of treatment. (A) Cell cycle analysis demonstrated a G1 arrest in DND-41 and TALL-1, but no effects were observed in Jurkat and Loucy. Means and standard deviations of three independent experiments are shown. Significance levels were calculated by one-way repeated measures ANOVA; Dunnett's post hoc test; *p<0.05, **p<0.01, ***p<0.001. (B) Representative Western blots showing a general induction of p27kip1 (except for Loucy), which inversely correlated with SKP2 expression and the G1 arrest.

As the cytoplasmic accumulation or mislocalization of p27kip1 may have an oncogenic function and enhance cell migration and metastasis (Besson et al., 2004; Ishii et al., 2004), we also investigated potential changes in the subcellular distribution of the protein upon compound treatment. In this context, it is important to note that only two out of five SKP2 inhibitors previously investigated were able to increase nuclear p27kip1 at the expense of cytoplasmic protein (Pavlides et al., 2013).

For this purpose, after 48 hours of drug treatment the T-ALL cell lines were subjected to protein fractionation and analysis by Western blotting for the localization and expression levels of p27kip1 as well as SKP2 and KPC1, the main regulators responsible for p27kip1 degradation in the nucleus and cytoplasm, respectively (Fig. 30). In the untreated T-ALL cell lines the localization of p27kip1 was predominantly nuclear with the already well-known exception of Loucy in which no protein was detected. KPC1 was restricted to the cytoplasmic fraction and SKP2 was found in both fractions but with a clear trend towards a nuclear localization.

The most significant findings of this analysis are the distinctive changes in the subcellular distribution of p27kip1 in T-ALL1 upon treatment with the compounds. As shown in Fig. 29B treatment with C25 results in an overall increase of total p27kip1 protein, which is obviously associated with an accumulation in the cytoplasmic compartment (Fig. 30). Remarkably, this cytoplasmic mislocalization differed form the expected induction of nuclear p27kip1, which would be required to elicit a G1 arrest (Fig. 29A). On the other hand, the minor induction of nuclear p27kip1 may be sufficient to induce cell cycle arrest.

In contrast, C1 evoked an accumulation in the nuclear fraction (Fig. 30), which correlated with the G2 arrest (Fig. 28). This observation is in agreement with the findings in endometrial carcinoma cells, in which treatment of the cells with C1 increased p27kip1 levels in both fractions (Pavlides et al., 2013). However, since our data are derived from only two independent experiments their (statistical) significances need to be cautiously interpreted.

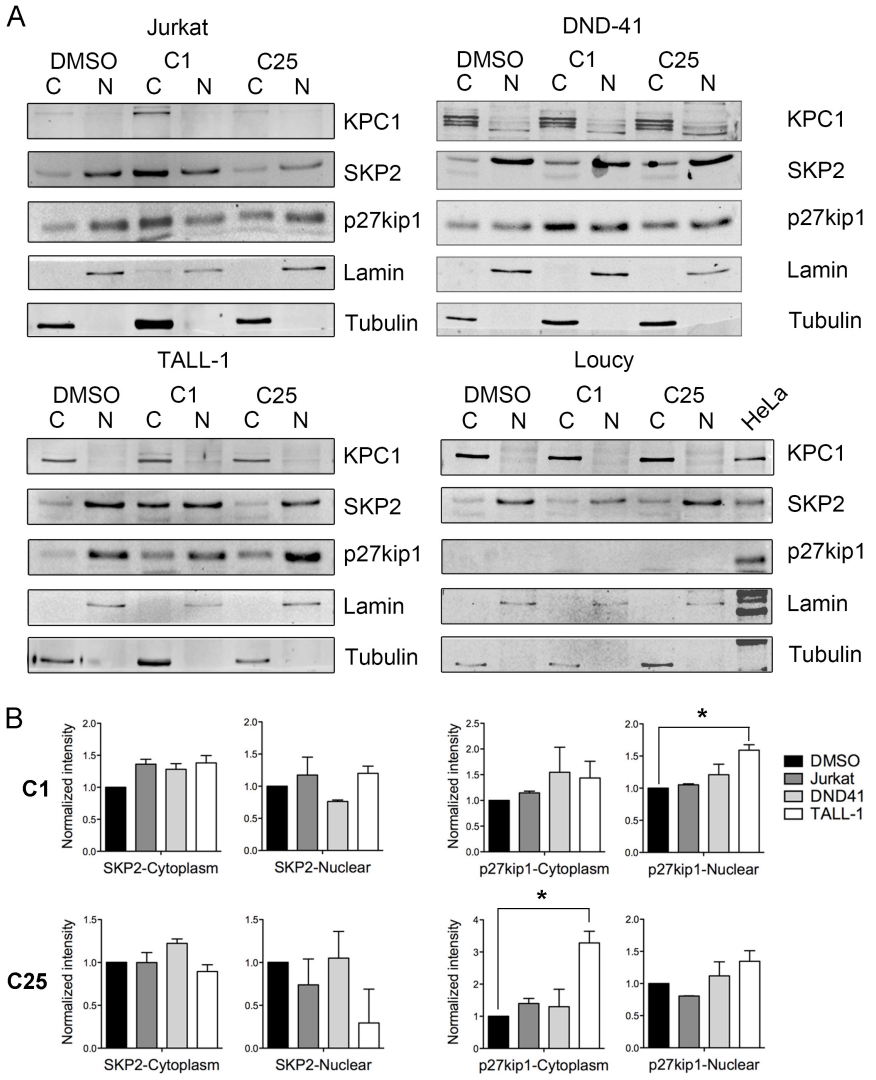

Figure 30. Subcellular localization of p27kip1, KPC1, and SKP2 upon treatment with C1 and C25. Cells were treated for 48 hours with C1 (6 μM for Jurkat and DND-41; 2,5 μM for TALL-1 and Loucy) or C25 (20 μM). (A) Protein lysates from cytoplasmic and nuclear fractions were immunoblotted with the indicated antibodies. Lamin and tubulin were used as controls for the nuclear and cytoplasmic fractions, respectively, and HeLa served as positive control. Representative Western blots of one of two independent experiments are shown. (B) Western blots were imaged using Li-Cor Odyssey system and semi-quantified using the Li-Cor Image Studio Lite software. Means and standard deviations of two independent experiments are shown. Significance levels were determined by one-way ANOVA test followed by Bonferroni's post hoc analysis; *p<0.05.

In summary, our data show that targeting SKP2 may provide an option for therapeutic intervention. However, it seems that the effects elicited by the two compounds tested are cell type and probably mutational background-dependent. This notion is strongly supported by the different sensitivities of the T-ALL cell lines towards the SKP2 inhibitors and the distinct effects on proliferation, cell cycle and apoptosis.

III.3. Treatment combinations of SKP2 inhibitors with glucocorticoids, γ-secretase or AKT inhibitors

In order to determine the consequences of combining small molecule inhibitors of SKP2 with contemporary frontline treatments (glucocorticoids) or therapeutic agents currently in development (γ-secretase and AKT inhibitors), we treated T-ALL cell lines with different drug combinations and evaluated their combinatorial influence on proliferation, cell cycle and apoptosis.

SKP2 inhibitors in combination with glucocorticoids

Glucocorticoids (GCs), such as dexamethasone (DEX) or prednisone are essential components of acute leukemia treatment and reduce cell proliferation, induce cell cycle arrest and apoptosis. Resistance to GCs is associated with an unfavorable prognosis and patients who relapse often show increased resistance to glucocorticoid therapy (Inaba et al., 2013).

Intriguingly, a recent publication showed that in T-lymphoma cells the p27kip1-SKP2 axis mediates GC-induced cell cycle arrest (Kullmann et al., 2013). Treatment with DEX increased p27kip1 protein levels, mediated by the GC-induced reduction of mRNA and protein levels of its negative regulator SKP2, indicating that both players might be considered as potential drug targets to improve therapies of T-cell malignancies.

Based on these observations, we sought to investigate whether SKP2 inhibitors could synergize with GCs in the induction of apoptosis. For this purpose, we selected the cell lines Jurkat, which is known to be highly resistant to GCs, DND-41 a GC-sensitive cell line, and Loucy, which shows a moderate response DEX treatment (De Keersmaecker et al., 2008). These cell lines were treated with 100 nM DEX, a concentration used in other studies (Kullmann et al., 2013; Real et al., 2009), and 20 μM of C25 or the lower concentrations of C1 used beforehand for each of the cell lines: 4 μM for Jurkat, 2,5 μM for DND-41 and Loucy.

First, we evaluated the viability of the cells treated with the glucocorticoid DEX alone after 24, 48, and 72 hours of treatment and based on its effect on cell growth we confirmed the GC resistance profile of the cell lines (Fig. 31A). The combinations of DEX with C1 or C25 showed no effects, perhaps except for Loucy, which displayed a trend towards a further reduction in cell growth when treated with DEX and C1.

Because GCs induce apoptosis in leukemic cells, we also determined the apoptosis rates by Annexin V/PI staining and FACS analysis (Fig. 31B). Jurkat displayed the already known moderate apoptotic cell death upon administration of C1 but neither the combination of DEX with C1 nor C25 had an additive effect. In contrast, in the cell line Loucy we found a cooperative effect of DEX and the SKP2 inhibitor C1 on proliferation and apoptosis which was less pronounced but also detectable in DND-41 (Fig. 31B); but combining DEX with C25 had also no effect in these cell lines (Fig. 31B). Of note, since the data presented in Fig. 31 were obtained from only two independent experiments, we refrained from statistical analysis.

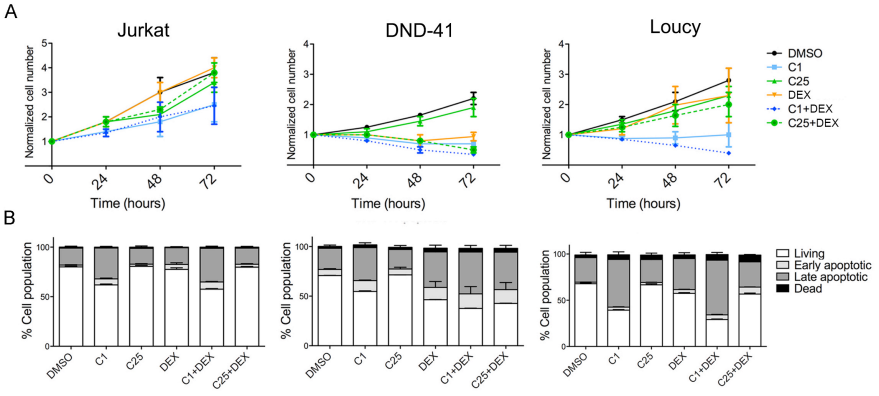

Figure 31. Proliferation and apoptosis of cells treated with SKP2 inhibitors alone or in combination with DEX. (A) Growth curves were generated based on cell viability determined by TB exclusion staining after 24, 48, and 72 hours of treatment. (B) Apoptosis/cell death was determined after 72 hours by Annexin V/PI double staining and FACS analysis. Means and standard deviations of two independent experiments are shown.

Several studies have demonstrated that GCs induce G1 arrest (Ausserlechner et al., 2004; Kullmann et al., 2013) and therefore, we also investigated the effects of combining the SKP2 inhibitors with DEX on cell cycle (Fig. 32). Of note, treatment of the T-ALL cell lines with C1 shows an accumulation of cells in G2 (Fig. 28), raising the question whether the combination of DEX and C1 would arrest the cells in both phases of the cell cycle and whether this effect might explain their additive effect on apoptosis and proliferation in some of the T-ALL cell lines (Fig. 32A).

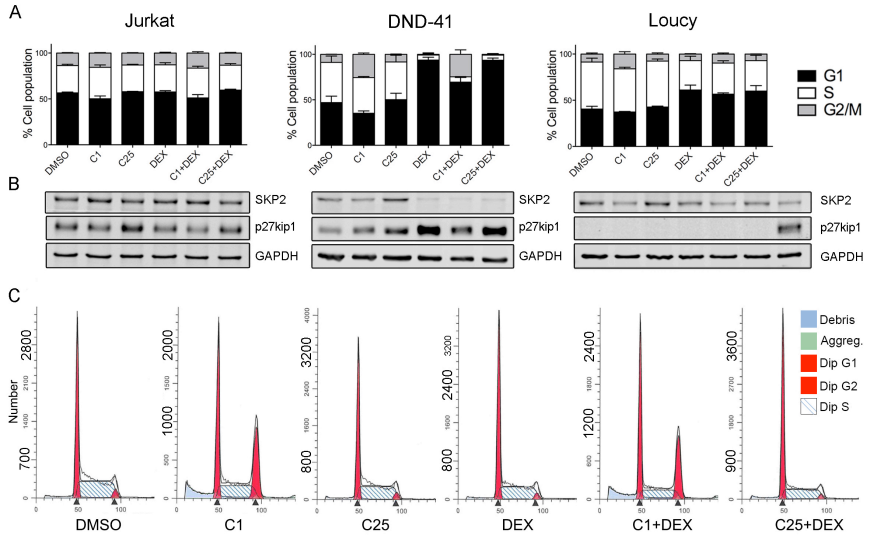

Figure 32. Cell cycle analysis of cells treated with SKP2 inhibitors alone or in combination with GC. (A) After 72 hours of treatment, cells were stained with PI and analyzed by flow cytometry and the percentages of cells in the different phases of the cell cycle were determined. Means and standard deviations of two independent experiments are shown. (B) Total protein lysates were immunoblotted with the indicated antibodies. HeLa was used as positive and GAPDH as a loading control. (C) Representative histograms of the cell line DND-41 indicating the cell cycle distribution upon drug treatment. Y-axis, total number of cells; X-axis, PI fluorescence intensity.

As expected from its GC resistance, Jurkat cells did not show any changes in cell cycle compared to the untreated control, and also neither an additive nor a synergistic effect with C1 nor C25 was detectable (Fig. 32A). Of note, Jurkat did not even display the G2 arrest usually seen with C1 (Fig. 28), which may be explained by its modest sensitivity to the

low concentration of the compound used for the combinatorial drug testing. Nevertheless, C25 treatment resulted in an induction of p27kip1.

In stark contrast, DND-41 cells displayed a G2 arrest upon treatment with C1, no changes with C25, and a massive arrest in G1 in the presence of DEX. Remarkably, the combination of C1 with DEX resulted in a simultaneous arrest in G1 and G2 (Fig. 32A, C) and, while the number of cells arrested in G1 decreased, the proportion of cells arrested in G2 became equal to that of the cells treated with C1 alone (Fig. 32C). Since the amount of cells in G2 was expanded at the expense of those arrested in G1, it seems that the effect of DEX (G1 arrest) is diminished by the effect exerted by C1 (G2 arrest). This dual effect may, however, be dependent on the proportions of cells in the different stages of cell cycle, their cycling times and the time to drug response.

On the contrary, the combination of C25 with GC only retained the effects of the DEX-induced G1 arrest and the cells showed no further response to this kind of treatment. However, the administration of GC with or without SKP2 inhibitor correlated with the previously described inverse effects of GC on SKP2 and p27kip1 protein levels (Kullmann et al., 2013). Notably, in the simultaneously G1/G2-arrested cells p27kip1 levels were lower than in the only G1-arrested ones, confirming the association of p27kip1 with G1 arrest.

As already shown, in Loucy only C1 has an effect on cell cycle (Fig. 28, Fig. 29). Due to the just moderate GC sensitivity of the cell line, DEX induced only a slight accumulation of the cells in G1, and combining C1 with DEX did not increase the percentage of cells arrested in G1 compared to cells treated with DEX alone (Fig. 32A), indicating that the increased apoptosis rate was responsible for the reduction in growth (Fig. 31). On the other hand, higher concentrations of C1 might elicit a more profound impact on cell cycle and the same G1/G2 arrest as observed in DND-41, which might already be indicated by the trend to a higher apoptotic rate in C1 and DEX treated cells (Fig. 31).

SKP2 inhibitors in combination with γ-secretase inhibitor

The high frequency of constitutive activation of NOTCH1 signaling in T-ALL makes NOTCH1 an attractive target for drug development (reviewed in (Purow, 2012)). Although γ-secretase inhibitor (GSI) treatment of T-ALL cell lines suppresses NOTCH1 activation, inhibits cell proliferation and induces cell cycle arrest, it has a limited effect on apoptosis and requires prolonged administration times (De Keersmaecker et al., 2008; O'Neil et al., 2007; Palomero et al., 2006a; Rao et al., 2009; Real et al., 2009). The limited antileukemic cytotoxicity together with strong adverse side effects is the main hindrance for a wider clinical use of GSIs. However, inhibition of NOTCH1 sensitizes GC-resistant T-ALL to GC-induced apoptosis and in mouse models this combination also protected the treated mice against the GSI-related gastrointestinal complications (De Keersmaecker et al., 2008; Real et al., 2009).

Furthermore, the combination of low doses of a GSI with the proteasome inhibitor Bortezomib synergistically decreased cell viability and proliferation and induced apoptosis in Jurkat and MOLT-4 cell lines as well as in *in vivo* models, providing a rationale for the combinatorial use of NOTCH1 and proteasome inhibitors (Yang et al., 2015). Based on the relation between NOTCH1 activation and the induction of *SKP2* (Dohda et al., 2007; Sarmento et al., 2005), we evaluated whether a combination of SKP2 inhibitors and GSIs would have a synergistic effect and whether GSIs might sensitize T-ALLs to the effects of the compounds C1 or C25.

For these experiments we selected two cell lines with active intracellular NOTCH1 (Fig. 33A), Jurkat being GSI-resistant and DND-41 GSI-sensitive, and first treated them with two different GSIs: DAPT (5 μM) or Compound E (CE; 1 μM). Our results confirmed the previously published findings regarding the GSI sensitivity of the two cell lines, i.e. their decreased proliferation and cell cycle arrest but no effect on apoptosis (data not shown). Since the effects of both GSIs were highly similar, we decided to use only CE for further experiments.

Next, we treated the two cell lines with the SKP2 inhibitors or CE alone or in combination and determined the cell viability after 72 hours of treatment (Fig. 33B). As expected, neither Jurkat nor DND-41 showed a significantly inhibited cell growth upon CE treatment alone, but whereas in Jurkat none of the combinations seemed to have a major effect, in DND-41 the combination of C1 and CE appeared to have at least a slight influence on proliferation (Fig. 33B).

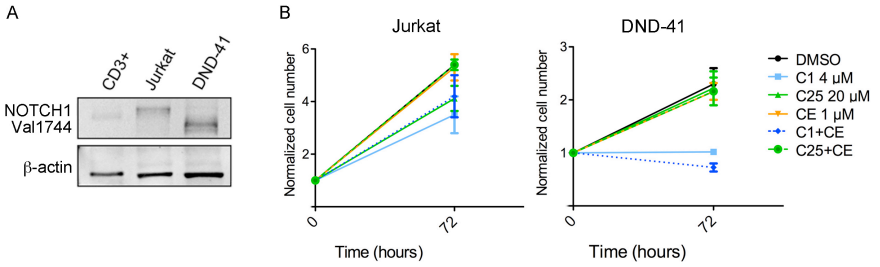

Figure 33. Cell growth of cell lines with activated NOTCH1 treated with SKP2 inhibitors alone or in combination with a γ-secretase inhibitor. (A) Western blot of active intracellular NOTCH1 in Jurkat and DND-41. Pooled CD3+ cells isolated from three healthy donors were used as negative and β-actin as loading control. (B) Proliferation curves based on cell viability determined by TB exclusion staining, after 72 hours of treatment with C1, C25 or CE, alone or in combination. Means and standard deviations of two independent experiments are shown.

To further investigate the interactions between CE and the compounds C1 and C25, we analyzed their combinatorial effects on apoptosis and cell death. The results obtained by Annexin V/PI double staining after 72 hours of drug administration were consistent with our previous data regarding apoptosis induction by C1. Moreover, they demonstrate that CE alone or in combination with the SKP2 inhibitors does not result in any changes as compared to the respective untreated controls and cells treated with C1 alone (Fig. 34).

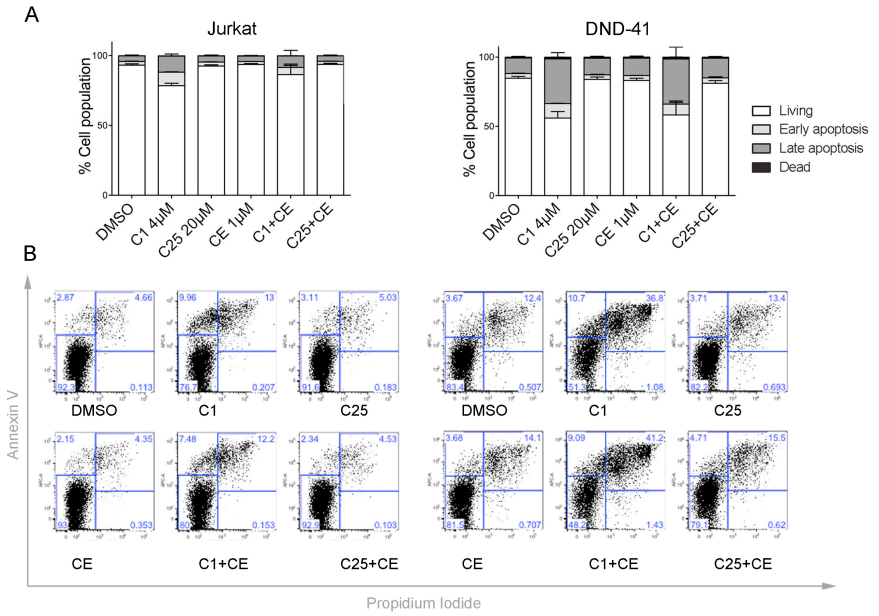

Figure 34. Apoptosis/cell death of cells treated with SKP2 inhibitors alone or in combination with a γ-secretase inhibitor. Annexin V/PI double staining followed by FACS analysis served to determine the cytotoxic effects of CE in combination with SKP2 inhibitors. Means and standard deviations of two independent experiments are shown. Representative dot plots of the flow cytometry measurements. Left lower gate, living cells; left upper gate early and right upper gate late apoptotic cells; right lower gate, dead cells.

Since treatment with CE has been shown to effectively block NOTCH1 signaling and to induce a modest G1 arrest in GSI-sensitive cells (Real et al., 2009), we analyzed also these parameters (Fig. 35). In both cell lines Western blot analysis showed a loss of intracellular NOTCH1 (ICN1) (Fig. 35B), confirming that CE efficiently inhibited the cleavage responsible for the release of NOTCH1 from the membrane. NOTCH1 inhibition was also accompanied by an increase of p27kip1 protein levels, substantiating the relationship between NOTCH1 signaling and p27kip1 expression (Sarmento et al., 2005).

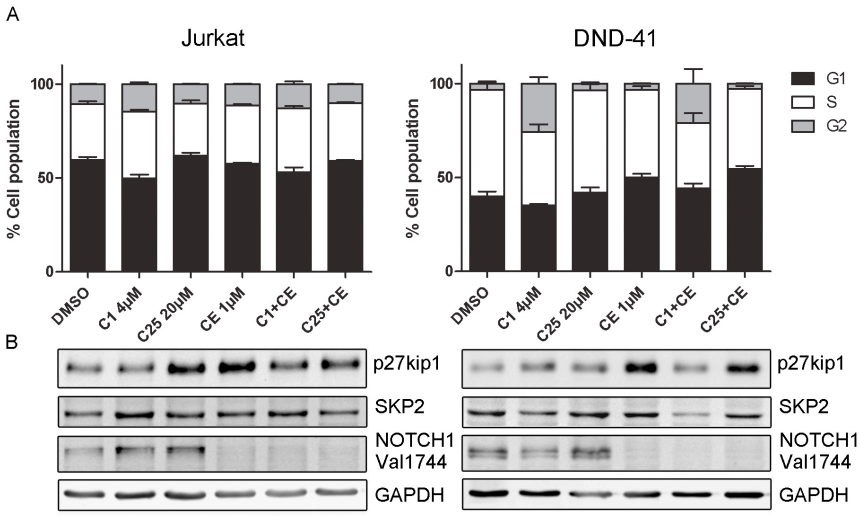

Figure 35. Cell cycle analysis and protein levels in cells treated with SKP2 inhibitors alone or in combination with a γ-secretase inhibitor. (A) FACS analysis of cells stained with propidium iodide after 72 hours of drug treatment. Means and standard deviations of two independent experiments are shown. (B) Representative Western blots showing the expression of p27kip1, SKP2, and intracellular NOTCH1. GAPDH was used as loading control.

As expected, Jurkat, which is GSI-resistant, was insensitive to CE treatment or its combination with the SKP2 inhibitors in terms of reduced proliferation, apoptosis or cell cycle, and no differences in these processes were detected (Fig. 34, Fig. 35). Since in Jurkat GSI treatment results in an efficient reduction of ICN1 but has no other effects it has been suggested that its GSI resistance might be NOTCH1-independent (Palomero et al., 2008). This finding may be due to the mutational inactivation of FBXW7, which inhibits NOTCH1 degradation and would not be affected by GSI treatment, and/or inactivation of PTEN. Interestingly, in Jurkat also the upregulation of p27kip1 is obviously not sufficient to induce a G1 arrest.

In the GSI-sensitive cell line DND-41, both CE alone and its combination with C25 induced a G1 arrest (Fig. 35A), which was accompanied by increased p27kip1 protein levels (Fig. 35B). Notably, the combination of CE with C1 had a less pronounced effect compared to that seen for the

combination of this SKP2 inhibitor with dexamethasone (Fig. 32), but similarly, resulted in a decrease of G1-arrested cells as compared to CE alone and an accumulation of G2-arrested cells as consequence of C1 treatment (Fig. 35A). These distinctive cell cycle arrests are also reflected by the p27kip1 levels, which are higher in G1-arrested as compared to G2-arrested cell populations (Fig. 35B).

Intriguingly, in neither of the two cell lines inhibition of NOTCH1 signaling had an impact on SKP2 protein expression (Fig. 35B), which at least under these experimental conditions, contradicts that NOTCH1 regulates *SKP2* transcription (Dohda et al., 2007; Sarmento et al., 2005), indicating that p27kip1 induction occurs independently of SKP2 downregulation.

SKP2 inhibitors in combination with AKT inhibitor

The PI3K/AKT pathway is linked to the pathogenesis of T-ALL via the mutational inactivation or posttranslational silencing of its main negative regulator PTEN (Larson Gedman et al., 2009; Silva et al., 2008). Loss of PTEN function and/or NOTCH1-induced upregulation of its negative regulators *HES1* and *MYC* are implicated in the activation of the PI3K/AKT/mTOR pathway-induced resistance to γ-secretase inhibitors (Palomero et al., 2008; Palomero et al., 2007; Shepherd et al., 2013).

Furthermore, SKP2 can promote AKT ubiquitination and membrane translocation (Chan et al., 2012), and in a feedback loop, AKT can directly (by promoter binding) or indirectly (via controlling E2F expression) regulate *SKP2* transcription (Mamillapalli et al., 2001; Reichert et al., 2007); or SKP2 activity by phosphorylating it and promoting its cytoplasmic mislocalization (Gao et al., 2009; Lin et al., 2009). Interestingly, it has been shown that inactivation of AKT using an inhibitor (MK-2206) has a synergistic effect in combination with GSIs or can sensitize GC-resistant cells (Loucy and Jurkat) to prednisone (Piovan et al., 2013; Yang et al., 2015).

Our previous experiments showed that the PTEN-inactivated cell lines Jurkat and Loucy are resistant to the SKP2 inhibitor C25. Based on the

findings outlined above and on the *CDKN1B*-p27kip1 regulatory network, we hypothesized that combining C25 with MK-2206 might increase p27kip1 protein levels via two different routes (Fig. 36). First, by inhibiting the formation of the SKP1-SKP2 complex, C25 might prevent p27kip1 degradation by SKP2 (1). Second, C25 by mimicking genetic deficiency of SKP2 has been shown to restrict activation of AKT (2). MK-2206 by inhibiting AKT would, thus, down-regulate SKP2 activity (3), and finally, MK-2206 would allow transcription of *CDKN1B* and consequently upregulation of the p27kip1 protein via the FOXOs (4) (Fig. 36).

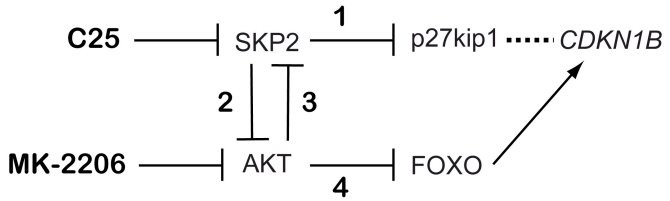

Figure 36. Hypothesis regarding the different ways of regulation of *CDKN1B*-p27kip1 via the SKP2-AKT axis.

Based on this concept, we aimed to gain first hints to verify this hypothesis. Therefore, we treated T-ALL cell lines with different PTEN status for 48 hours with C25 (20 µM) or MK-2206 (4 µM) alone or in combination and analyzed the levels of AKT Ser473 phosphorylation (pAKT) by intracellular phosphoprotein analysis using flow cytometry. Indeed, cells lacking functional PTEN, like Jurkat and Loucy, showed high levels of pAKT compared to the PTEN wild-type cell line TALL-1 (Fig. 37). While treatment with the AKT inhibitor was clearly effective and resulted in a drop of pAKT levels, C25 did not have any influence on AKT phosphorylation.

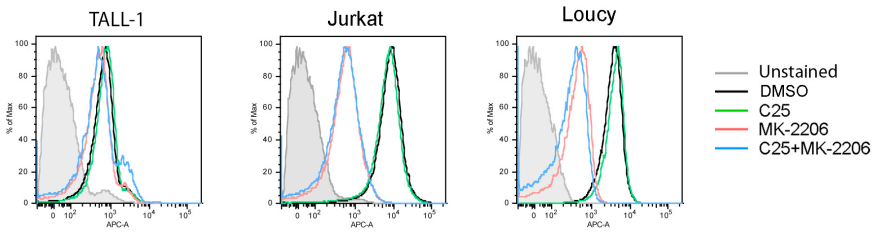

Figure 37. Detection of phosphorylated AKT in T-ALL cell lines treated with C25, MK-2206 or both. Levels of pAKT (Ser473) were determined after 48 hours of treatment by intracellular phosphoprotein analysis using flow cytometry. Shifts to the right indicate higher pAKT levels. Representative histograms of one out of three independent experiments are shown.

We then analyzed changes in cell growth and apoptosis in the PTEN mutated cell lines upon treatment with C25, MK-2206 or in combination (Fig. 38). Cell viability analysis by TB exclusion staining revealed a decrease in the proliferation of Jurkat cells when exposed to MK-2206, however, its combination with C25 did not show any additive effect (Fig. 38A). In Loucy only a minor decrease in cell growth was observed without any difference between MK-2206 alone or in combination with C25 (Fig. 38A). The evaluation of cell death rates detected an increase in the number of apoptotic cells in both MK-2206 treated cell lines and addition of C25 to MK-2206 appears to sensitize Jurkat to the cytotoxic effect of the AKT inhibitor but not Loucy (Fig. 38B).

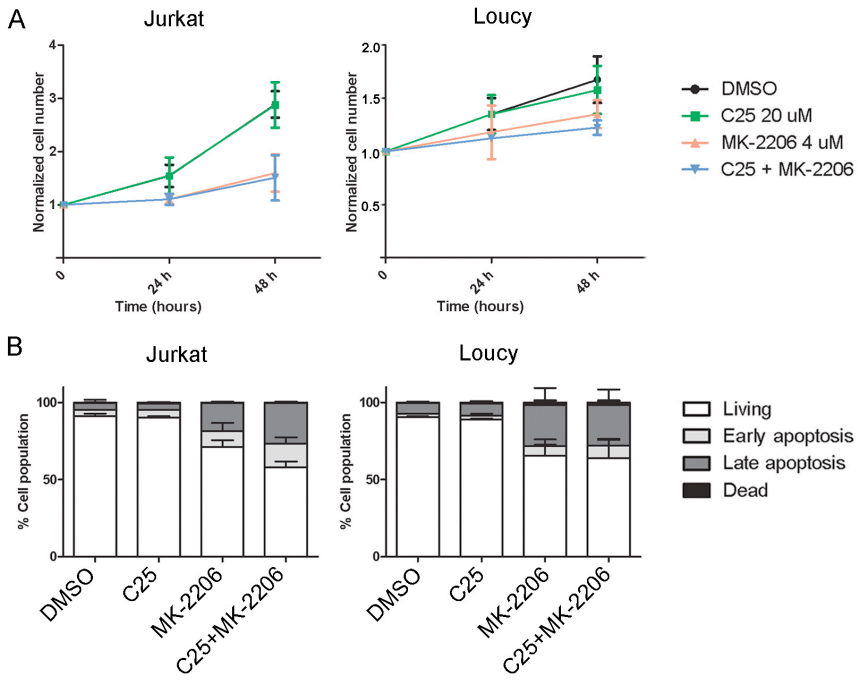

Figure 38. Cell proliferation and apoptosis in cells treated with C25, MK-2206 or both. (A) Growth curves were established based on cell viability assessed by trypan blue exclusion staining after 48 hours of drug treatment. (B) The percentages of apoptotic cells were determined by Annexin V/PI double staining and flow cytometry analysis. Means and standard deviations of two independent experiments are shown.

Because one of the expected consequences of combining these two compounds would be an increase of p27kip1, by a decrease of SKP2 or the induction of *CDKN1B* transcription (Fig. 36), we further analyzed their influence on the expression levels of the involved proteins and cell cycle (Fig. 39). Remarkably, an at least minor increase in the G1-arrested cell population was detected in the resistant cell line Jurkat when both compounds were combined (Fig. 39A). Even though this effect was not statistically significant when compared to MK-2206 alone, it was in line with the slightly increased apoptotic rate shown in Fig. 38B. Consistent with these finding, Western blot analysis showed a correlation between G1 arrest and the accumulation of p27kip1 protein, which inversely correlated with SKP2 levels (Fig. 39B).

In Loucy cells the arrest in G1 was as well evident upon MK-2206 treatment alone, however, no further increase was seen when C25 was added (Fig. 39A). As in Jurkat, also in Loucy SKP2 protein levels showed a marked reduction when cells were treated with the AKT inhibitor but no p27kip1 protein was detected, indicating that also in this scenario the G1 arrest occurs in a p27kip1-independent manner (Fig. 39B).

Although these data are rather preliminary and substantiating them will require a number of additional experiments, they nevertheless indicate that in the cell line Jurkat, in which compound C25 alone, despite a moderate induction of p27kip1, has no other effects at all, its combination with AKT inhibitors may have a sensitizing influence. This notion is supported by the greater impact on SKP2 and p27kip1 protein levels, which may after prolonged treatment times also result in increased cell cycle arrest and/or cell death.

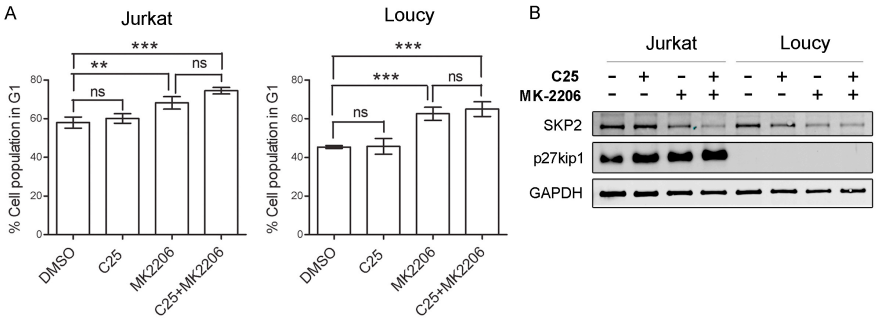

Figure 39. Effects of C25, MK-2206 or both on cell cycle and protein expression. (A) After 48 hours of drug treatment cells were stained with propidium iodide and analyzed by flow cytometry for cell cycle. Percentages of cells in G1 are depicted. Means and standard deviations of two independent experiments are shown. Significance levels were determined by one-way repeated measures ANOVA with Bonferroni post hoc test; *p<0.05, **p<0.01, ***p<0.001. (B) Representative Western blots of drug treated cells for SKP2 and p27kip1 expression. GAPDH was used as loading control.

DISCUSSION

DISCUSSION I

1. Complexity of *CDKN1B* transcriptional regulation

In this study we have confirmed that *CDKN1B* deletions are a recurrent genetic event in pediatric T-ALL (Mullighan et al., 2007; Remke et al., 2009) and have, for the first time, characterized *CDKN1B*-deleted patients in more detail. We have also verified that in both, T-ALL cell lines and primary leukemia samples low levels of *CDKN1B* expression are as well found in non-deleted cases (Remke et al., 2009), suggesting that other mechanisms of suppression may exist.

One of the main objectives of this work was to analyze whether somatic mutations in several genes frequently detected in T-ALL are involved in *CDKN1B* transcriptional regulation and whether they independently or in conjunction modulate *CDKN1B* expression (Fig. 8). Mutation screening of *NOTCH1*, *FBXW7*, and *PTEN* in the *CDKN1B*-deleted and wild-type cases revealed that the frequencies of alterations of these genes did neither differ between the two groups nor from unselected T-ALL cohorts retrieved from the literature (Table 6). Furthermore, we did not find any clear correlation between specific mutations or patterns of mutations and *CDKN1B* transcript levels (Fig. 14). Although in most cases activated NOTCH1 signaling was associated with the expression of one of its target, *HES1*, in the T-ALL cell lines and primary leukemia samples, the expected inverse correlation between *HES1* and *CDKN1B* transcription levels was not readily apparent (Fig. 15).

However, in contrast to cellular or mouse model systems, in which this relationship has been firmly established (Monahan et al., 2009; Murata et al., 2005), in full-blown leukemia this correlation may be masked by the influence of other factors we have not taken into consideration. Therefore, our data do not exclude an involvement of the analyzed genetic alterations in *CDKN1B* transcriptional regulation, but suggest that other mechanisms as well contribute to its modulation. This notion is supported by the enormous heterogeneity and complexity of somatic mutation

patterns in T-ALL, whose functions are not fully understood yet and remain to be determined. For example, very recent data show that also TLX1 is capable of binding to the *CDKN1B* promoter (Durinck et al., 2015) and may thus, also be involved in its transcriptional repression or, as shown for *TAL1* regulation (Mansour et al., 2014), somatic mutations in non-coding intergenic elements may create super-enhancers and regulate gene expression.

In this regard, the cell Loucy exemplifies that complete transcriptional repression of *CDKN1B* may occur via yet undetermined mechanisms. In this cell line, we have excluded the presence of a homozygous deletion of the gene, but neither any *CDKN1B* transcripts nor any p27kip1 protein were detectable (Fig. 9). Also treatment with a proteasome inhibitor was not able to induce any accumulation of p27kip1 (Fig. 23), corroborating that a suppressive mechanism acts on the transcriptional level. Even though inactivation of *CDKN1B* by DNA hypermethylation is a rare event in T-ALL (Kraszewska et al., 2012), we can at this point, however, not rule out that DNA methylation is responsible for the silencing of *CDKN1B*. Further analysis will be required in order to determine whether demethylating agents such as 5-azacytidine may abrogate the complete transcriptional repression of *CDKN1B* in Loucy or whether other epigenetic modifications may play a role in its regulation (Baylin and Ohm, 2006; Riedel et al., 2015).

On other hand, the emerging role of long non-coding RNAs (lncRNA) as regulators of gene expression adds an extra layer of complexity to the mechanisms of transcriptional activation or repression. The regulatory functions of lncRNAs, although still poorly understood, are related to many biological processes including cell cycle and consequently, also to cancer development (Hung et al., 2011; Liz and Esteller, 2015). As previously shown, for example, for *PTEN*, pseudogenes have a coding-independent function and compete for microRNA binding, thereby establishing a functional relationship between the mRNAs produced by the *PTEN* tumor suppressor gene and its pseudogene *PTENP1* (Guo et al., 2015;

Johnsson et al., 2013; Poliseno et al., 2010). Two recent studies, which showed that NOTCH1 signaling regulates the lncRNA landscape in T-ALL (Durinck et al., 2014; Trimarchi et al., 2014), emphasize not only the role of NOTCH1 signaling but also that of lncRNAs in leukemogenesis in general.

Hence, the transcriptional regulation of *CDKN1B* may still be more complex than anticipated and the entire spectrum of its regulatory factors remains to be determined.

2. *CDKN1B*-deleted pediatric T-ALL is associated with *MEF2C* expression

Our study revealed a high incidence of *MEF2C*-dysregulated cases within the *CDKN1B*-deleted cohort, or *vice versa*, a high frequency of *CDKN1B* deletions in *MEF2C* expressing T-ALL, which strongly suggests an association between these two genetic events (Table 6). In addition, we found that *CDKN1B*-deleted cases frequently belong to the *HOXA* subtype. Together, these data support the notion that *CDKN1B* deletions may preferentially occur in T-ALL associated with an expression signature indicating an immature phenotype of the leukemia (Homminga et al., 2011). However, this assumption is only based on the presence of specific genetic lesions and the ectopic expression of *MEF2C* and not on gene expression profiling data.

MEF2C dysregulated T-ALL (Homminga et al., 2011) closely resembles other defined T-ALL subtypes, such as early T-cell phenotype ALL (ETP-ALL) (Coustan-Smith et al., 2009), immature T-ALL (Soulier et al., 2005) or the *LYL* expressing subgroup (Ferrando et al., 2002), supporting a unifying genetic basis of these leukemias, which is associated with a transcriptional program related to hematopoietic stem cells and myeloid progenitors. As result of their very early arrest in T-cell differentiation, it has been suggested that these leukemias show lower frequencies of prototypical T-ALL-specific genetic lesions, such as deletions of the cell cycle regulator and tumor suppressors *CDKN2A/B* and a mutational

spectrum more similar to myeloid tumors (Haydu and Ferrando, 2013; Zhang et al., 2012). Consistent with this observation, we also found a lower incidence of *CDKN2A/B* deletions in the *CDKN1B*-deleted and *MEF2C* expressing cases, corroborating their lower incidence in rather immature T-ALL. Importantly, in *MEF2C*-dysregulated cases either *CDKN1B* or *CDKN2A/B* or simultaneously both cell cycle regulators may be affected, increasing the percentage of cases with at least one cell cycle regulator defect to the >75% usually observed for *CDKN2A/B* in unselected T-ALL cohorts. This finding indicates that haploinsufficiency of *CDKN1B* may represent an alternative mechanism to impair cell cycle control and to enforce cell cycle progression.

Furthermore, these data corroborate the notion that *CDKN1B* is indeed the main target within the relatively large 12p13 deletions. Nevertheless, we cannot rule out that also the haploinsufficiency of other genes, such as *ETV6*, affected by the 12p13 deletions, are involved in T-ALL leukemogenesis. However, in one of the patients the heterozygous deletion involved only the *CDKN1B* locus, without compromising *ETV6*, and haploinsufficiency of *CDKN1B* also contributes to the development of T-cell prolymphocytic leukemia (Hetet et al., 2000; Le Toriellec et al., 2008). Furthermore, in adult early immature T-ALL, *ETV6* mutations rather than deletions play a role in the pathogenesis of the disease (Van Vlierberghe et al., 2011).

Intriguingly, even though *MEF2C* is considered as one of the driving oncogenes in ETP-ALL (Homminga et al., 2011), in our study most cases expressing increased levels of *MEF2C* did not show the typical immunophenotypic characteristics of ETP-ALL (Table 8), neither by the initial nor the refined criteria associated with the immature/*MEF2C*-dysregulated cluster (Coustan-Smith et al., 2009; Zuurbier et al., 2014). Therefore, based on our data, we propose that *MEF2C* expression alone may not serve as denominator for ETP-ALL, at least not according to its current immunological definition criteria, which, however, are still controversially discussed.

Since glucocorticoids (GCs) are essential components of childhood ALL therapy and a poor response to GCs is a strong predictor of an adverse outcome, it is interesting to note that *in vitro* drug sensitivity testing showed that the blast cells of *MEF2C*-dysregulated ETP-ALL are more resistant to prednisolone treatment (Zuurbier et al., 2014). In line with this finding, *MEF2C* expression in primary leukemia samples was significantly associated with a higher rate of resistance of the patients to GC treatment (Fig.20). However, it remains to be determined whether MEF2C may be directly linked to the GC pathway.

In summary, these data provide evidence that *CDKN1B*-deleted cases have a lower frequency of *CDKN2A/B* deletions and preferentially belong to an immature/*MEF2C*-dysregulated T-ALL subtype. Furthermore, we suggest that *MEF2C* dysregulation, though associated with, is not exclusively found in early T-cell phenotype leukemia and that *MEF2C* expression may be predictive of the response to GC treatment, warranting further studies in this direction.

DISCUSSION II

SKP2 is one of the key players regulating the degradation of p27kip1 and the overexpression of the former and low levels of the latter have been observed in many types of human cancer (Hao and Huang, 2015), providing a rationale to therapeutically target SKP2. The improvement of screening methods, *in vitro* and *in silico* has facilitated the discovery of a number of compounds, which, in contrast to the unspecific effects of general proteasome inhibitors, like Bortezomib, target specific components of the SCF complex (Chan et al., 2013; Chan et al., 2014; Wu et al., 2012).

In this study we tested two of these new small molecule inhibitors of SKP2, C1 and C25, described to interact at the interface between SKP2 and p27kip1 or preventing the SKP1-SKP2 association and formation of the SCF-SKP2 complex, respectively (Chan et al., 2013; Wu et al., 2012), for their effects in T-ALL cell lines.

1. Effects of SKP2 inhibitors on cell cycle and apoptosis in T-ALL cell lines

Our first observation was a remarkably different sensitivity of the T-ALL cell lines tested towards the compounds. While C25 had no effects regarding apoptosis in any of the cell lines, they displayed major differences in their sensitivity to compound C1. Whereas Loucy was highly sensitive to C1 and showed massive apoptosis even when the drug was applied at low concentrations, Jurkat, known to be resistant to many of the current therapeutic agents, also required much higher doses of C1 to drive the cells into cell death (Fig. 26). Generally, induction of apoptosis was accompanied by a reduction in SKP2 levels and it has been shown that SKP2 downregulation or its knockdown correlates with BCL-2 expression, indicating that SKP2 may control apoptosis via regulating BCL-2 (Chan et al., 2010; Hao and Huang, 2015; Lee and McCormick,

2005). Notably, Loucy expresses much higher levels of BCL-2 than Jurkat (Peirs et al., 2014), which might provide an explanation for its high sensitivity to compound C1; however, we have not yet analyzed changes in BCL-2 expression in our experimental model system.

In addition, rather unexpectedly, C25 had different effects on cell cycle arrest than described in the original publication (Chan et al., 2013). While in a prostate cancer cell line (PC-3) C25 induced a G2 arrest, treatment of the T-ALL cell lines DND-41 and TALL-1 resulted in the induction of a G1 arrest (Fig. 29), which correlated with an increase of p27kip1. A similar phenomenon in terms of its impact on G1 or G2 checkpoint arrest in different cell types has also been described for compound C1 (Wu et al., 2012). Whereas in the prostate cancer cell line LNCaP C1 triggered a G1 arrest, in the breast cancer cell line MCF-7 the number of cells in G1 decreased while the G2/M population increased (Wu et al., 2012). As an explanation for these findings, the authors argued that a similar cell cycle phenotype was observed upon knockdown of SKP2 in mouse embryonic fibroblasts and that this effect was reversed when p27kip1 was simultaneously knocked out and that therefore, p27kip1 has also a pivotal role in G2/M checkpoint control.

Notably, in at least some of the T-ALL cell lines the C1-induced G2/M arrest at the expense of G1-arrested cells was accompanied by a reduction of p27kip1 protein levels, indicating that the G2 arrest occurs independent of p27kip1 (Fig. 28). This notion is strongly supported by the effects that compound C1 elicited in the T-ALL cell line Loucy. Even though Loucy completely lacks p27kip1 protein, quite unexpectedly, Loucy was the most sensitive cell line in terms of apoptosis and also achieved a G2/M arrest (Fig. 28), providing compelling evidence that the arrest at this checkpoint occurs independent of p27kip1 as well as in the absence of the upregulation of any of the other two CIP/KIP proteins (data not shown). Nevertheless, the G2/M arrest was accompanied by a drop in SKP2 levels. This highly enigmatic behavior of Loucy cells is difficult to reconcile, but on the one hand, suggests that compound C1 – although

claimed to be highly specific (Wu et al., 2012) – may have additional, so far unrecognized off-target effects, and, on the other hand, that the G2/M arrest has to occur via other routes which, at this point, remain elusive. In this context it is important to note, that all T-ALL cell lines investigated are TP53 mutant, indicating that the G2 arrest is also TP53-independent. These observations argue against the assumption of Wu and colleagues that in cells lacking p27kip1 treatment with C1 will not alter the cell cycle profile, because the inhibitor requires p27kip1 in order to cause changes in cell cycle (Wu et al., 2012).

An additional point, which requires consideration when targeting SKP2, is that fact that in order to evoke a cell cycle arrest a stabilization of nuclear p27kip1 is essential. Furthermore, since cytoplasmic mislocalization of p27kip1 is potentially oncogenic and promotes cell motility, migration and metastasis formation (Baldassarre et al., 1999; Besson et al., 2004; Denicourt et al., 2007; Masciullo et al., 1999; Singh et al., 1998), its upregulation in the cytoplasmic compartment may have unwanted effects. Therefore, only SKP2 inhibitors, which specifically prevent degradation of nuclear p27kip1 without causing an accumulation of 27kip1 in the cytoplasm will have the desired therapeutic effects.

Interestingly, in all T-ALL cell lines the ground state of the subcellular distribution of p27kip1 showed that the protein was present in both compartments, which is different from other highly aggressive malignancies, in which a complete nuclear exclusion has been observed (Chu et al., 2008; Viglietto et al., 2002b). In terms of the induction of p27kip by the SKP2 inhibitors in the nucleus, in the cytoplasm or in both, the two compounds had again different effects (Fig. 30). While treatment with C1 showed a trend to induce an accumulation of nuclear p27kip1, C25 increased p27kip1 levels in the cytoplasmic fraction, at least in the cell line TALL-1 (Fig. 30). This observation is in line with the finding that only two out of five SKP2 targeting compounds increased nuclear and simultaneously decreased cytoplasmic p27kip1 (Pavlides et al., 2013).

Together, although SKP2 is certainly an attractive molecular target, the currently available different small molecule inhibitors of SKP2 appear to elicit different effects in a cell type and mutational background-dependent manner, complicating the testing of their effectiveness. While in prostate cancer cell lines C25 regulated cancer cell proliferation and survival (Chan et al., 2013) in the analyzed T-ALL cell lines its impact was different and it generally did not inhibit cell growth or induce apoptosis. In contrast, apart from inducing a G2 rather than a G1 arrest, C1 inhibited proliferation and increased apoptotic rates in a cell line and dosage-dependent manner, which is, at least to some extent, more in line with the observations using this compound in solid tumor cell lines (Wu et al., 2012).

In addition, using SKP2 as molecular target may under certain circumstances have other effects, which need to be taken into account. Since MYC is also a substrate of SKP2-mediated degradation, blocking SKP2 might have a deleterious effect and upregulate MYC and consequently, possibly also activate AKT signaling via inhibiting PTEN (Kim et al., 2003; Palomero et al., 2007; von der Lehr et al., 2003). Furthermore, in case *CDKN1B* is transcriptionally silenced and/or in a haploinsufficient state, SKP2 inhibition may result in an increase of cyclin E (Koutsami et al., 2008), whose upregulation enhances genomic instability and in various malignancies is associated with a poor prognosis (Akli and Keyomarsi, 2003; Nakayama et al., 2000). In such cases, blocking of SKP2 activity would be only effective when the levels of p27kip1 are upregulated above a certain threshold, and therefore able to exert its negative effect on cell cycle progression. If p27kip1 levels remain below this threshold, the protein would be sequestered by the cyclin-CDK complexes, promoting cyclin E-CDK activity (Koutsami et al., 2008).

This scenario may well apply at least to those T-ALLs that express very low levels of *CDKN1B* transcripts or display homozygous genomic deletions. Consequently, one of the essential remaining questions is whether targeting exclusively SKP2-p27kip1 in patients with p27kip1

haploinsufficiency would reach the threshold to exert its desired negative effects on the proliferation of the leukemic cells.

In summary, extensive analysis of the specificity and impact of small molecule inhibitors of SKP2 in terms of interfering with substrate recognition or SCF complex formation and accumulation of proteins in the different subcellular compartments in a tumor type and mutational background-dependent manner is an essential prerequisite to avoid an undesirable response of the tumor cells.

2. Combination therapies in T-ALL

The development of targeted anticancer therapies exploits the genetic and biochemical characteristics unique to malignant cells and the constellation of specific genetic lesions present in the individual tumors provides the rational for the selection of a single drug or a combination of agents for cancer therapy. It has become increasingly clear that a single drug may not be effective in eradicating the tumor cells and may evoke escape mechanisms and tumor resistance, and therefore, the combinatorial use of several drugs is the current strategy.

Consequently, we determined whether the combination of the small molecule inhibitors of SKP2 with some of the contemporary and essential therapeutic agents used in T-ALL, like GCs, and some drugs currently under development, like γ-secretase or AKT inhibitors, might have any additive, synergistic or sensitizing effects in otherwise resistant T-ALL cell lines. Generally the combination of the SKP2 inhibitors with other drugs had no significant influence on proliferation, cell cycle arrest or apoptosis. However, our preliminary data, nevertheless, show some remarkable consequences for particular drug combinations.

An interesting effect was observed in the GC-sensitive cell line DND-41. In this cell line treatment with dexamethasone (DEX) resulted in the expected massive G1 arrest and the previously described GC-mediated changes in SKP2 (significant downregulation) and p27kip1 (upregulation) expression (Kullmann et al., 2013) and the characteristic G2/M arrest

caused by C1 (Fig. 32). However, the combinatorial treatment with both drugs decreased the cell cycle effect of DEX (G1 arrest) at the expense of the one exerted by C1 (G2 arrest), thus leading to a simultaneous arrest in G1 and G2. Although the proportion of arrested cells with DEX alone or DEX and C1 in both cases amounted to almost 100% (Fig. 32), in the latter scenario (G1+G2 arrest), although the response was not significant, a higher proportion of the cells underwent apoptosis (Fig. 31). This influence will certainly be highly dependent on the relative proportions of the cells in the different cell cycle stages and the time to drug response, but may in fact lead to a faster induction of apoptosis. However, the verification that this is indeed the case will require both time-course experiments and combinations of different drug dosages.

The only moderately GC-sensitive cell lines Loucy showed a similar response as DND-41 but the effect of DEX was less pronounced and the combination treatment had only a minor impact on cell cycle arrest (Fig. 32). Nevertheless, DEX together with C1 resulted in a reduction of SKP2 and an increased apoptotic rate (Fig. 31). Since SKP2 may control apoptosis by regulating BCL-2 (Chan et al., 2010; Hao and Huang, 2015; Lee and McCormick, 2005) and BCL-2 inhibitors synergize with GCs in driving BCL-2 expressing T-ALL into cell death (Anderson et al., 2014; Peirs et al., 2014), possibly the combination of DEX and SKP2 inhibitors leading to a SKP2 downregulation may have similar consequences.

In the highly GC-resistant cell line Jurkat expressing very low levels of BCL-2 (Peirs et al., 2014), simultaneous application of DEX and SKP2 inhibition had no consequences at all (Fig. 31, Fig. 32), suggesting that this drug combination has only an effect in *a priori* GC-sensitive cells expressing BCL-2. Notably, in the more GC-resistant T-ALL cell lines, DEX treatment neither results in an upregulation of p27kip1 nor in a repression of its negative regulator SKP2 (Fig. 32), suggesting that the p27kip1-SKP2 axis, unlike in GC-sensitive cells (Kullmann et al., 2013), is somehow non-functional in GC-resistant leukemia.

Regarding the combinatorial effects of the SKP2 inhibitors with a γ-secretase inhibitor or simultaneous inhibition of AKT there were no significant changes detectable, indicating that the drugs have no additive, synergistic or sensitizing effects. Remarkably, however, while inhibition of NOTCH1 signaling induced p27kip1 levels, paradoxically, the SKP2 levels remained unaffected (Fig. 35), suggesting that NOTCH1, at least in the T-ALL cell lines Jurkat and DND-41, regulates p27kip1 not necessarily via the previously described NOTCH1-(MYC)-SKP2-p27kip1 axes (Dohda et al., 2007; Sarmento et al., 2005) but potentially via its regulation of *HES1* (Fig. 8) (Murata et al., 2005). However, further analysis of the transcript and protein expression of all potential players in this regulatory pathway will be required to determine how p27kip is exactly upregulated.

Nonetheless, it remains to be determined whether administration of these drug combinations might at different schedules, including pre-treatment with one or the other drug, sensitize the cells to SKP2 inhibition, or the other way around, whether SKP2 inhibition might sensitize cells to the other therapeutic agents. The same holds true for any of the SKP2 inhibitor drug combinations used in this study, which may have different effects when other administration schedules are used.

Importantly, some studies have proven that specific therapeutic agents may not be unconditionally combined with each other, and that the exact timing, dosage and order of administration may determine whether a combination has synergistic or antagonistic effects. This complication is exemplified by the finding that simultaneous application of GSIs and the tyrosine kinase inhibitor (TKI) imatinib antagonizes the inhibitory effect of the TKI, whereas pretreatment with a GSI sensitized the cells to the effect of the TKI, but not the swapped drug administration (De Keersmaecker et al., 2008).

In addition, while inhibition of the PI3K/mTOR pathway alone appears to result in an upregulation of the NOTCH1-MYC pathway, targeting both the PI3K/mTOR and the NOTCH1 pathways enhances cell cycle arrest and cell death (Shepherd et al., 2013), underlining the importance of testing

not only single drugs but also combinations and analyzing their effects not only on the respective pathway but also for interferences with other signaling cascades.

Remarkably, however, a recent study indicates that also combining targeted anticancer drugs may elicit unanticipated effects on clonal dynamics and selection processes and inadvertently promote the outgrowth of resistant cells. One example for such an effect is the finding that treatment of mice with a PI3K inhibitor invariable resulted in the emergence of drug resistant clones, which downregulated NOTCH1 signaling and exhibited cross-resistance to γ-secretase inhibitors. Thus, dual inhibition of PI3K and NOTCH1 signaling might promote drug resistance in T-ALL (Dail et al., 2014).

In conclusion, our findings emphasize the high relevance of defining the transcriptional and/or protein status of *CDKN1B*-p27kip1 and its regulatory network in the context of T-ALL before SKP2 inhibition may be envisioned as therapeutic approach. Furthermore, they raise the question whether the compounds C1 and C25, although it has been claimed that they are highly specific, may under certain circumstances have so far unrecognized (off-target) effects.

Hence, before the “dream target” of cancer therapy (Chan et al., 2014) will become a realistic option, the development of more specific small molecules and their extensive testing in a tumor type and mutational landscape-dependent manner will be required – and it is still a long way down the road until targeting SKP2 will come of age.

MATERIAL AND METHODS

Patients

All patients analyzed in this study were enrolled in the Austrian ALL-BFM 90, 95 or 2000 clinical trials and treated with informed consent obtained from the patients, their parents or legal guardians. Cytogenetic analysis and immunophenotyping were conducted as part of the routine diagnostic work-up of the patients. Array comparative genomic hybridization (aCGH) using BAC arrays of 102 pediatric T-ALL samples has been carried out in a previous study (M. Pisecker, R. Ullmann; S. Strehl, *unpublished data*) as described elsewhere (Attarbaschi et al., 2010; Cheng et al., 2005; Erdogan et al., 2006). Fluorescence in situ hybridization (FISH) analysis was performed by M. König according to standard procedures and using appropriate probe sets for the detection of the leukemia-specific genetic alterations of interest.

Cell culture

The human T-ALL cell lines Jurkat, RPMI-8402, HSB-2, MOLT-4, CCRF-CEM, and Loucy were obtained from the German Collection of Microorganisms and Cell Cultures (DSMZ); and T-ALL1, MOLT-16, and DND-41 were a kind gift from F. Speleman (Ghent University, Belgium). All cell lines were grown in RPMI-1640 medium containing 1% penicillin/streptomycin, 2 mM glutamine and 10% fetal bovine serum (FBS); for Loucy and TALL-1 20% FBS was used. Cells were maintained at 37°C in a humidified atmosphere with 5% CO_2.

Isolation of CD3+ T-cells

CD3+ T-lymphocytes were isolated from peripheral blood of healthy donors using a whole blood column kit with anti-CD3+ magnetic microbeads (Milteny Biotec) according to the manufacturer's recommendations. In order to increase the purity of the magnetically labeled fraction, the eluted fraction was enriched over a new, freshly prepared MS Column. Cell purity was determined by FACS analysis using an antibody cocktail containing anti-CD3 (PeTR), anti-CD45 (PerCP), anti-

CD56 (PeCy7), anti-CD33 (PE) (BD Bioscience), anti-CD19 (APC) (eBioscience), and anti-CD15 (FITC) (Dako).

DNA isolation

DNA was isolated using a standard high-salt extraction method. First, the cells were washed in 1xPBS and the cell pellet resuspended in 400 µl of RSB buffer (10 mM Tris/HCl pH 7.4, 10 mM NaCl, 3 mM $MgCl_2$) and 1 µl RNAse A (10mg/ml), followed by the addition of an equal volume of TENS buffer (100 mM Tris/HCl pH 8.0, 40 mM EDTA pH 8.0, 200 mM NaCl, 1% SDS) including 4 µl of proteinase K (10mg/ml) and incubated for at least 3 hours or over-night at 37°C After the addition of 220 µl 5 M NaCl and centrifugation, the supernatant was added to two volumes of absolut ethanol and mixed. The DNA fibers were transferred to a fresh tube and washed in 70% ethanol, air-dried, and finally resuspended in TE buffer (10 mM Tris, 0.1 mM EDTA; pH 8.0). DNA concentrations were measured using a Nanodrop Spectrophotometer.

RNA isolation and reverse transcription (RT)

Total RNA was extracted using the RNeasy Mini kit (Qiagen) according to the manufacturer's instructions. RNA concentrations were determined using a Nanodrop Spectrophotometer. In addition, the quality of the RNA was controlled using a 2100 Bioanalyzer (Agilent) and only samples with a RIN value of ≥5 were used for the gene expression studies.

1 µg total RNA was reverse transcribed with a mixture of 200 units M-MLV reverse transcriptase, 500 ng random hexamer primers, 500 ng oligo-dT18, 20 units RNasin, and 2 mM dNTPs (Promega) in a total volume of 20 µl at 42°C for for 1 hour. The cDNAs were diluted to 100 µl with water and 2 µl of these samples were used for each reaction.

Mutation screening

Mutation screening was carried by direct sequencing of PCR products. PCR reactions were carried out using genomic DNA or cDNA as

templates and primer sets encompassing the mutation hot spots of *NOTCH1*: heterodimerization (HD), transmembrane (TM), and PEST domains encoded by exons 26-27, 28, and 34, respectively; *FBXW7*: WD40 domains encoded by exons 8–12, and *PTEN*: C2-domain encoded by exon 7. Primers used for the mutation screening are listed in Table MM.1.

Mutations in *NOTCH1* and *FBXW7* were analyzed by PCR amplification of cDNA using the Hot-Start Taq polymerase (Qiagen) according to manufacturer's instructions and the following cycling conditions: initial denaturation at 95°C for 14 min followed by 35-37 cycles 95°C for 30 sec, 60-62°C for 30 sec, and 72°C for 45 sec; and a final extension step at 72°C for 7 min. For *PTEN*, PCRs were performed using genomic DNA and Taq DNA Polymerase (Sigma Aldrich) according to the manufacturer's instructions and the cycling parameters 94°C for 4 min; 35-37 cycles of 94°C for 30 sec, 58-60°C for 30 sec and 72°C for 30 sec; and a final extension step at 72°C for 7 min.

PCR products were purified either by using the QIAquick PCR Purification Kit (Qiagen) or the QIAquick Gel Extraction Kit (Qiagen) according to the manufacturer's recommendations. The purified PCR products were directly sequenced by Microsynth (Vienna, Austria) and the obtained sequences were analyzed using the Sequencher 5.0.1 software and compared to the following reference sequences: *NOTCH1* (NM_017617), *FBXW7* (NM_018315), and *PTEN* (NG_007466.2).

Cloning

The TOPO® TA Cloning® Kit from Invitrogen was used for cloning. 4 µl of fresh PCR product were added to the reaction mix composed of 1 µl salt solution (1.2 M NaCl + 0.06 M $MgCl_2$), 1 µl TOPO® vector to a final volume of 6 µl. The reaction was gently mixed and incubated for 5 min at room temperature (22–23°C) and placed on ice. JM-109 or TOP10 One Shot® E. coli competent cells were transformed with 2 µl of the reaction mix. The bacteria were incubated on ice for 30 min followed by incubation

at 42°C for 45 sec and incubation on ice for 5 min. Subsequently, 250 µl SOC medium was added and the transformed cells were placed under agitation at 37°C for 60 min. Cells were plated on LB-agar plates containing 100 µg/ml ampicilin and incubated overnight at 37°C. Single colonies were picked the next day.

Colony PCR

Direct PCR of intact bacteria (colony PCR) was performed for screening of the desired inserts using the universal M13 primers (Table MM.2) and the Hot-Start Taq polymerase (QIAGEN) according to manufacturer's instructions and the following cycling conditions: initial denaturation at 95°C for 14 min, followed by 30 cycles 95°C for 30 sec, 55°C for 30 sec, and 72°C for 60 sec; and a final extension step at 72°C for 7 min. Aliquots of the amplification products were loaded on a 1,5% agarose gels and the clones carrying the correct inserts were selected for PCR product purification using the QIAquick PCR Purification Kit (Qiagen) followed by direct sequencing with the T7 and T3 universal primers (Table MM.2) by Microsynth (Vienna, Austria). Sequences were analyzed with the Sequencher v.5.0 software.

Standard genomic PCR

To determine the genomic integrity of the *CDKN1B* gene in the cell line Loucy, we performed a standard genomic PCR using primer pairs covering different regions of the *CDKN1B* locus. 100 ng of genomic DNA and the Hot-Start Taq polymerase (QIAGEN) were used for the reaction and the cycling conditions were as follows: initial denaturation at 95°C for 14 min followed by 36 cycles 95°C for 30 sec, 60°C for 30 sec, and 72°C for 30 sec; and a final extension step at 72°C for 7 min. PCR products were then loaded in a 2% agarose gels.

Quantitative PCR (qPCR)

RT-qPCR. Quantitative expression analysis of *CDKN1B*, *HES1*, *SKP2*, *MYC*, and *MEF2C* transcript levels was carried out using the IQ™ SYBR® Green Supermix (Biorad) and an ABI 7500-fast Real-Time PCR system with the following cycling conditions: 1 cycle at 95°C for 30 sec, 1 cycle at 95°C for 2 min, 40 cycles at 95°C for 15 sec alternating with 60°C for 30 sec, followed by 1 cycle at 95°C for 1 min, 1 cycle at 40°C for 1 min, and finally 110 cycles at 40-94.5°C each for 10 sec. The transcript values were analyzed with the 7500 System Software (Applied Biosystems) and normalized using the ΔΔCt method, relative to the expression of the reference gene *GUSB* and to a pool of highly enriched CD3+ T-cells. The primers used for RT-qPCR are listed in Table MM.3.

Genomic qPCR. 10 ng DNA isolated from primary leukemia samples or normal human DNA was amplified using the same conditions as described for RT-qPCR. Two different *CDKN1B*-specific primer pairs located in the 5'-UTR and exon 3 of the gene were used and *SATB1* (3p23) and *PPP3CA* (4q24) generally not affected by copy number alterations in T-ALL served as controls for data normalization. Cut-offs of ≤0.75 and ≤0.35 were used to determine hemizygous and homozygous *CDKN1B* deletions, respectively. All primers used for genomic qPCR are listed in Table MM.3.

Protein preparation

For total protein extraction, cells were washed with PBS and lysed in an appropriate volume of hypertonic buffer (20 mM Tris-HCl pH 7.5, 400 mM NaCl, 0.5% NP-40, 0.3% Triton-X-100, and a protease inhibitor cocktail (phenylmethanesulfonylfluoride (PMSF), aprotinin, leupeptin, and pepstatin). After incubation and centrifugation for 30 min at 16000 g at 4°C, the supernatants containing the proteins were collected.

For protein fractionation, cells were washed with ice-cold PBS and lysed in hypotonic buffer containing 10 mM Tris pH 7.5, 10 mM KCl, and protease inhibitor cocktail, with the addition of 0.25% NP-40. After

incubation and centrifugation, the supernatants were collected as cytosolic protein fraction. The pellets were resuspended in hypertonic buffer, incubated on ice, and following a centrifugation step, the supernatants were used as nuclear fraction.

The protein concentrations were determined using Bradford analysis (Biorad Laboratories) according to the manufacturer's recommendations.

Western blotting

For immunoblotting, protein samples containing 5x SDS loading buffer and preheated for 5 min at 96°C, were analyzed by SDS-PAGE using 10% SDS-polyacrylamide gels in Tris-glycine SDS running buffer (25 mM Tris, 192 mM glycine, 0.1% SDS) and electroblotted onto nitrocellulose membranes (Whatman) at 400 mA for 1 hour on ice in transfer buffer (25 mM Tris, 192 mM glycine, 20% methanol). Protein transfer was checked with Ponceau staining (Sigma). The membranes were washed in 1x TBS-T (50 mM Tris, 150 mM NaCl, pH 7.5 containing 0.1% Tween-20) and blocked in 1x TBS containing blocking reagent (Roche). Primary and secondary antibodies were diluted in 1x TBS containing 0.5x blocking reagent and NaN_3 and incubated over-night at 4°C (in case of primary antibodies) or for 1 hour at room temperature (for the secondary antibodies), followed by three washes in 1x TBS-T.

Blots were scanned at 700 and 800 nm using the Odyssey imaging system (Li-COR). Semi-quantification of Western blots was performed using the Li-COR software Image Studio Lite.

All antibodies and dilutions used are provided in Table MM.4.

Drug treatment of T-ALL cell lines

The respective T-ALL cell lines were cultured in a density between 0.5-0.6.10^5 cells per ml and treated with a single dose of the different compounds at the final concentrations provided in Table MM.4. For combination treatments mostly the lower concentration of C1 for the respective cell lines was used.

For determining growth rates, cell cycle analysis and Western blotting after 24 or 48 hours of incubation appropriate aliquots were taken out from the cultures and without changing the medium the remaining cells were further incubated. After 72 hours of treatment the entire cell population was uses for further analysis.

Except for a few of the drug combinations, always three independent experiments using different batches of the cell lines were conducted. The number of experiments for each individual drug treatment or combination of drugs is described in detail in the “Results”

Trypan blue exclusion staining for cell viability

Trypan blue (TB) exclusion staining was used to determine cell viability. Aliquots of the cell suspensions were stained with TB after 24, 48, and 72 hours and counted using a hemocytometer. The total number of cells per ml for each condition and time-point was normalized to the starting density (time point 0).

Cell cycle analysis

To monitor changes in the cell cycle the DNA content of the cells using the Cycletest^{TM} Plus DNA Reagent Kit (Becton Dickinson) was used. Cells were counted using the hematology analyzer Sysmex. $5x10^5$ cells were resuspended and washed in BD-Buffer. The cells were then incubated for 10 min at room temperature in a solution containing trypsin for the digestion of cell membranes and cytoskeletons followed by addition of a solution containing trypsin inhibitor and ribonuclease A in order to inhibit the trypsin activity and to digest the RNA, and incubated for another 10 min at room temperature. Propidium Iodide (PI) solution was added to a final concentration of 125 µg/ml and the cells were incubated at 4°C for one hour in the dark. The samples were measured on a BD Fortessa flow cytometer and analyzed with the ModFit LT V3.3 software.

Detection of apoptosis

Apoptotic cells were detected using the Annexin V Apoptosis Detection Kit APC (eBioscience) according to the manufacturer's recommendations. 1-5.10^5 cells were resuspended in 1x binding buffer in a final volume of 100 µl followed by the addition of the Annexin V-APC conjugated antibody (1:50) and propidium Iodide (1:50). The samples were incubated for one hour at 4ºC in the dark, and analyzed by flow cytometry on a BD Fortessa and the results were further processed with the FlowJo v.9.8 software.

Intracellular phosphoprotein analysis

For intracellular phosphoprotein staining (Krutzik and Nolan, 2003; Schulz et al., 2012), cells were harvested and fixed with 2% methanol-free formaldehyde (Polysciences) for 15 min at room temperature. Cells were centrifuged and permeabilized by the addition of ice-cold methanol while vortexing and immediately transferred to −20°C for 1 to 3 hours. After centrifugation, the cells were resuspended in PBS supplemented with 0.02% bovine serum albumin and stained for 1 hour at room temperature using the phospho-AKT (S473)-647 conjugated antibody (Table MM.4.).

Statistical analysis

Results are presented as means and standard deviations. Statistical significances were determined by one-way ANOVA or two-ways ANOVA with Bonferroni or Dunnett's post-test as well as the Mann-Whitney test and 2-tailed Fisher´s exact test for comparison between patient groups. Graph Pad Prism software v.5 was used for the analysis. The specific statistical tests used for the individual analysis are provided in the "Results".

Table MM.1. Primers used for mutation screening

Gene/primer name	Template	Primer sequence 5'→ 3'
NOTCH1		
NOTCH1 ex25-F1	cDNA	GCCTCTTCGACGGCTTTGAC
NOTCH1 ex28-R1	cDNA	TTGCTGGCCTCAGACACTTTG
NOTCH1 ex34-F1	cDNA	TCCCCGTTCCAGCAGTCTC
NOTCH1 ex34-R1	cDNA	GCTCGGCTCTCCACTCAGG
NOTCH1 ex34-F2	cDNA	AGCGCCCTGTCCCAGATG
NOTCH1 ex34-R2	cDNA	GCACACAGACGCCCGAAG
NOTCH1_27F	gDNA	AGGCCGTGCAGAGTAAGTGT
NOTCH1_28R	gDNA	CCACGAAGAACAGAAGCACA
NOTCH1_g26F *	gDNA	GCTGAGGGAGGACCTGAACTTGG
NOTCH1_g26R *	gDNA	CCTGAGCTGGAATGCTGCCTCTA
NOTCH1_g27F *	gDNA	CATGGGCCTCAGTGTCCT
NOTCH1_g27R *	gDNA	TAGCAACTGGCACAAACAGC
NOTCH1g28-F4 *	gDNA	GCGTAGCCGCTGCCTGAT
NOTCH1g28-R3 *	gDNA	CAGACTCCCGGTGAGGATGC
FBXW7		
FBXW7ex9-F1	cDNA	TGGAGTATGGTCATCACAAATGAG
FBXW7ex11-R1	cDNA	TGTATCAAGAGATCCACTCACCAC
FBXW7-F2	gDNA	ATTCCCAGCAAGGACAGTTG
FBXW7-R2	gDNA	ATGTAATTCGGCGTCGTTGT
FBXW7-F3	gDNA	ACGCCGAATTACATCTGTCC
FBXW7-R3	gDNA	AGTTCTCCTCGCCTCCAGTT
FBXW7-F4	gDNA	CCTGCTACAAGCAGCTCAGA
FBXW7-R4	gDNA	TATTGAACACAGCGGACTGC
FBXW7-F5	gDNA	GTGTTTGGGATGTGGAGACA
FBXW7-R5	gDNA	GTCCACATCAAAGTCCAGCAC
FBXW7-R6	gDNA	ATGCAATTCCCTGTCTCCAC
PTEN		
PTENint6-F1	gDNA	TCATTTATTTCAGTTGATTTGCTTG
PTENint7-R1	gDNA	TTGGTCCCATGCTAATTTCTTC
gPTEN-int4-F1	gDNA	TTGTATGCAACATTTCTAAAGTT
gPTEN-int5-R1	gDNA	ATCTGTTTTCCAATAAATTCTCA
gPTEN-int5-F1	gDNA	ACGACCCAGTTACCATAGC
gPTEN-int6-R1	gDNA	TAGCCCAATGAGTTGAACA
gPTEN-int7-F1	gDNA	GATTGCCTTATAATAGTCTTTGTG
gPTEN-int8-R1	gDNA	TTTTTGACGCTGTGTACATT

gDNA, genomic DNA; F, forward primer; R, reverse primer
*** primer sequences from Sulis et al., 2008**

Table MM.2. Other primers used

Gene/primer name	Template	Primer sequence 5'→ 3'
T7	vector	TAATACGACTCACTATAGGG
T3	vector	ATTAACCCTCACTAAAGGGA
M13 F	vector	GTAAAACGACGGCCAG
M13 R	vector	CAGGAAACAGCTATGAC
NKX2-5-F *	cDNA	TCTATCCACGTGCCTACAGC
NKX2-5-R *	cDNA	TGGACGTGAGTTTCAGCACG
NKX2-2-F *	cDNA	GGACATCTTAGACCTGCCGG
NKX2-2-R *	cDNA	TTGGAGCTTGAGTCCTGAGG
CDKN1B_1_F	gDNA	CTTTGGCTTCTTCCCTAGGC
CDKN1B_1_R	gDNA	ATGGTTCGCTCAGCCTTAAC
CDKN1B_2_F	gDNA	AGGTTTGTTGGCAGCAGTAC
CDKN1B_2_R	gDNA	GAGCGCGGCCTTAAGGTG
CDKN1B_3_F	gDNA	CCATTTGATCAGCGGAGACT
CDKN1B_3_R	gDNA	AGATGTCAAACGTGCGAGTG
CDKN1B_4_F	gDNA	TAGAATGTGTTTGGGGCCCC
CDKN1B_4_R	gDNA	CAAACAGACAAGCAGTGGGC
CDKN1B_5_F	gDNA	TTGGGGCAAAAATCCGAGGT
CDKN1B_5_R	gDNA	TGTTTACACAGCCCGAAGTGA

gDNA, genomic DNA; F, forward primer; R, reverse primer
*** primer sequences from Nagel, 2003**

Table MM.3. Primers used for quantitative PCR

Gene/primer name	Template	Primer sequence 5'→ 3'
GUSB-ENF1102	cDNA	GAAAATATGTGGTTGGAGAGCTCATT
GUSB-ENR1162	cDNA	CCGAGTGAAGATCCCCTTTTTA
CDKN1B_ex2_F3	cDNA	CGTCAAACGTAAACAGCTCG
CDKN1B_ex3_R3	cDNA	ACAGGATGTCCATTCCATGA
HES1_ex3F2	cDNA	ACGACACCGGATAAACCAA
HES1_ex3-4-R1	cDNA	TGCCGCGAGCTATCTTTCTT
MYC-F1	cDNA	AACAGGAACTATGACCTCG
MYC-R1	cDNA	AGCAGCTCGAATTTCTTC
SKP2_F1	cDNA	AGCCCGACAGTGAGAACATC
SKP2_R1	cDNA	GAAGGGAGTCCCATGAAACA
PPP3CA (TSS)	gDNA	GCGGCTGGTGGCACTGACAT
PPP3CA (TSS)	gDNA	CACACACGAGCACCCACCCC
SATB1 (exon 1)	gDNA	CGGCCGGGATGAGTCAACTA
SATB1 (exon 1)	gDNA	GGGCTGCTTCTCTCGCTCTC
CDKN1B_F4 (5´UTR)	gDNA	ATAAGTGCCGCGTCTACTCC
CDKN1B_R2 (5´UTR)	gDNA	CGCTCAGCCTTAACCCAGAA
CDKN1B_F7 (exon 3)	gDNA	CCGCAACCAATGGATCTCCT
CDKN1B_R7 (exon 3)	gDNA	CAGGGGAGGGGGAGAAAAAC

gDNA, genomic DNA; TSS, transcriptional start site; UTR, untranslated region

Table MM.4a. List of primary antibodies

Antibody	Host species & dilution		kDa	Manufacturer	Application
NOTCH1-Val1744	rabbit	1:500	100-120	Cell signaling	WB
p27kip1	rabbit	1:200	25-27	Santa Cruz	WB
MYC (sc40)	mouse	1:1000	60	Santa Cruz	WB
HES1	mouse	1:500	30-35	Sigma	WB
SKP2	rabbit	1:500	48	Cell signaling	WB
PTEN	rabbit	1:1000	54	Cell signaling	WB
FOXO3	rabbit	1:1000	97	Cell signaling	WB
RNF123/KPC (M01) (3F8)	mouse	1:500	140	Abnova	WB
PARP	mouse	1:1000	116/90	Becton Dickinson	WB
GAPDH sc-32233 (6C5)	mouse	1:1000	37	Santa Cruz	WB
lamin A/C	rabbit	1:1000	72-55	Cell signaling	WB
tubulin (CP06)	mouse	1:5000	55	Merck	WB
β-actin (C4)	mouse	1:5000	43	Santa Cruz	WB
Antibody	**Host species & dilution**		**Fluorochrome**	**Manufacturer**	**Application**
p-AKT (S473) (D9E)	rabbit	1:250	647Conj	Cell signaling	FACS

WB, Western blotting; FACS, fluorescence activated cell sorting

Table MM.4b. List of secondary antibodies

Host species	Fluorochrome	Dilution	Manufacturer	Application
Anti-mouse	680 conjugated	1:15000	Thermo Scientific	WB
	800 conjugated	1:12500	Thermo Scientific	WB
Anti rabbit	800 conjugated	1:12500	Thermo Scientific	WB

WB, Western blotting

Table MM.5. List of compounds

Compound	Manufacturer	Catalogue number	Dissolved in	Concentration used
Dexamethasone	Sigma	D4902	EtOH	100 nM
DAPT (GSI-IX)	Selleckchem	S2215	DMSO	5 μM
Compound E (GSI-XXI)	Merck Millipore	565790	DMSO	1 μM
MK-2206 (AKT inhibitor)	Selleckchem	S1078	DMSO	4 μM
MG-132	Selleckchem	S2619	DMSO	20 μM
C1, SKP2 E3 Ligase Inhibitor I	Merck Millipore	500519	DMSO	2.5-8 μM
C25, SKP2 E3 Ligase Inhibitor III	Merck Millipore	506305	DMSO	20 μM

ANNEX

Colomer-Lahiguera S, Strehl S. Complexity of NOTCH1 juxtamembrane insertion mutations in T-cell acute lymphoblastic leukemia. Leuk Lymphoma. 2016 May 3;57(5):1219–22. DOI: 10.3109/10428194.2015.1080366

REFERENCES

Aifantis, I., Raetz, E., and Buonamici, S. (2008). Molecular pathogenesis of T-cell leukaemia and lymphoma. Nat Rev Immunol *8*, 380-390.

Akli, S., and Keyomarsi, K. (2003). Cyclin E and its low molecular weight forms in human cancer and as targets for cancer therapy. Cancer Biol Ther *2*, S38-47.

Aleem, E., and Arceci, R. J. (2015). Targeting cell cycle regulators in hematologic malignancies. Front Cell Dev Biol *3*, 16.

Anderson, N. M., Harrold, I., Mansour, M. R., Sanda, T., McKeown, M., Nagykary, N., Bradner, J. E., Lan Zhang, G., Look, A. T., and Feng, H. (2014). BCL2-specific inhibitor ABT-199 synergizes strongly with cytarabine against the early immature LOUCY cell line but not more-differentiated T-ALL cell lines. Leukemia *28*, 1145-1148.

Andersson, E. R., and Lendahl, U. (2014). Therapeutic modulation of Notch signalling--are we there yet? Nat Rev Drug Discov *13*, 357-378.

Asada, M., Yamada, T., Ichijo, H., Delia, D., Miyazono, K., Fukumuro, K., and Mizutani, S. (1999). Apoptosis inhibitory activity of cytoplasmic p21(Cip1/WAF1) in monocytic differentiation. EMBO J *18*, 1223-1234.

Asnafi, V., Buzyn, A., Le Noir, S., Baleydier, F., Simon, A., Beldjord, K., Reman, O., Witz, F., Fagot, T., Tavernier, E.*, et al.* (2009). NOTCH1/FBXW7 mutation identifies a large subgroup with favorable outcome in adult T-cell acute lymphoblastic leukemia (T-ALL): a Group for Research on Adult Acute Lymphoblastic Leukemia (GRAALL) study. Blood *113*, 3918-3924.

Aster, J. C., Pear, W. S., and Blacklow, S. C. (2008). Notch signaling in leukemia. Annu Rev Pathol *3*, 587-613.

Attarbaschi, A., Pisecker, M., Inthal, A., Mann, G., Janousek, D., Dworzak, M., Potschger, U., Ullmann, R., Schrappe, M., Gadner, H.*, et al.* (2010). Prognostic relevance of TLX3 (HOX11L2) expression in childhood T-cell acute lymphoblastic leukaemia treated with Berlin-Frankfurt-Munster (BFM) protocols containing early and late re-intensification elements. Br J Haematol *148*, 293-300.

Ausserlechner, M. J., Obexer, P., Bock, G., Geley, S., and Kofler, R. (2004). Cyclin D3 and c-MYC control glucocorticoid-induced cell cycle arrest but not apoptosis in lymphoblastic leukemia cells. Cell Death Differ *11*, 165-174.

Baldassarre, G., Belletti, B., Bruni, P., Boccia, A., Trapasso, F., Pentimalli, F., Barone, M. V., Chiappetta, G., Vento, M. T., Spiezia, S.*, et al.* (1999). Overexpressed cyclin D3 contributes to retaining the growth inhibitor p27 in the cytoplasm of thyroid tumor cells. J Clin Invest *104*, 865-874.

Baldassarre, G., Belletti, B., Nicoloso, M. S., Schiappacassi, M., Vecchione, A., Spessotto, P., Morrione, A., Canzonieri, V., and Colombatti, A. (2005). p27(Kip1)-stathmin interaction influences sarcoma cell migration and invasion. Cancer Cell *7*, 51-63.

Bandapalli, O. R., Zimmermann, M., Kox, C., Stanulla, M., Schrappe, M., Ludwig, W. D., Koehler, R., Muckenthaler, M. U., and Kulozik, A. E. (2013). NOTCH1 activation clinically antagonizes the unfavorable effect of PTEN inactivation in BFM-treated children with precursor T-cell acute lymphoblastic leukemia. Haematologica *98*, 928-936.

Baylin, S. B., and Ohm, J. E. (2006). Epigenetic gene silencing in cancer - a mechanism for early oncogenic pathway addiction? Nat Rev Cancer *6*, 107-116.

Belletti, B., Pellizzari, I., Berton, S., Fabris, L., Wolf, K., Lovat, F., Schiappacassi, M., D'Andrea, S., Nicoloso, M. S., Lovisa, S.*, et al.* (2010). p27kip1 controls cell morphology and motility by regulating microtubule-dependent lipid raft recycling. Mol Cell Biol *30*, 2229-2240.

Besson, A., Assoian, R. K., and Roberts, J. M. (2004). Regulation of the cytoskeleton: an oncogenic function for CDK inhibitors? Nat Rev Cancer *4*, 948-955.

Besson, A., Dowdy, S. F., and Roberts, J. M. (2008). CDK inhibitors: cell cycle regulators and beyond. Dev Cell *14*, 159-169.

Besson, A., Gurian-West, M., Chen, X., Kelly-Spratt, K. S., Kemp, C. J., and Roberts, J. M. (2006). A pathway in quiescent cells that controls p27Kip1 stability, subcellular localization, and tumor suppression. Genes Dev *20*, 47-64.

Besson, A., Hwang, H. C., Cicero, S., Donovan, S. L., Gurian-West, M., Johnson, D., Clurman, B. E., Dyer, M. A., and Roberts, J. M. (2007). Discovery of an oncogenic activity in p27Kip1 that causes stem cell expansion and a multiple tumor phenotype. Genes Dev *21*, 1731-1746.

Borriello, A., Bencivenga, D., Criscuolo, M., Caldarelli, I., Cucciolla, V., Tramontano, A., Borgia, A., Spina, A., Oliva, A., Naviglio, S., and Della Ragione, F. (2011). Targeting p27Kip1 protein: its relevance in the therapy of human cancer. Expert Opin Ther Targets *15*, 677-693.

Breit, S., Stanulla, M., Flohr, T., Schrappe, M., Ludwig, W. D., Tolle, G., Happich, M., Muckenthaler, M. U., and Kulozik, A. E. (2006). Activating NOTCH1 mutations predict favorable early treatment response and long-term outcome in childhood precursor T-cell lymphoblastic leukemia. Blood *108*, 1151-1157.

Bretones, G., Acosta, J. C., Caraballo, J. M., Ferrandiz, N., Gomez-Casares, M. T., Albajar, M., Blanco, R., Ruiz, P., Hung, W. C., Albero, M. P.*, et al.* (2011). SKP2 oncogene is a direct MYC target gene and MYC down-regulates p27(KIP1) through SKP2 in human leukemia cells. J Biol Chem *286*, 9815-9825.

Brunet, A., Bonni, A., Zigmond, M. J., Lin, M. Z., Juo, P., Hu, L. S., Anderson, M. J., Arden, K. C., Blenis, J., and Greenberg, M. E. (1999). Akt promotes cell survival by phosphorylating and inhibiting a Forkhead transcription factor. Cell *96*, 857-868.

Burgering, B. M., and Kops, G. J. (2002). Cell cycle and death control: long live Forkheads. Trends Biochem Sci *27*, 352-360.

Cardozo, T., and Pagano, M. (2004). The SCF ubiquitin ligase: insights into a molecular machine. Nat Rev Mol Cell Biol *5*, 739-751.

Carracedo, A., and Pandolfi, P. P. (2008). The PTEN-PI3K pathway: of feedbacks and cross-talks. Oncogene *27*, 5527-5541.

Cave, H., Suciu, S., Preudhomme, C., Poppe, B., Robert, A., Uyttebroeck, A., Malet, M., Boutard, P., Benoit, Y., Mauvieux, L.*, et al.* (2004). Clinical significance of HOX11L2 expression linked to t(5;14)(q35;q32), of HOX11 expression, and of SIL-TAL fusion in childhood T-cell malignancies: results of EORTC studies 58881 and 58951. Blood *103*, 442-450.

Chan, C. H., Lee, S. W., Wang, J., and Lin, H. K. (2010). Regulation of Skp2 expression and activity and its role in cancer progression. Scientific World Journal *10*, 1001-1015.

Chan, C. H., Li, C. F., Yang, W. L., Gao, Y., Lee, S. W., Feng, Z., Huang, H. Y., Tsai, K. K., Flores, L. G., Shao, Y., *et al.* (2012). The Skp2-SCF E3 ligase regulates Akt ubiquitination, glycolysis, herceptin sensitivity, and tumorigenesis. Cell *149*, 1098-1111.

Chan, C. H., Morrow, J. K., Li, C. F., Gao, Y., Jin, G., Moten, A., Stagg, L. J., Ladbury, J. E., Cai, Z., Xu, D., *et al.* (2013). Pharmacological inactivation of Skp2 SCF ubiquitin ligase restricts cancer stem cell traits and cancer progression. Cell *154*, 556-568.

Chan, C. H., Morrow, J. K., Zhang, S., and Lin, H. K. (2014). Skp2: a dream target in the coming age of cancer therapy. Cell Cycle *13*, 679-680.

Chan, S. M., Weng, A. P., Tibshirani, R., Aster, J. C., and Utz, P. J. (2007). Notch signals positively regulate activity of the mTOR pathway in T-cell acute lymphoblastic leukemia. Blood *110*, 278-286.

Chandramohan, V., Jeay, S., Pianetti, S., and Sonenshein, G. E. (2004). Reciprocal control of Forkhead box O 3a and c-Myc via the phosphatidylinositol 3-kinase pathway coordinately regulates p27Kip1 levels. J Immunol *172*, 5522-5527.

Cheng, L., Samad, O. A., Xu, Y., Mizuguchi, R., Luo, P., Shirasawa, S., Goulding, M., and Ma, Q. (2005). Lbx1 and Tlx3 are opposing switches in determining GABAergic versus glutamatergic transmitter phenotypes. Nat Neurosci *8*, 1510-1515.

Chu, I. M., Hengst, L., and Slingerland, J. M. (2008). The Cdk inhibitor p27 in human cancer: prognostic potential and relevance to anticancer therapy. Nat Rev Cancer *8*, 253-267.

Clappier, E., Collette, S., Grardel, N., Girard, S., Suarez, L., Brunie, G., Kaltenbach, S., Yakouben, K., Mazingue, F., Robert, A., *et al.* (2010). NOTCH1 and FBXW7 mutations have a favorable impact on early response to treatment, but not on outcome, in children with T-cell acute lymphoblastic leukemia (T-ALL) treated on EORTC trials 58881 and 58951. Leukemia *24*, 2023-2031.

Connor, M. K., Kotchetkov, R., Cariou, S., Resch, A., Lupetti, R., Beniston, R. G., Melchior, F., Hengst, L., and Slingerland, J. M. (2003). CRM1/Ran-mediated nuclear export of p27(Kip1) involves a nuclear export signal and links p27 export and proteolysis. Mol Biol Cell *14*, 201-213.

Conter, V., Bartram, C. R., Valsecchi, M. G., Schrauder, A., Panzer-Grumayer, R., Moricke, A., Arico, M., Zimmermann, M., Mann, G., De Rossi, G., *et al.* (2010). Molecular response to treatment redefines all prognostic factors in children and adolescents with B-cell precursor acute lymphoblastic leukemia: results in 3184 patients of the AIEOP-BFM ALL 2000 study. Blood *115*, 3206-3214.

Coustan-Smith, E., Mullighan, C. G., Onciu, M., Behm, F. G., Raimondi, S. C., Pei, D., Cheng, C., Su, X., Rubnitz, J. E., Basso, G., *et al.* (2009). Early T-cell precursor leukaemia: a subtype of very high-risk acute lymphoblastic leukaemia. Lancet Oncol *10*, 147-156.

Cullion, K., Draheim, K. M., Hermance, N., Tammam, J., Sharma, V. M., Ware, C., Nikov, G., Krishnamoorthy, V., Majumder, P. K., and Kelliher, M. A. (2009). Targeting the Notch1 and mTOR pathways in a mouse T-ALL model. Blood *113*, 6172-6181.

D'Angio, M., Valsecchi, M. G., Testi, A. M., Conter, V., Nunes, V., Parasole, R., Colombini, A., Santoro, N., Varotto, S., Caniglia, M., *et al.* (2015). Clinical features

and outcome of SIL/TAL1-positive T-cell acute lymphoblastic leukemia in children and adolescents: a 10-year experience of the AIEOP group. Haematologica *100*, e10-13.

Dadi, S., Le Noir, S., Payet-Bornet, D., Lhermitte, L., Zacarias-Cabeza, J., Bergeron, J., Villarese, P., Vachez, E., Dik, W. A., Millien, C.*, et al.* (2012). TLX homeodomain oncogenes mediate T cell maturation arrest in T-ALL via interaction with ETS1 and suppression of TCRalpha gene expression. Cancer Cell *21*, 563-576.

Dail, M., Wong, J., Lawrence, J., O'Connor, D., Nakitandwe, J., Chen, S. C., Xu, J., Lee, L. B., Akagi, K., Li, Q.*, et al.* (2014). Loss of oncogenic Notch1 with resistance to a PI3K inhibitor in T-cell leukaemia. Nature *513*, 512-516.

Dansen, T. B., and Burgering, B. M. (2008). Unravelling the tumor-suppressive functions of FOXO proteins. Trends Cell Biol *18*, 421-429.

De Keersmaecker, K., Lahortiga, I., Mentens, N., Folens, C., Van Neste, L., Bekaert, S., Vandenberghe, P., Odero, M. D., Marynen, P., and Cools, J. (2008). In vitro validation of gamma-secretase inhibitors alone or in combination with other anti-cancer drugs for the treatment of T-cell acute lymphoblastic leukemia. Haematologica *93*, 533-542.

De Keersmaecker, K., Marynen, P., and Cools, J. (2005). Genetic insights in the pathogenesis of T-cell acute lymphoblastic leukemia. Haematologica *90*, 1116-1127.

De Keersmaecker, K., Real, P. J., Gatta, G. D., Palomero, T., Sulis, M. L., Tosello, V., Van Vlierberghe, P., Barnes, K., Castillo, M., Sole, X.*, et al.* (2010). The TLX1 oncogene drives aneuploidy in T cell transformation. Nat Med *16*, 1321-1327.

Deangelo, D. J., Stone, R. M., Silverman, L. B., Stock, W., Attar, E. C., Fearen, I., Dallob, A., Matthews, C., Stone, J., Freedman, S. J., and Aster, J. (2006). A phase I clinical trial of the notch inhibitor MK-0752 in patients with T-cell acute lymphoblastic leukemia/lymphoma (T-ALL) and other leukemias. J Clin Oncol (Meeting Abstracts) *24*.

Dehan, E., and Pagano, M. (2005). Skp2, the FoxO1 hunter. Cancer Cell *7*, 209-210.

Denicourt, C., Saenz, C. C., Datnow, B., Cui, X. S., and Dowdy, S. F. (2007). Relocalized p27Kip1 tumor suppressor functions as a cytoplasmic metastatic oncogene in melanoma. Cancer Res *67*, 9238-9243.

Dijkers, P. F., Medema, R. H., Pals, C., Banerji, L., Thomas, N. S., Lam, E. W., Burgering, B. M., Raaijmakers, J. A., Lammers, J. W., Koenderman, L., and Coffer, P. J. (2000). Forkhead transcription factor FKHR-L1 modulates cytokine-dependent transcriptional regulation of p27(KIP1). Mol Cell Biol *20*, 9138-9148.

Dohda, T., Maljukova, A., Liu, L., Heyman, M., Grander, D., Brodin, D., Sangfelt, O., and Lendahl, U. (2007). Notch signaling induces SKP2 expression and promotes reduction of p27Kip1 in T-cell acute lymphoblastic leukemia cell lines. Exp Cell Res *313*, 3141-3152.

Durinck, K., Van Loocke, W., Van der Meulen, J., Van de Walle, I., Ongenaert, M., Rondou, P., Wallaert, A., de Bock, C. E., Van Roy, N., Poppe, B.*, et al.* (2015). Characterization of the genome-wide TLX1 binding profile in T-cell acute lymphoblastic leukemia. Leukemia.

Durinck, K., Wallaert, A., Van de Walle, I., Van Loocke, W., Volders, P. J., Vanhauwaert, S., Geerdens, E., Benoit, Y., Van Roy, N., Poppe, B.*, et al.* (2014). The Notch driven long non-coding RNA repertoire in T-cell acute lymphoblastic leukemia. Haematologica *99*, 1808-1816.

Erdogan, F., Chen, W., Kirchhoff, M., Kalscheuer, V. M., Hultschig, C., Muller, I., Schulz, R., Menzel, C., Bryndorf, T., Ropers, H. H., and Ullmann, R. (2006). Impact of low copy repeats on the generation of balanced and unbalanced chromosomal aberrations in mental retardation. Cytogenet Genome Res *115*, 247-253.

Fero, M. L., Randel, E., Gurley, K. E., Roberts, J. M., and Kemp, C. J. (1998). The murine gene p27Kip1 is haplo-insufficient for tumour suppression. Nature *396*, 177-180.

Fero, M. L., Rivkin, M., Tasch, M., Porter, P., Carow, C. E., Firpo, E., Polyak, K., Tsai, L. H., Broudy, V., Perlmutter, R. M.*, et al.* (1996). A syndrome of multiorgan hyperplasia with features of gigantism, tumorigenesis, and female sterility in p27(Kip1)-deficient mice. Cell *85*, 733-744.

Ferrando, A. A., and Look, A. T. (2003). Gene expression profiling in T-cell acute lymphoblastic leukemia. Semin Hematol *40*, 274-280.

Ferrando, A. A., Neuberg, D. S., Staunton, J., Loh, M. L., Huard, C., Raimondi, S. C., Behm, F. G., Pui, C. H., Downing, J. R., Gilliland, D. G.*, et al.* (2002). Gene expression signatures define novel oncogenic pathways in T cell acute lymphoblastic leukemia. Cancer Cell *1*, 75-87.

Flohr, T., Schrauder, A., Cazzaniga, G., Panzer-Grumayer, R., van der Velden, V., Fischer, S., Stanulla, M., Basso, G., Niggli, F. K., Schafer, B. W.*, et al.* (2008). Minimal residual disease-directed risk stratification using real-time quantitative PCR analysis of immunoglobulin and T-cell receptor gene rearrangements in the international multicenter trial AIEOP-BFM ALL 2000 for childhood acute lymphoblastic leukemia. Leukemia *22*, 771-782.

Fogelstrand, L., Staffas, A., Wasslavik, C., Sjogren, H., Soderhall, S., Frost, B. M., Forestier, E., Degerman, S., Behrendtz, M., Heldrup, J.*, et al.* (2014). Prognostic implications of mutations in NOTCH1 and FBXW7 in childhood T-ALL treated according to the NOPHO ALL-1992 and ALL-2000 protocols. Pediatr Blood Cancer *61*, 424-430.

Frescas, D., and Pagano, M. (2008). Deregulated proteolysis by the F-box proteins SKP2 and beta-TrCP: tipping the scales of cancer. Nat Rev Cancer *8*, 438-449.

Fujita, N., Sato, S., and Tsuruo, T. (2003). Phosphorylation of p27Kip1 at threonine 198 by p90 ribosomal protein S6 kinases promotes its binding to 14-3-3 and cytoplasmic localization. J Biol Chem *278*, 49254-49260.

Gao, C., Liu, S. G., Zhang, R. D., Li, W. J., Zhao, X. X., Cui, L., Wu, M. Y., Zheng, H. Y., and Li, Z. G. (2014). NOTCH1 mutations are associated with favourable long-term prognosis in paediatric T-cell acute lymphoblastic leukaemia: a retrospective study of patients treated on BCH-2003 and CCLG-2008 protocol in China. Br J Haematol.

Gao, D., Inuzuka, H., Tseng, A., Chin, R. Y., Toker, A., and Wei, W. (2009). Phosphorylation by Akt1 promotes cytoplasmic localization of Skp2 and impairs APCCdh1-mediated Skp2 destruction. Nat Cell Biol *11*, 397-408.

Gimenes-Teixeira, H. L., Lucena-Araujo, A. R., Dos Santos, G. A., Zanette, D. L., Scheucher, P. S., Oliveira, L. C., Dalmazzo, L. F., Silva-Junior, W. A., Falcao, R. P., and Rego, E. M. (2013). Increased expression of miR-221 is associated with shorter overall survival in T-cell acute lymphoid leukemia. Exp Hematol Oncol *2*, 10.

Gordon, W. R., Roy, M., Vardar-Ulu, D., Garfinkel, M., Mansour, M. R., Aster, J. C., and Blacklow, S. C. (2009). Structure of the Notch1-negative regulatory region: implications for normal activation and pathogenic signaling in T-ALL. Blood *113*, 4381-4390.

Graux, C., Cools, J., Michaux, L., Vandenberghe, P., and Hagemeijer, A. (2006). Cytogenetics and molecular genetics of T-cell acute lymphoblastic leukemia: from thymocyte to lymphoblast. Leukemia *20*, 1496-1510.

Graux, C., Stevens-Kroef, M., Lafage, M., Dastugue, N., Harrison, C. J., Mugneret, F., Bahloula, K., Struski, S., Gregoire, M. J., Nadal, N.*, et al.* (2009). Heterogeneous patterns of amplification of the NUP214-ABL1 fusion gene in T-cell acute lymphoblastic leukemia. Leukemia *23*, 125-133.

Guo, X., Deng, L., Deng, K., Wang, H., Shan, T., Zhou, H., Liang, Z., Xia, J., and Li, C. (2015). Pseudogene PTENP1 Suppresses Gastric Cancer Progression by Modulating PTEN. Anticancer Agents Med Chem.

Gutierrez, A., Dahlberg, S. E., Neuberg, D. S., Zhang, J., Grebliunaite, R., Sanda, T., Protopopov, A., Tosello, V., Kutok, J., Larson, R. S.*, et al.* (2010). Absence of biallelic TCRgamma deletion predicts early treatment failure in pediatric T-cell acute lymphoblastic leukemia. J Clin Oncol *28*, 3816-3823.

Gutierrez, A., and Look, A. T. (2010). Molecular targeted therapies in T-cell acute lymphoblastic leukemia. In Molecularly Targeted Therapy for Childhood Cancer, P.J. Houghton, and R.J. Arceci, eds. (Springer).

Gutierrez, A., Sanda, T., Grebliunaite, R., Carracedo, A., Salmena, L., Ahn, Y., Dahlberg, S., Neuberg, D., Moreau, L. A., Winter, S. S.*, et al.* (2009). High frequency of PTEN, PI3K, and AKT abnormalities in T-cell acute lymphoblastic leukemia. Blood *114*, 647-650.

Hao, Z., and Huang, S. (2015). E3 ubiquitin ligase Skp2 as an attractive target in cancer therapy. Front Biosci (Landmark Ed) *20*, 474-490.

Hara, T., Kamura, T., Nakayama, K., Oshikawa, K., Hatakeyama, S., and Nakayama, K. (2001). Degradation of p27(Kip1) at the G(0)-G(1) transition mediated by a Skp2-independent ubiquitination pathway. J Biol Chem *276*, 48937-48943.

Harper, J. W., Adami, G. R., Wei, N., Keyomarsi, K., and Elledge, S. J. (1993). The p21 Cdk-interacting protein Cip1 is a potent inhibitor of G1 cyclin-dependent kinases. Cell *75*, 805-816.

Haydu, J. E., and Ferrando, A. A. (2013). Early T-cell precursor acute lymphoblastic leukaemia. Curr Opin Hematol *20*, 369-373.

Hengst, L., and Reed, S. I. (1996). Translational control of p27Kip1 accumulation during the cell cycle. Science *271*, 1861-1864.

Hershko, D. D. (2008). Oncogenic properties and prognostic implications of the ubiquitin ligase Skp2 in cancer. Cancer *112*, 1415-1424.

Hetet, G., Dastot, H., Baens, M., Brizard, A., Sigaux, F., Grandchamp, B., and Stern, M. H. (2000). Recurrent molecular deletion of the 12p13 region, centromeric to ETV6/TEL, in T-cell prolymphocytic leukemia. Hematol J *1*, 42-47.

Hochegger, H., Takeda, S., and Hunt, T. (2008). Cyclin-dependent kinases and cell-cycle transitions: does one fit all? Nat Rev Mol Cell Biol *9*, 910-916.

Homminga, I., Pieters, R., Langerak, A. W., de Rooi, J. J., Stubbs, A., Verstegen, M., Vuerhard, M., Buijs-Gladdines, J., Kooi, C., Klous, P.*, et al.* (2011). Integrated transcript and genome analyses reveal NKX2-1 and MEF2C as potential oncogenes in T cell acute lymphoblastic leukemia. Cancer Cell *19*, 484-497.

Homminga, I., Pieters, R., and Meijerink, J. P. (2012). NKL homeobox genes in leukemia. Leukemia *26*, 572-581.

Huang, H., Regan, K. M., Wang, F., Wang, D., Smith, D. I., van Deursen, J. M., and Tindall, D. J. (2005). Skp2 inhibits FOXO1 in tumor suppression through ubiquitin-mediated degradation. Proc Natl Acad Sci U S A *102*, 1649-1654.

Huang, S., Shu, L., Dilling, M. B., Easton, J., Harwood, F. C., Ichijo, H., and Houghton, P. J. (2003). Sustained activation of the JNK cascade and rapamycin-induced apoptosis are suppressed by p53/p21(Cip1). Mol Cell *11*, 1491-1501.

Hung, T., Wang, Y., Lin, M. F., Koegel, A. K., Kotake, Y., Grant, G. D., Horlings, H. M., Shah, N., Umbricht, C., Wang, P.*, et al.* (2011). Extensive and coordinated transcription of noncoding RNAs within cell-cycle promoters. Nat Genet *43*, 621-629.

Hunger, S. P., and Mullighan, C. G. (2015). Redefining ALL classification: toward detecting high-risk ALL and implementing precision medicine. Blood *125*, 3977-3987.

Inaba, H., Greaves, M., and Mullighan, C. G. (2013). Acute lymphoblastic leukaemia. The Lancet *381*, 1943-1955.

Inaba, H., and Pui, C. H. (2010). Glucocorticoid use in acute lymphoblastic leukaemia. Lancet Oncol *11*, 1096-1106.

Inoue, T., Kamiyama, J., and Sakai, T. (1999). Sp1 and NF-Y synergistically mediate the effect of vitamin D(3) in the p27(Kip1) gene promoter that lacks vitamin D response elements. J Biol Chem *274*, 32309-32317.

Inukai, T., Kiyokawa, N., Campana, D., Coustan-Smith, E., Kikuchi, A., Kobayashi, M., Takahashi, H., Koh, K., Manabe, A., Kumagai, M.*, et al.* (2012). Clinical significance of early T-cell precursor acute lymphoblastic leukaemia: results of the Tokyo Children's Cancer Study Group Study L99-15. Br J Haematol *156*, 358-365.

Ishii, T., Fujishiro, M., Masuda, M., Goshima, Y., Kitamura, H., Teramoto, S., and Matsuse, T. (2004). Effects of p27Kip1 on cell cycle status and viability in A549 lung adenocarcinoma cells. Eur Respir J *23*, 665-670.

Jarriault, S., Le Bail, O., Hirsinger, E., Pourquie, O., Logeat, F., Strong, C. F., Brou, C., Seidah, N. G., and Isra l, A. (1998). Delta-1 activation of notch-1 signaling results in HES-1 transactivation. Mol Cell Biol *18*, 7423-7431.

Jaruga-Killeen, E., and Rayford, W. (2005). TNF receptor 1 is involved in the induction of apoptosis by the cyclin dependent kinase inhibitor p27Kip1 in the prostate cancer cell line PC-3. FASEB J *19*, 139-141.

Jenkinson, S., Kirkwood, A. A., Goulden, N., Vora, A., Linch, D. C., and Gale, R. E. (2015). Impact of PTEN abnormalities on outcome in pediatric patients with T-

cell acute lymphoblastic leukemia treated on the MRC UKALL2003 trial. Leukemia.

Jeon, M. J., Yang, W., Seo, H. S., Wang, E. S., and Shin, I. (2012). Down-regulation of estrogen receptor alpha (ERalpha) transcriptional activity by p27 is mediated by inhibition of ERalpha nuclear localization and modulation of the ERalpha transcriptional complex. Cell Signal *24*, 2249-2258.

Johnsson, P., Ackley, A., Vidarsdottir, L., Lui, W. O., Corcoran, M., Grander, D., and Morris, K. V. (2013). A pseudogene long-noncoding-RNA network regulates PTEN transcription and translation in human cells. Nat Struct Mol Biol *20*, 440-446.

Joshi, I., Minter, L. M., Telfer, J., Demarest, R. M., Capobianco, A. J., Aster, J. C., Sicinski, P., Fauq, A., Golde, T. E., and Osborne, B. A. (2008). Notch signaling mediates G1/S cell cycle progression in T cells via cyclin D3 and its dependent kinases. Blood.

Kamiyama, J., Inoue, T., Ohtani-Fujita, N., Minami, S., Yamagishi, H., and Sakai, T. (1999). The ubiquitous transcription factor NF-Y positively regulates the transcription of human p27Kip1 through a CCAAT box located in the 5-upstream region of the p27Kip1 gene. FEBS Lett *455*, 281-285.

Kamura, T., Hara, T., Matsumoto, M., Ishida, N., Okumura, F., Hatakeyama, S., Yoshida, M., Nakayama, K., and Nakayama, K. I. (2004). Cytoplasmic ubiquitin ligase KPC regulates proteolysis of p27(Kip1) at G1 phase. Nat Cell Biol *6*, 1229-1235.

Kanzawa, T., Komata, T., Kyo, S., Germano, I. M., Kondo, Y., and Kondo, S. (2003). Down-regulation of telomerase activity in malignant glioma cells by p27KIP1. Int J Oncol *23*, 1703-1708.

Katayose, Y., Kim, M., Rakkar, A. N., Li, Z., Cowan, K. H., and Seth, P. (1997). Promoting apoptosis: a novel activity associated with the cyclin-dependent kinase inhibitor p27. Cancer Res *57*, 5441-5445.

Keller, U. B., Old, J. B., Dorsey, F. C., Nilsson, J. A., Nilsson, L., MacLean, K. H., Chung, L., Yang, C., Spruck, C., Boyd, K.*, et al.* (2007). Myc targets Cks1 to provoke the suppression of p27Kip1, proliferation and lymphomagenesis. EMBO J *26*, 2562-2574.

Kikuchi, A., Hayashi, Y., Kobayashi, S., Hanada, R., Moriwaki, K., Yamamoto, K., Fujimoto, J., Kaneko, Y., and Yamamori, S. (1993). Clinical significance of TAL1 gene alteration in childhood T-cell acute lymphoblastic leukemia and lymphoma. Leukemia *7*, 933-938.

Kim, S. Y., Herbst, A., Tworkowski, K. A., Salghetti, S. E., and Tansey, W. P. (2003). Skp2 regulates Myc protein stability and activity. Mol Cell *11*, 1177-1188.

Kleppe, M., Lahortiga, I., El Chaar, T., De Keersmaecker, K., Mentens, N., Graux, C., Van Roosbroeck, K., Ferrando, A. A., Langerak, A. W., Meijerink, J. P.*, et al.* (2010). Deletion of the protein tyrosine phosphatase gene PTPN2 in T-cell acute lymphoblastic leukemia. Nat Genet *42*, 530-535.

Knoechel, B., Roderick, J. E., Williamson, K. E., Zhu, J., Lohr, J. G., Cotton, M. J., Gillespie, S. M., Fernandez, D., Ku, M., Wang, H.*, et al.* (2014). An epigenetic mechanism of resistance to targeted therapy in T cell acute lymphoblastic leukemia. Nat Genet *46*, 364-370.

Koutsami, M., Velimezi, G., Kotsinas, A., Evangelou, K., Papavassiliou, A. G., Kittas, C., and Gorgoulis, V. G. (2008). Is exclusive Skp2 targeting always beneficial in cancer therapy? Blood *112*, 4777-4779.

Koyama, D., Kikuchi, J., Hiraoka, N., Wada, T., Kurosawa, H., Chiba, S., and Furukawa, Y. (2014). Proteasome inhibitors exert cytotoxicity and increase chemosensitivity via transcriptional repression of Notch1 in T-cell acute lymphoblastic leukemia. Leukemia *28*, 1216-1226.

Kraszewska, M. D., Dawidowska, M., Larmonie, N. S., Kosmalska, M., Sedek, L., Szczepaniak, M., Grzeszczak, W., Langerak, A. W., Szczepanski, T., Witt, M., and Polish Pediatric Leukemia Lymphoma Study, G. (2012). DNA methylation pattern is altered in childhood T-cell acute lymphoblastic leukemia patients as compared with normal thymic subsets: insights into CpG island methylator phenotype in T-ALL. Leukemia *26*, 367-371.

Krivtsov, A. V., Twomey, D., Feng, Z., Stubbs, M. C., Wang, Y., Faber, J., Levine, J. E., Wang, J., Hahn, W. C., Gilliland, D. G.*, et al.* (2006). Transformation from committed progenitor to leukaemia stem cell initiated by MLL-AF9. Nature *442*, 818-822.

Krutzik, P. O., and Nolan, G. P. (2003). Intracellular phospho-protein staining techniques for flow cytometry: monitoring single cell signaling events. Cytometry A *55*, 61-70.

Kullmann, M., Gopfert, U., Siewe, B., and Hengst, L. (2002). ELAV/Hu proteins inhibit p27 translation via an IRES element in the p27 5'UTR. Genes Dev *16*, 3087-3099.

Kullmann, M. K., Grubbauer, C., Goetsch, K., Jakel, H., Podmirseg, S. R., Trockenbacher, A., Ploner, C., Cato, A. C., Weiss, C., Kofler, R., and Hengst, L. (2013). The p27-Skp2 axis mediates glucocorticoid-induced cell cycle arrest in T-lymphoma cells. Cell Cycle *12*, 2625-2635.

Larrea, M. D., Hong, F., Wander, S. A., da Silva, T. G., Helfman, D., Lannigan, D., Smith, J. A., and Slingerland, J. M. (2009). RSK1 drives p27Kip1 phosphorylation at T198 to promote RhoA inhibition and increase cell motility. Proc Natl Acad Sci U S A *106*, 9268-9273.

Larrea, M. D., Liang, J., Da Silva, T., Hong, F., Shao, S. H., Han, K., Dumont, D., and Slingerland, J. M. (2008). Phosphorylation of p27Kip1 regulates assembly and activation of cyclin D1-Cdk4. Mol Cell Biol *28*, 6462-6472.

Larson Gedman, A., Chen, Q., Kugel Desmoulin, S., Ge, Y., LaFiura, K., Haska, C. L., Cherian, C., Devidas, M., Linda, S. B., Taub, J. W., and Matherly, L. H. (2009). The impact of NOTCH1, FBW7 and PTEN mutations on prognosis and downstream signaling in pediatric T-cell acute lymphoblastic leukemia: a report from the Children's Oncology Group. Leukemia *23*, 1417-1425.

le Sage, C., Nagel, R., and Agami, R. (2007). Diverse ways to control p27Kip1 function: miRNAs come into play. Cell Cycle *6*, 2742-2749.

Le Toriellec, E., Despouy, G., Pierron, G., Gaye, N., Joiner, M., Bellanger, D., Vincent-Salomon, A., and Stern, M. H. (2008). Haploinsufficiency of CDKN1B contributes to leukemogenesis in T-cell prolymphocytic leukemia. Blood *111*, 2321-2328.

Lee, J., and Kim, S. S. (2009). The function of p27 KIP1 during tumor development. Exp Mol Med *41*, 765-771.

Lee, M. H., Reynisdottir, I., and Massague, J. (1995). Cloning of p57KIP2, a cyclin-dependent kinase inhibitor with unique domain structure and tissue distribution. Genes Dev *9*, 639-649.

Lee, S. H., and McCormick, F. (2005). Downregulation of Skp2 and p27/Kip1 synergistically induces apoptosis in T98G glioblastoma cells. J Mol Med (Berl) *83*, 296-307.

Levkau, B., Koyama, H., Raines, E. W., Clurman, B. E., Herren, B., Orth, K., Roberts, J. M., and Ross, R. (1998). Cleavage of p21Cip1/Waf1 and p27Kip1 mediates apoptosis in endothelial cells through activation of Cdk2: role of a caspase cascade. Mol Cell *1*, 553-563.

Li, X., Gounari, F., Protopopov, A., Khazaie, K., and von Boehmer, H. (2008). Oncogenesis of T-ALL and nonmalignant consequences of overexpressing intracellular NOTCH1. J Exp Med *205*, 2851-2861.

Liang, J., Shao, S. H., Xu, Z. X., Hennessy, B., Ding, Z., Larrea, M., Kondo, S., Dumont, D. J., Gutterman, J. U., Walker, C. L.*, et al.* (2007). The energy sensing LKB1-AMPK pathway regulates p27(kip1) phosphorylation mediating the decision to enter autophagy or apoptosis. Nat Cell Biol *9*, 218-224.

Liang, J., Zubovitz, J., Petrocelli, T., Kotchetkov, R., Connor, M. K., Han, K., Lee, J. H., Ciarallo, S., Catzavelos, C., Beniston, R.*, et al.* (2002). PKB/Akt phosphorylates p27, impairs nuclear import of p27 and opposes p27-mediated G1 arrest. Nat Med *8*, 1153-1160.

Lin, H. K., Wang, G., Chen, Z., Teruya-Feldstein, J., Liu, Y., Chan, C. H., Yang, W. L., Erdjument-Bromage, H., Nakayama, K. I., Nimer, S.*, et al.* (2009). Phosphorylation-dependent regulation of cytosolic localization and oncogenic function of Skp2 by Akt/PKB. Nat Cell Biol *11*, 420-432.

Liz, J., and Esteller, M. (2015). lncRNAs and microRNAs with a role in cancer development. Biochim Biophys Acta.

Ma, M., Wang, X., Tang, J., Xue, H., Chen, J., Pan, C., Jiang, H., and Shen, S. (2012). Early T-cell precursor leukemia: a subtype of high risk childhood acute lymphoblastic leukemia. Front Med *6*, 416-420.

Malecki, M. J., Sanchez-Irizarry, C., Mitchell, J. L., Histen, G., Xu, M. L., Aster, J. C., and Blacklow, S. C. (2006). Leukemia-associated mutations within the NOTCH1 heterodimerization domain fall into at least two distinct mechanistic classes. Mol Cell Biol *26*, 4642-4651.

Malumbres, M. (2014). Cyclin-dependent kinases. Genome Biol *15*, 122.

Malumbres, M., and Barbacid, M. (2009). Cell cycle, CDKs and cancer: a changing paradigm. Nat Rev Cancer *9*, 153-166.

Mamillapalli, R., Gavrilova, N., Mihaylova, V. T., Tsvetkov, L. M., Wu, H., Zhang, H., and Sun, H. (2001). PTEN regulates the ubiquitin-dependent degradation of the CDK inhibitor p27(KIP1) through the ubiquitin E3 ligase SCF(SKP2). Curr Biol *11*, 263-267.

Mansour, M. R., Abraham, B. J., Anders, L., Berezovskaya, A., Gutierrez, A., Durbin, A. D., Etchin, J., Lawton, L., Sallan, S. E., Silverman, L. B.*, et al.* (2014). Oncogene regulation. An oncogenic super-enhancer formed through somatic mutation of a noncoding intergenic element. Science *346*, 1373-1377.

Mansur, M. B., Emerenciano, M., Brewer, L., Sant'Ana, M., Mendonca, N., Thuler, L. C., Koifman, S., and Pombo-de-Oliveira, M. S. (2009). SIL-TAL1 fusion gene negative impact in T-cell acute lymphoblastic leukemia outcome. Leuk Lymphoma *50*, 1318-1325.

Mansur, M. B., Hassan, R., Barbosa, T. C., Splendore, A., Jotta, P. Y., Yunes, J. A., Wiemels, J. L., and Pombo-de-Oliveira, M. S. (2012). Impact of complex NOTCH1 mutations on survival in paediatric T-cell leukaemia. BMC Cancer *12*, 9.

Masciullo, V., Sgambato, A., Pacilio, C., Pucci, B., Ferrandina, G., Palazzo, J., Carbone, A., Cittadini, A., Mancuso, S., Scambia, G., and Giordano, A. (1999). Frequent loss of expression of the cyclin-dependent kinase inhibitor p27 in epithelial ovarian cancer. Cancer Res *59*, 3790-3794.

Maser, R. S., Choudhury, B., Campbell, P. J., Feng, B., Wong, K. K., Protopopov, A., O'Neil, J., Gutierrez, A., Ivanova, E., Perna, I.*, et al.* (2007). Chromosomally unstable mouse tumours have genomic alterations similar to diverse human cancers. Nature *447*, 966-971.

McGuire, E. A., Hockett, R. D., Pollock, K. M., Bartholdi, M. F., O'Brien, S. J., and Korsmeyer, S. J. (1989). The t(11;14)(p15;q11) in a T-cell acute lymphoblastic leukemia cell line activates multiple transcripts, including Ttg-1, a gene encoding a potential zinc finger protein. Mol Cell Biol *9*, 2124-2132.

Medema, R. H., Kops, G. J., Bos, J. L., and Burgering, B. M. (2000). AFX-like Forkhead transcription factors mediate cell-cycle regulation by Ras and PKB through p27kip1. Nature *404*, 782-787.

Medina, R., Zaidi, S. K., Liu, C. G., Stein, J. L., van Wijnen, A. J., Croce, C. M., and Stein, G. S. (2008). MicroRNAs 221 and 222 bypass quiescence and compromise cell survival. Cancer Res *68*, 2773-2780.

Meijerink, J. P. (2010). Genetic rearrangements in relation to immunophenotype and outcome in T-cell acute lymphoblastic leukaemia. Best Pract Res Clin Haematol *23*, 307-318.

Millard, S. S., Vidal, A., Markus, M., and Koff, A. (2000). A U-rich element in the 5' untranslated region is necessary for the translation of p27 mRNA. Mol Cell Biol *20*, 5947-5959.

Miyamoto, T., Horiuchi, A., Kashima, H., Suzuki, A., Yamada, T., Kurai, M., Konishi, I., and Shiozawa, T. (2010). Inverse correlation between Skp2 and p27(Kip1) in normal endometrium and endometrial carcinoma. Gynecol Endocrinol *26*, 220-229.

Monahan, P., Rybak, S., and Raetzman, L. T. (2009). The notch target gene HES1 regulates cell cycle inhibitor expression in the developing pituitary. Endocrinology *150*, 4386-4394.

Mullighan, C. G., Goorha, S., Radtke, I., Miller, C. B., Coustan-Smith, E., Dalton, J. D., Girtman, K., Mathew, S., Ma, J., Pounds, S. B.*, et al.* (2007). Genome-wide analysis of genetic alterations in acute lymphoblastic leukaemia. Nature *446*, 758-764.

Murata, K., Hattori, M., Hirai, N., Shinozuka, Y., Hirata, H., Kageyama, R., Sakai, T., and Minato, N. (2005). Hes1 directly controls cell proliferation through the transcriptional repression of p27Kip1. Mol Cell Biol *25*, 4262-4271.

Mussolin, L., Holmes, A. B., Romualdi, C., Sales, G., D'Amore, E. S., Ghisi, M., Pillon, M., Rosolen, A., and Basso, K. (2014). An aberrant microRNA signature in

childhood T-cell lymphoblastic lymphoma affecting CDKN1B expression, NOTCH1 and growth factor signaling pathways. Leukemia.

Nagel, S., Kaufmann, M., Drexler, H. G., and MacLeod, R. A. (2003). The cardiac homeobox gene NKX2-5 is deregulated by juxtaposition with BCL11B in pediatric T-ALL cell lines via a novel t(5;14)(q35.1;q32.2). Cancer Res *63*, 5329-5334.

Nagel, S., Meyer, C., Quentmeier, H., Kaufmann, M., Drexler, H. G., and MacLeod, R. A. (2008). MEF2C is activated by multiple mechanisms in a subset of T-acute lymphoblastic leukemia cell lines. Leukemia *22*, 600-607.

Nagel, S., Scherr, M., Kel, A., Hornischer, K., Crawford, G. E., Kaufmann, M., Meyer, C., Drexler, H. G., and MacLeod, R. A. (2007). Activation of TLX3 and NKX2-5 in t(5;14)(q35;q32) T-cell acute lymphoblastic leukemia by remote 3'-BCL11B enhancers and coregulation by PU.1 and HMGA1. Cancer Res *67*, 1461-1471.

Nakayama, K., Ishida, N., Shirane, M., Inomata, A., Inoue, T., Shishido, N., Horii, I., Loh, D. Y., and Nakayama, K. (1996). Mice lacking p27(Kip1) display increased body size, multiple organ hyperplasia, retinal dysplasia, and pituitary tumors. Cell *85*, 707-720.

Nakayama, K., Nagahama, H., Minamishima, Y. A., Matsumoto, M., Nakamichi, I., Kitagawa, K., Shirane, M., Tsunematsu, R., Tsukiyama, T., Ishida, N.*, et al.* (2000). Targeted disruption of Skp2 results in accumulation of cyclin E and p27(Kip1), polyploidy and centrosome overduplication. EMBO J *19*, 2069-2081.

Nakayama, K., Nagahama, H., Minamishima, Y. A., Miyake, S., Ishida, N., Hatakeyama, S., Kitagawa, M., Iemura, S., Natsume, T., and Nakayama, K. I. (2004). Skp2-mediated degradation of p27 regulates progression into mitosis. Dev Cell *6*, 661-672.

Nakayama, K. I., and Nakayama, K. (2006). Ubiquitin ligases: cell-cycle control and cancer. Nat Rev Cancer *6*, 369-381.

Naruse, I., Hoshino, H., Dobashi, K., Minato, K., Saito, R., and Mori, M. (2000). Over-expression of p27kip1 induces growth arrest and apoptosis mediated by changes of pRb expression in lung cancer cell lines. Int J Cancer *88*, 377-383.

Neumann, M., Heesch, S., Gokbuget, N., Schwartz, S., Schlee, C., Benlasfer, O., Farhadi-Sartangi, N., Thibaut, J., Burmeister, T., Hoelzer, D.*, et al.* (2012). Clinical and molecular characterization of early T-cell precursor leukemia: a high-risk subgroup in adult T-ALL with a high frequency of FLT3 mutations. Blood Cancer J *2*, e55.

O'Hagan, R. C., Ohh, M., David, G., de Alboran, I. M., Alt, F. W., Kaelin, W. G., Jr., and DePinho, R. A. (2000). Myc-enhanced expression of Cul1 promotes ubiquitin-dependent proteolysis and cell cycle progression. Genes Dev *14*, 2185-2191.

O'Neil, J., Grim, J., Strack, P., Rao, S., Tibbitts, D., Winter, C., Hardwick, J., Welcker, M., Meijerink, J. P., Pieters, R.*, et al.* (2007). FBW7 mutations in leukemic cells mediate NOTCH pathway activation and resistance to gamma-secretase inhibitors. J Exp Med *204*, 1813-1824.

Orlando, S., Gallastegui, E., Besson, A., Abril, G., Aligue, R., Pujol, M. J., and Bachs, O. (2015). p27Kip1 and p21Cip1 collaborate in the regulation of transcription by recruiting cyclin-Cdk complexes on the promoters of target genes. Nucleic Acids Res.

Pagano, M. (2004). Control of DNA synthesis and mitosis by the Skp2-p27-Cdk1/2 axis. Mol Cell *14*, 414-416.

Pagano, M., Tam, S. W., Theodoras, A. M., Beer-Romero, P., Del Sal, G., Chau, V., Yew, P. R., Draetta, G. F., and Rolfe, M. (1995). Role of the ubiquitin-proteasome pathway in regulating abundance of the cyclin-dependent kinase inhibitor p27. Science *269*, 682-685.

Paik, J. H., Kollipara, R., Chu, G., Ji, H., Xiao, Y., Ding, Z., Miao, L., Tothova, Z., Horner, J. W., Carrasco, D. R.*, et al.* (2007). FoxOs are lineage-restricted redundant tumor suppressors and regulate endothelial cell homeostasis. Cell *128*, 309-323.

Palomero, T., Barnes, K. C., Real, P. J., Bender, J. L., Sulis, M. L., Murty, V. V., Colovai, A. I., Balbin, M., and Ferrando, A. A. (2006a). CUTLL1, a novel human T-cell lymphoma cell line with t(7;9) rearrangement, aberrant NOTCH1 activation and high sensitivity to gamma-secretase inhibitors. Leukemia *20*, 1279-1287.

Palomero, T., Dominguez, M., and Ferrando, A. A. (2008). The role of the PTEN/AKT Pathway in NOTCH1-induced leukemia. Cell Cycle *7*, 965-970.

Palomero, T., Lim, W. K., Odom, D. T., Sulis, M. L., Real, P. J., Margolin, A., Barnes, K. C., O'Neil, J., Neuberg, D., Weng, A. P.*, et al.* (2006b). NOTCH1 directly regulates c-MYC and activates a feed-forward-loop transcriptional network promoting leukemic cell growth. Proc Natl Acad Sci U S A *103*, 18261-18266.

Palomero, T., Sulis, M. L., Cortina, M., Real, P. J., Barnes, K., Ciofani, M., Caparros, E., Buteau, J., Brown, K., Perkins, S. L.*, et al.* (2007). Mutational loss of PTEN induces resistance to NOTCH1 inhibition in T-cell leukemia. Nat Med *13*, 1203-1210.

Park, M. J., Taki, T., Oda, M., Watanabe, T., Yumura-Yagi, K., Kobayashi, R., Suzuki, N., Hara, J., Horibe, K., and Hayashi, Y. (2009). FBXW7 and NOTCH1 mutations in childhood T cell acute lymphoblastic leukaemia and T cell non-Hodgkin lymphoma. Br J Haematol *145*, 198-206.

Pateras, I. S., Apostolopoulou, K., Niforou, K., Kotsinas, A., and Gorgoulis, V. G. (2009). p57KIP2: "Kip"ing the cell under control. Mol Cancer Res *7*, 1902-1919.

Pavletich, N. P. (1999). Mechanisms of cyclin-dependent kinase regulation: structures of Cdks, their cyclin activators, and Cip and INK4 inhibitors. J Mol Biol *287*, 821-828.

Pavlides, S. C., Huang, K. T., Reid, D. A., Wu, L., Blank, S. V., Mittal, K., Guo, L., Rothenberg, E., Rueda, B., Cardozo, T., and Gold, L. I. (2013). Inhibitors of SCF-Skp2/Cks1 E3 ligase block estrogen-induced growth stimulation and degradation of nuclear p27kip1: therapeutic potential for endometrial cancer. Endocrinology *154*, 4030-4045.

Peirs, S., Matthijssens, F., Goossens, S., Van de Walle, I., Ruggero, K., de Bock, C. E., Degryse, S., Cante-Barrett, K., Briot, D., Clappier, E.*, et al.* (2014). ABT-199 mediated inhibition of BCL-2 as a novel therapeutic strategy in T-cell acute lymphoblastic leukemia. Blood *124*, 3738-3747.

Piovan, E., Yu, J., Tosello, V., Herranz, D., Ambesi-Impiombato, A., Da Silva, A. C., Sanchez-Martin, M., Perez-Garcia, A., Rigo, I., Castillo, M.*, et al.* (2013). Direct reversal of glucocorticoid resistance by AKT inhibition in acute lymphoblastic leukemia. Cancer Cell *24*, 766-776.

Pippa, R., Espinosa, L., Gundem, G., Garcia-Escudero, R., Dominguez, A., Orlando, S., Gallastegui, E., Saiz, C., Besson, A., Pujol, M. J.*, et al.* (2012). p27Kip1 represses transcription by direct interaction with p130/E2F4 at the promoters of target genes. Oncogene *31*, 4207-4220.

Poliseno, L., Salmena, L., Zhang, J., Carver, B., Haveman, W. J., and Pandolfi, P. P. (2010). A coding-independent function of gene and pseudogene mRNAs regulates tumour biology. Nature *465*, 1033-1038.

Polyak, K., Lee, M. H., Erdjument-Bromage, H., Koff, A., Roberts, J. M., Tempst, P., and Massague, J. (1994). Cloning of p27Kip1, a cyclin-dependent kinase inhibitor and a potential mediator of extracellular antimitogenic signals. Cell *78*, 59-66.

Przybylski, G. K., Dik, W. A., Grabarczyk, P., Wanzeck, J., Chudobska, P., Jankowski, K., von Bergh, A., van Dongen, J. J., Schmidt, C. A., and Langerak, A. W. (2006). The effect of a novel recombination between the homeobox gene NKX2-5 and the TRD locus in T-cell acute lymphoblastic leukemia on activation of the NKX2-5 gene. Haematologica *91*, 317-321.

Pui, C. H., and Evans, W. E. (2006). Treatment of acute lymphoblastic leukemia. N Engl J Med *354*, 166-178.

Purow, B. (2012). Notch inhibition as a promising new approach to cancer therapy. Adv Exp Med Biol *727*, 305-319.

Rao, S. S., O'Neil, J., Liberator, C. D., Hardwick, J. S., Dai, X., Zhang, T., Tyminski, E., Yuan, J., Kohl, N. E., Richon, V. M.*, et al.* (2009). Inhibition of NOTCH signaling by gamma secretase inhibitor engages the RB pathway and elicits cell cycle exit in T-cell acute lymphoblastic leukemia cells. Cancer Res *69*, 3060-3068.

Real, P. J., Tosello, V., Palomero, T., Castillo, M., Hernando, E., de Stanchina, E., Sulis, M. L., Barnes, K., Sawai, C., Homminga, I.*, et al.* (2009). Gamma-secretase inhibitors reverse glucocorticoid resistance in T cell acute lymphoblastic leukemia. Nat Med *15*, 50-58.

Reichert, M., Saur, D., Hamacher, R., Schmid, R. M., and Schneider, G. (2007). Phosphoinositide-3-kinase signaling controls S-phase kinase-associated protein 2 transcription via E2F1 in pancreatic ductal adenocarcinoma cells. Cancer Res *67*, 4149-4156.

Reiter, A., Schrappe, M., Ludwig, W. D., Hiddemann, W., Sauter, S., Henze, G., Zimmermann, M., Lampert, F., Havers, W., Niethammer, D., and et al. (1994). Chemotherapy in 998 unselected childhood acute lymphoblastic leukemia patients. Results and conclusions of the multicenter trial ALL-BFM 86. Blood *84*, 3122-3133.

Remke, M., Pfister, S., Kox, C., Toedt, G., Becker, N., Benner, A., Werft, W., Breit, S., Liu, S., Engel, F.*, et al.* (2009). High-resolution genomic profiling of childhood T-ALL reveals frequent copy-number alterations affecting the TGF-beta and PI3K-AKT pathways and deletions at 6q15-16.1 as a genomic marker for unfavorable early treatment response. Blood *114*, 1053-1062.

Renneville, A., Kaltenbach, S., Clappier, E., Collette, S., Micol, J. B., Nelken, B., Lepelley, P., Dastugue, N., Benoit, Y., Bertrand, Y.*, et al.* (2010). Wilms tumor 1 (WT1) gene mutations in pediatric T-cell malignancies. Leukemia *24*, 476-480.

Riedel, S. S., Neff, T., and Bernt, K. M. (2015). Histone profiles in cancer. Pharmacol Ther.

Riz, I., and Hawley, R. G. (2005). G1/S transcriptional networks modulated by the HOX11/TLX1 oncogene of T-cell acute lymphoblastic leukemia. Oncogene *24*, 5561-5575.

Roderick, J. E., Tesell, J., Shultz, L. D., Brehm, M. A., Greiner, D. L., Harris, M. H., Silverman, L. B., Sallan, S. E., Gutierrez, A., Look, A. T.*, et al.* (2014). c-Myc inhibition prevents leukemia initiation in mice and impairs the growth of relapsed and induction failure pediatric T-ALL cells. Blood *123*, 1040-1050.

Rodriguez-Rodriguez, S., Wang, L., Zhang, H., Zollman, A., Cardoso, A., and Carlesso, N. (2014). SKP2 Is Dispensable for Normal T-Cell Development but Required for T-Cell Leukemogenesis. Blood *124*, 2214-2214.

Rosner, M., Hanneder, M., Siegel, N., Valli, A., Fuchs, C., and Hengstschlager, M. (2009). Skp2 inversely correlates with p27 and tuberin in transformed cells. Amino Acids *37*, 257-262.

Roti, G., and Stegmaier, K. (2014). New Approaches to Target T-ALL. Front Oncol *4*, 170.

Roy, A., and Banerjee, S. (2015). p27 and leukemia: cell cycle and beyond. J Cell Physiol *230*, 504-509.

Royer-Pokora, B., Fleischer, B., Ragg, S., Loos, U., and Williams, D. (1989). Molecular cloning of the translocation breakpoint in T-ALL 11;14 (p13;q11): genomic map of TCR alpha and delta region on chromosome 14q11 and long-range map of region 11p13. Hum Genet *82*, 264-270.

Russo, A. A., Jeffrey, P. D., Patten, A. K., Massague, J., and Pavletich, N. P. (1996). Crystal structure of the p27Kip1 cyclin-dependent-kinase inhibitor bound to the cyclin A-Cdk2 complex. Nature *382*, 325-331.

Sarmento, L. M., Huang, H., Limon, A., Gordon, W., Fernandes, J., Tavares, M. J., Miele, L., Cardoso, A. A., Classon, M., and Carlesso, N. (2005). Notch1 modulates timing of G1-S progression by inducing SKP2 transcription and p27 Kip1 degradation. J Exp Med *202*, 157-168.

Sawai, C. M., Freund, J., Oh, P., Ndiaye-Lobry, D., Bretz, J. C., Strikoudis, A., Genesca, L., Trimarchi, T., Kelliher, M. A., Clark, M.*, et al.* (2012). Therapeutic targeting of the cyclin D3:CDK4/6 complex in T cell leukemia. Cancer Cell *22*, 452-465.

Schrappe, M., Reiter, A., Ludwig, W. D., Harbott, J., Zimmermann, M., Hiddemann, W., Niemeyer, C., Henze, G., Feldges, A., Zintl, F.*, et al.* (2000). Improved outcome in childhood acute lymphoblastic leukemia despite reduced use of anthracyclines and cranial radiotherapy: results of trial ALL-BFM 90. German-Austrian-Swiss ALL-BFM Study Group. Blood *95*, 3310-3322.

Schulz, K. R., Danna, E. A., Krutzik, P. O., and Nolan, G. P. (2012). Single-cell phospho-protein analysis by flow cytometry. Curr Protoc Immunol *Chapter 8*, Unit 8 17 11-20.

Serres, M. P., Zlotek-Zlotkiewicz, E., Concha, C., Gurian-West, M., Daburon, V., Roberts, J. M., and Besson, A. (2011). Cytoplasmic p27 is oncogenic and cooperates with Ras both in vivo and in vitro. Oncogene *30*, 2846-2858.

Servant, M. J., Coulombe, P., Turgeon, B., and Meloche, S. (2000). Differential regulation of p27(Kip1) expression by mitogenic and hypertrophic factors: Involvement of transcriptional and posttranscriptional mechanisms. J Cell Biol *148*, 543-556.

Shepherd, C., Banerjee, L., Cheung, C. W., Mansour, M. R., Jenkinson, S., Gale, R. E., and Khwaja, A. (2013). PI3K/mTOR inhibition upregulates NOTCH-MYC signalling leading to an impaired cytotoxic response. Leukemia *27*, 650-660.

Sherr, C. J., and Roberts, J. M. (1999). CDK inhibitors: positive and negative regulators of G1-phase progression. Genes Dev *13*, 1501-1512.

Silva, A., Yunes, J. A., Cardoso, B. A., Martins, L. R., Jotta, P. Y., Abecasis, M., Nowill, A. E., Leslie, N. R., Cardoso, A. A., and Barata, J. T. (2008). PTEN posttranslational inactivation and hyperactivation of the PI3K/Akt pathway sustain primary T cell leukemia viability. J Clin Invest *118*, 3762-3774.

Singh, S. P., Lipman, J., Goldman, H., Ellis, F. H., Jr., Aizenman, L., Cangi, M. G., Signoretti, S., Chiaur, D. S., Pagano, M., and Loda, M. (1998). Loss or altered subcellular localization of p27 in Barrett's associated adenocarcinoma. Cancer Res *58*, 1730-1735.

Slingerland, J., and Pagano, M. (2000). Regulation of the cdk inhibitor p27 and its deregulation in cancer. J Cell Physiol *183*, 10-17.

Soulier, J., Clappier, E., Cayuela, J. M., Regnault, A., Garcia-Peydro, M., Dombret, H., Baruchel, A., Toribio, M. L., and Sigaux, F. (2005). HOXA genes are included in genetic and biologic networks defining human acute T-cell leukemia (T-ALL). Blood *106*, 274-286.

Starostina, N. G., and Kipreos, E. T. (2012). Multiple degradation pathways regulate versatile CIP/KIP CDK inhibitors. Trends Cell Biol *22*, 33-41.

Sulis, M. L., Williams, O., Palomero, T., Tosello, V., Pallikuppam, S., Real, P. J., Barnes, K., Zuurbier, L., Meijerink, J. P., and Ferrando, A. A. (2008). NOTCH1 extracellular juxtamembrane expansion mutations in T-ALL. Blood *112*, 733-740.

Tammam, J., Ware, C., Efferson, C., O'Neil, J., Rao, S., Qu, X., Gorenstein, J., Angagaw, M., Kim, H., Kenific, C.*, et al.* (2009). Down-regulation of the Notch pathway mediated by a gamma-secretase inhibitor induces anti-tumour effects in mouse models of T-cell leukaemia. Br J Pharmacol *158*, 1183-1195.

Thompson, B. J., Buonamici, S., Sulis, M. L., Palomero, T., Vilimas, T., Basso, G., Ferrando, A., and Aifantis, I. (2007). The SCFFBW7 ubiquitin ligase complex as a tumor suppressor in T cell leukemia. J Exp Med *204*, 1825-1835.

Tosello, V., Mansour, M. R., Barnes, K., Paganin, M., Sulis, M. L., Jenkinson, S., Allen, C. G., Gale, R. E., Linch, D. C., Palomero, T.*, et al.* (2009). WT1 mutations in T-ALL. Blood *114*, 1038-1045.

Toyoshima, H., and Hunter, T. (1994). p27, a novel inhibitor of G1 cyclin-Cdk protein kinase activity, is related to p21. Cell *78*, 67-74.

Trimarchi, T., Bilal, E., Ntziachristos, P., Fabbri, G., Dalla-Favera, R., Tsirigos, A., and Aifantis, I. (2014). Genome-wide mapping and characterization of Notch-regulated long noncoding RNAs in acute leukemia. Cell *158*, 593-606.

Tzoneva, G., and Ferrando, A. A. (2012). Recent advances on NOTCH signaling in T-ALL. Curr Top Microbiol Immunol *360*, 163-182.

van Grotel, M., Meijerink, J. P., Beverloo, H. B., Langerak, A. W., Buys-Gladdines, J. G., Schneider, P., Poulsen, T. S., den Boer, M. L., Horstmann, M., Kamps, W. A.*, et al.* (2006). The outcome of molecular-cytogenetic subgroups in pediatric T-cell acute lymphoblastic leukemia: a retrospective study of patients treated according to DCOG or COALL protocols. Haematologica *91*, 1212-1221.

Van Vlierberghe, P., Ambesi-Impiombato, A., Perez-Garcia, A., Haydu, J. E., Rigo, I., Hadler, M., Tosello, V., Della Gatta, G., Paietta, E., Racevskis, J.*, et al.* (2011). ETV6 mutations in early immature human T cell leukemias. J Exp Med *208*, 2571-2579.

Van Vlierberghe, P., and Ferrando, A. (2012). The molecular basis of T cell acute lymphoblastic leukemia. J Clin Invest *122*, 3398-3406.

Van Vlierberghe, P., Homminga, I., Zuurbier, L., Gladdines-Buijs, J., van Wering, E. R., Horstmann, M., Beverloo, H. B., Pieters, R., and Meijerink, J. P. (2008). Cooperative genetic defects in TLX3 rearranged pediatric T-ALL. Leukemia *22*, 762-770.

Van Vlierberghe, P., Palomero, T., Khiabanian, H., Van der Meulen, J., Castillo, M., Van Roy, N., De Moerloose, B., Philippe, J., Gonzalez-Garcia, S., Toribio, M. L.*, et al.* (2010). PHF6 mutations in T-cell acute lymphoblastic leukemia. Nat Genet *42*, 338-342.

Van Vlierberghe, P., van Grotel, M., Beverloo, H. B., Lee, C., Helgason, T., Buijs-Gladdines, J., Passier, M., van Wering, E. R., Veerman, A. J., Kamps, W. A.*, et al.* (2006). The cryptic chromosomal deletion del(11)(p12p13) as a new activation mechanism of LMO2 in pediatric T-cell acute lymphoblastic leukemia. Blood *108*, 3520-3529.

Vervoorts, J., and Luscher, B. (2008). Post-translational regulation of the tumor suppressor p27(KIP1). Cell Mol Life Sci *65*, 3255-3264.

Viglietto, G., Motti, M. L., Bruni, P., Melillo, R. M., D'Alessio, A., Califano, D., Vinci, F., Chiappetta, G., Tsichlis, P., Bellacosa, A.*, et al.* (2002a). Cytoplasmic relocalization and inhibition of the cyclin-dependent kinase inhibitor p27(Kip1) by PKB/Akt-mediated phosphorylation in breast cancer. Nat Med *8*, 1136-1144.

Viglietto, G., Motti, M. L., and Fusco, A. (2002b). Understanding p27(kip1) deregulation in cancer: down-regulation or mislocalization. Cell Cycle *1*, 394-400.

Vilimas, T., Mascarenhas, J., Palomero, T., Mandal, M., Buonamici, S., Meng, F., Thompson, B., Spaulding, C., Macaroun, S., Alegre, M. L.*, et al.* (2007). Targeting the NF-kappaB signaling pathway in Notch1-induced T-cell leukemia. Nat Med *13*, 70-77.

von der Lehr, N., Johansson, S., Wu, S., Bahram, F., Castell, A., Cetinkaya, C., Hydbring, P., Weidung, I., Nakayama, K., Nakayama, K. I.*, et al.* (2003). The F-box protein Skp2 participates in c-Myc proteosomal degradation and acts as a cofactor for c-Myc-regulated transcription. Mol Cell *11*, 1189-1200.

Wander, S. A., Zhao, D., and Slingerland, J. M. (2011). p27: a barometer of signaling deregulation and potential predictor of response to targeted therapies. Clin Cancer Res *17*, 12-18.

Wang, C., Hou, X., Mohapatra, S., Ma, Y., Cress, W. D., Pledger, W. J., and Chen, J. (2005). Activation of p27Kip1 Expression by E2F1. A negative feedback mechanism. J Biol Chem *280*, 12339-12343.

Wang, Z., Liu, P., Inuzuka, H., and Wei, W. (2014). Roles of F-box proteins in cancer. Nat Rev Cancer *14*, 233-247.

Weng, A. P., Ferrando, A. A., Lee, W., Morris, J. P. t., Silverman, L. B., Sanchez-Irizarry, C., Blacklow, S. C., Look, A. T., and Aster, J. C. (2004). Activating mutations of NOTCH1 in human T cell acute lymphoblastic leukemia. Science *306*, 269-271.

Weng, A. P., Millholland, J. M., Yashiro-Ohtani, Y., Arcangeli, M. L., Lau, A., Wai, C., Del Bianco, C., Rodriguez, C. G., Sai, H., Tobias, J.*, et al.* (2006). c-Myc is an important direct target of Notch1 in T-cell acute lymphoblastic leukemia/lymphoma. Genes Dev *20*, 2096-2109.

Wu, J., Lee, S. W., Zhang, X., Han, F., Kwan, S. Y., Yuan, X., Yang, W. L., Jeong, Y. S., Rezaeian, A. H., Gao, Y.*, et al.* (2013). Foxo3a transcription factor is a negative regulator of Skp2 and Skp2 SCF complex. Oncogene *32*, 78-85.

Wu, L., Grigoryan, A. V., Li, Y., Hao, B., Pagano, M., and Cardozo, T. J. (2012). Specific small molecule inhibitors of Skp2-mediated p27 degradation. Chem Biol *19*, 1515-1524.

Yang, L., Zhang, S., George, S. K., Teng, R., You, X., Xu, M., Liu, H., Sun, X., Amin, H. M., and Shi, W. (2015). Targeting Notch1 and proteasome as an effective strategy to suppress T-cell lymphoproliferative neoplasms. Oncotarget *6*, 14953-14969.

Yang, W., Shen, J., Wu, M., Arsura, M., FitzGerald, M., Suldan, Z., Kim, D. W., Hofmann, C. S., Pianetti, S., Romieu-Mourez, R.*, et al.* (2001). Repression of transcription of the p27(Kip1) cyclin-dependent kinase inhibitor gene by c-Myc. Oncogene *20*, 1688-1702.

Zhang, J., Ding, L., Holmfeldt, L., Wu, G., Heatley, S. L., Payne-Turner, D., Easton, J., Chen, X., Wang, J., Rusch, M.*, et al.* (2012). The genetic basis of early T-cell precursor acute lymphoblastic leukaemia. Nature *481*, 157-163.

Zhu, Y. M., Zhao, W. L., Fu, J. F., Shi, J. Y., Pan, Q., Hu, J., Gao, X. D., Chen, B., Li, J. M., Xiong, S. M.*, et al.* (2006). NOTCH1 mutations in T-cell acute lymphoblastic leukemia: prognostic significance and implication in multifactorial leukemogenesis. Clin Cancer Res *12*, 3043-3049.

Zuurbier, L., Gutierrez, A., Mullighan, C. G., Cante-Barrett, K., Gevaert, A. O., de Rooi, J., Li, Y., Smits, W. K., Buijs-Gladdines, J. G., Sonneveld, E.*, et al.* (2014). Immature MEF2C-dysregulated T-cell leukemia patients have an early T-cell precursor acute lymphoblastic leukemia gene signature and typically have non-rearranged T-cell receptors. Haematologica *99*, 94-102.

Zuurbier, L., Homminga, I., Calvert, V., te Winkel, M. L., Buijs-Gladdines, J. G., Kooi, C., Smits, W. K., Sonneveld, E., Veerman, A. J., Kamps, W. A.*, et al.* (2010). NOTCH1 and/or FBXW7 mutations predict for initial good prednisone response but not for improved outcome in pediatric T-cell acute lymphoblastic leukemia patients treated on DCOG or COALL protocols. Leukemia *24*, 2014-2022.

Zuurbier, L., Petricoin, E. F., 3rd, Vuerhard, M. J., Calvert, V., Kooi, C., Buijs-Gladdines, J. G., Smits, W. K., Sonneveld, E., Veerman, A. J., Kamps, W. A.*, et al.* (2012). The significance of PTEN and AKT aberrations in pediatric T-cell acute lymphoblastic leukemia. Haematologica *97*, 1405-1413.